MASS TRANSFER EQUILIBRIA AND KINETICS OF GRANULAR FILTER MATERIALS FOR PHOSPHORUS IN URBAN WATER

By

TINGTING WU

A DISSERTATION PRESENTED TO THE GRADUATE SCHOOL
OF THE UNIVERSITY OF FLORIDA IN PARTIAL FULFILLMENT
OF THE REQUIREMENTS FOR THE DEGREE OF
DOCTOR OF PHILOSOPHY

UNIVERSITY OF FLORIDA

2010

This work is dedicated to my father, Changzhi Wu; my mother, Yuqing Ma; and my brother Yue Wu.

ACKNOWLEDGMENTS

I wish to express my sincerest and deepest appreciation and gratitude to my advisor, Dr. John J. Sansalone, for his guidance and encouragement throughout my research. His patience and support helped me overcome difficult situations and finish this dissertation. His words of urgings and careful reading and reviewing of all my writing will never be forgotten. I came to UF to gain knowledge and capability to take me to a higher professional level, what I come away with is so much more.

In the same vein, I want to thank my doctoral committee---Dr. James P. Heaney, Dr. Joseph J. Delfino and Dr. Mark W. Clark, for their valuable support and advices on my research.

My thanks also go to the past and present members of my group, for many fond memories and insightful discussions involving our research. I am grateful to Mr. Gary Scheiffele and Mr. Bill Brubaker for helping me with the analysis conducted in PERC.

Many friends have helped me overcome setbacks and stay focused on my graduate study. I greatly value their friendship and deeply appreciate their belief in me. Special thanks go to Fangyuan Hua, my previous roommate, for being such a great companion and helping each other stay affirmative through these years.

Finally, I would like to express my heart-felt gratitude to my parents and brother. They are always behind me and I could hardly accomplish anything without the love and support of my family.

TABLE OF CONTENTS

page

LIST OF TABLES

LIST OF FIGURES

Abstract Of Dissertation Presented To The Graduate School
Of The University Of Florida In Partial Fulfillment Of The Requirements For The Degree
Of Doctor Of Philosophy

MASS TRANSFER EQUILIBRIA AND KINETICS OF GRANULAR FILTER MATERIALS FOR PHOSPHORUS IN URBAN WATER

By

Tingting Wu

December 2010

Chair: John J. Sansalone
Major: Environmental Engineering Sciences

This study examined a suite of granular filter substrates as potential adsorptive-filtration media for P control in urban water.

The batch equilibria between dissolved phosphorus (DP) and three engineered AlOx coated media (soil-based, $AOCM_c$; pumice-based, $AOCM_p$; Portland cement concrete-based, $AOCM_{pcc}$) were investigated. Media isotherms are evaluated with surrogate matrix in de-ionized (DI) water, municipal wet weather flow (rainfall-runoff) and dry weather (wastewater) matrices. Compared to the uncoated media substrates, AOCM provides statistically significantly higher equilibra capacity. Wet and dry weather flow matrices had lower DP adsorption compared to the DI matrix due to competitive effects, in particular SO_4^{2-}. As compared to $AOCM_c$ and $AOCM_p$ isotherms $AOCM_{pcc}$ exhibited an increasing mass transfer gradient with increasing DP concentration; driven by surface precipitation. A series of granular filter materials were also tested in batch equilibrium experiments using the equivalent surrogate matrix of DI water. Results were modeled using Freundlich isotherm equation. Another unified sorption variable, K_u was calculated and served as a more appropriate parameter for media evaluation and

comparison. At C_e = 0.03 mg/L, K_u values ranged from 25.68 to 0.09 L/g for the media tested in this study, indicating a significant variability of the media capacity.

This study also examined the kinetics of DP mass transfer from the aqueous matrix to the media. A 2nd order potential driving model is utilized for the overall rate process. Comparing synthetic- and actual rainfall-runoff matrices demonstrated that actual runoff produced slower overall rate kinetics for $AOCM_c$ and $AOCM_p$ primarily due to the presence of competitive ions (SO_4^{2-}) while elevated Ca^{2+} at the alkaline surface of $AOCM_{pcc}$ offset the effect of SO_4^{2-}, through surface precipitation. Commercially available media exhibited a large variance of capacities.

Column breakthrough experiments of DP from granular media were also conducted. Thomas model was utilized to simulate the breakthrough curves of AOCM. The effect of surface loading rate on breakthrough behavior was investigated and novel mathematical correlations were developed to relate Thomas model parameters (K_T and q_0) with surface loading rates. Additionally, $AOCM_c$ and $AOCM_{pcc}$ were examined in rainfall-runoff and wastewater, respectively.

CHAPTER 1
GLOBAL INTRODUCTION

Phosphorus (P) has been recognized as a primary nutrient discharged in excess to surface waters and ground water; and such enrichment by phosphorus is regarded as a main reason for eutrophication (U.S. Geological Survey, 1999; Markris et al., 2004; Yoshida et al., 2004; Oleszkiewicz and Barnard, 2006; Endards and Withers, 2007). P can be generated from point sources, for example domestic and industrial wastewater; and nonpoint sources such as agricultural and urban runoff (Namasivayam and Sangeetha, 2004). The built environs as the interface that transforms rainfall into runoff, is a major nonpoint source and pathway of nutrients including P and urban runoff has been noted to contain high phosphorus concentrations that can be accelerating the eutrophication resulting in aesthetic, chemical and ecological degradation of receiving waters (USEPA 1993, Bowes et al. 2005; Kim et al. 2008). While WEF/ASCE (1998) documented that the event mean concentration (EMC) for total phosphorus (TP) 0.33 mg/L and dissolved phosphorus is 0.12 mg/L; it has been reported that EMC of TP in urban runoff ranged from 0.03 to 5.29 mg/L (Davis, 2007) and for highway runoff the median TP ranged from 0.19 to 1.8 mg/L (Drapper et al., 2000). Dean et al. (2005) reported that urban runoff transported DP from 0.3 to 1.4 mg/L (EMC) in an urban pavement catchment. A desired goal for prevention of plant nuisances in flowing waters not discharging directly to lakes or impoundments is 0.1 mg/L (USEPA, 1986). Oğuz (2005) reported that TP concentration over 0.03 mg/L will likely trigger algal blooms in confined water bodies. Especially, EPA recently proposed new numeric nutrients criteria for Florida's lakes and flowing waters, which are summarized in Table 1-1 the specific values for different water bodies.

However, while the technology exists and is relatively mature for treating point sources, control of nonpoint sources has not kept pace with point source control, in part because of the much greater challenges associated with diffuse, stochastic and variable loadings and with technology that is still developing. Many physical, chemical and biological control technologies applied to nonpoint loads can be disadvantaged by unfavorable cost/benefit relationships, low or variable effectiveness, or restrained by operational instability (for example desorption from media systems or lack of maintenance) and lack of sustainability (Karaca, 2004; Sansalone, 2005; Huang et al., 2008).

P occurs in the forms of both dissolved phosphorus (DP) and particulate phosphorus (PP) and mainly exists as phosphate in aqua-systems (Wei et al., 2008; Chitrakar et al., 2006). Regarding the control of P loadings in urban rainfall-runoff, many phosphorus treatment methods have been investigated, such as constructed wetland systems (Gervin and Brix 2001; Seo et al. 2005), filtration, infiltration and detention/retention basins (Dechesne et al. 2005; Hunt et al. 2008; Hsieh et al, 2007), in-situ filtration (Sansalone and Teng 2005, Teng and Sansalone 2004), storm-treat systems (Sonstrom et al. 2002), urban wet detention ponds (Wu et al. 1996; Comings et al. 2000; Wang et al. 2004), and vegetative controls (Barrett et al. 1998). While sedimentation occurs in all unit operations, whether by design or otherwise, designs based strictly on sedimentation through overflow rate concepts are limited in populated urban area since there is generally a requirement of large operational area and volume, if suspended particulate matter (PM) requires separation. Additionally, sedimentation is

a mechanism to separate PM, not soluble phosphorus, which, unfortunately, is very biologically active, and imparts the most negative influence on our surface waters.

For over a decade adsorptive-filtration has attracted interest; for example through deployment of economical filter substrates for DP adsorption. A category of the adsorptive media incarnations have included filter substrates that range from common non-engineered materials (Sakadevan and Bavor, 1998; Johansson, 1999; Bubba et al., 2003; Hsieh and Davis, 2005; Davis et al., 2006; Hsieh et al., 2007) to industrial by-products or wastes (Kostura et al., 2005; Drizo et al., 2006; Lu et al., 2008) in order to reduce the initial cost of media systems. These studies have demonstrated that many of these media do not have sufficient capacity for successful deployment to control DP (Bubba et al. 2003; Forbes et al. 2004, Kim et al. 2008, Sansalone and Ma 2009). Recently engineered media with Fe or Al coating has been reported to exhibit significantly improved adsorptive capacity as compared to non-engineered media (Ayoub et al., 2001; Arias et al., 2006; Boujelben et al., 2008; Sansalone and Ma 2009). However, while these recent studies have pointed to the role of metal oxides for phosphate adsorption, Liu et al 2005 (a, b) reported that media function and deployment is also influenced by the properties of the media substrate itself such as porosity, pore size distribution, strength and substrate chemistry. To date, research has focused on comparisons of economical substrates such as reuse or waste substrates (Agyei et al., 2002; Oğuz, 2005; Yang et al., 2006) without examining the role of the substrate as compared to substrate combined with an oxide coating for adsorption of phosphate. Additionally, if media and media substrates require comparison, testing that allows comparison between media for a given media phenomena under equivalent conditions

are required. The most common controlled surrogate aqueous matrix is de-ionized (D.I.) water which provides a consistent and reproducible matrix for media testing and facilitating media comparisons subject to different controlled loadings (Namasivayam and Sangeetha, 2004; Arias et al., 2006; Georgantas and Grigoopoulou, 2007; Boujelben et al., 2008). However, while such a consistent and reproducible matrix provides a vehicle for media comparability, studies have also shown that the equilibrium capacity of DP can be non-representative when comparing results from a DI matrix and an actual aqueous matrix subject to similar pH and DP concentrations (Millero et al., 2001; Chen et al., 2002; Shilton et al., 2005; Ádám et al., 2007, Sansalone and Ma 2009).

To date little quantitative evaluations of adsorptive-filter media for DP adsorption have been conducted, especially fixed-bed/column tests. However, there continues to be limited information available and large performance claims for phosphorus removal for both manufactured and natural filtration systems using un-quantified media. Media applications that do exist with reported information tend to experience high performance variability (Davis et al. 2006, Hsieh et al. 2007) or result in exporting phosphorus, or leaching of other pollutants such as metals or pH. Again, these challenges are due to the limited quantitative information of the behavior of the filter material. Successful deployment of any media system requires the comparison of media behavior on a rigorous and equal basis. In this study, three Al-oxide coated substrates: clayey soil-based ($AOCM_c$, 2 gradations), pumice-based ($AOCM_p$), and Portland cement concrete-based ($AOCM_{pcc}$, 2 gradations), along with their uncoated media substrates (UCM) served as controls, and a suite of non-engineered commercially available media,

including activated alumina, bioretention soil media, expanded shale (2 gradations), iron coated perlite, tire crumb B&G (2 gradations) and Zeolite-perlite-GAC are evaluated through three quantitative descriptions: equilibrium isotherms, kinetics and column breakthrough using controlled surrogate aqueous matrix of de-ionized (D.I.) water. Additionally, metal leaching and desorption tests are carried out to determine if metals leach out from the media materials during adsorption tests or the immobilized P can be easily sloughed off after adsorption. Furthermore, AOCM are examined utilizing aqueous matrices of synthetic runoff, actual rainfall-runoff and wastewater under three hypotheses: First, a media-based AlOx reactant, as a coating or admixture can significantly increase the capacity of a given substrate as compared to the substrate alone. Second, the physical and chemical indices of the substrate impact the capability of the resulting media with AlOx. Third, the chemistry of an actual runoff or wastewater matrix with competing solutes significantly affects the overall P mass transfer rates and media capacity.

Moreover, the application of batch experimental data is often difficult to apply to fixed-bed adsorption system and inferences from such data may lead to false direction without proper interpretation. Beyond equilibria, media capacity for a solute can be represented through breakthrough modeling under a known set of loading conditions (Köse and Öztürk, 2008). The time (or more appropriately volume treated) until a set breakthrough or exhaustion level are commonly-reported characteristics of a given media, system and set of loading conditions; while there has been more limited analytical model development to describe breakthrough in time and throughout the media profile (Aksu et al., 2007) unless carried out with an advective-dispersive

numerical model (Liu et al. 2005). However, introduction of lumped system parameters and constrained correlations have provided tractable analytical models for one-dimensional flow systems (Lee et al., 2000; Ko et al., 2001; Aksu et al., 2007). One such bed depth service time (BDST) model is the Thomas model that has been widely used in the design of fixed bed adsorption systems (Rao and Viraraghavan, 2002; Thirunavukkarasu et al., 2003; Aksu and Gönen, 2004; Aksu et al., 2007; Köse and Öztürk, 2008; Pokhrel and Viraraghavan, 2008; Sivakumar and Palanisamy, 2009). The main advantages of the Thomas model are simplicity and reasonable accuracy in predicting media breakthrough behavior for adsorptive media. Additionally the kinetics coefficient and adsorption capacity from the model can be determined from monitored data. Typically examined for a single SLR, examination across a range of SLRs can extend the use of the Thomas model to incorporate behavior subject to unsteady phenomena, for example for a fixed bed media absorber utilized after an equalizing or primary treatment operation of runoff (Erickson et al., 2007). While there have been many studies regarding the use of such models (Koh et al., 1998; Aksu and Gönen, 2004; Mantovaneli et al., 2004; Aksu et al., 2007; Köse and Öztürk, 2008), illustrating the relationship between these Thomas model parameters and SLR has not been demonstrated through a physical model. Given the variability in actual application, especially the stochastic loading of rainfall runoff, such relations will be of great practical significance and immediate benefits.

Table 1-1. Water quality standards for the state of Florida's lakes and flowing waters
(The final rule signature: Nov. 14, 2010)

Lake class	TP [mg/L]
Colored lakes > 40 PCU	0.050 – 0.157
Clear lakes, alkaline ≤ 40 PCU and > 50 mg/L $CaCO_3$	0.030 – 0.087
Clear lakes, acidic ≤ 40 PCU and < 50 mg/L $CaCO_3$	0.010 – 0.030

Watershed Regions	TP [mg/L]
Panhandle	0.043
Bone valley	0.739
Peninsula	0.107
North central	0.359

Waterway	TP [mg/L]
Canals	0.042

CHAPTER 2
BATCH EQUILIBRIA BETWEEN AQUEOUS PHOSPHORUS SPECIES AND ALUMINUM OXIDE COATED GRANULAR SUBSTRATES

Background

Phosphorus (P) can be generated from point sources, for example domestic and municipal wastewater; and nonpoint sources such as agricultural and urban runoff (Namasivayam and Sangeetha, 2004). The build environs of urban land uses represent an interface that transforms rainfall into runoff, while mobilizing and transporting nutrients including P. Urban runoff has been shown to contain high P concentrations, resulting in an adverse impact on receiving water bodies (Dean et al. 2005; Kim et al., 2008). As a primary limiting nutrient in surface waters a range of limits for discharge of have been identified; for example 0.03 mg/L of P was suggested as a criteria level with respect to excessive algae growth in lakes (Oğuz, 2005). With respect to control, advances in treatment of point source P, for example at a municipal wastewater treatment plant (WWTP) is economical and efficient compared to treatment of diffuse and stochastic loadings of nonpoint P (Shin and Han, 2004, Duda, 1993; UEPA 2003; Sansalone 2005).

For over a decade adsorptive-filtration has attracted interest; for example through deployment of economical filter substrates for phosphate adsorption (Gray et al., 2000; Liu and Yang, 2002; Mortula et al., 2007, Sansalone and Ma 2009). There is also a significant body of research that has demonstrated that P in runoff can be adsorbed by soils (Edzwald et al., 1976; Wang and Tzou, 1995; Fontes and Weed, 1996). In part, this adsorption can be attributed to Al and Fe oxides. For example, Al oxides can range from 9.4 to 12.3 g/kg; while Fe oxides can range from 10.8 to 23.3 g/kg in silt loam and sandy loam soil (Morillo et al., 2004). In many soils Al and Fe-oxides are present

making soil a reactive substrate, specifically for phosphate species (Fontes and Weed, 1996; Nooney et al., 1998; Arias et al., 2006; Boujelben et al., 2008). Parfitt (1978) indicated that phosphate, within a broad concentration range was adsorbed on the oxide surfaces of clayey soils as binuclear bridging complexes by replacing two singly coordinated hydroxyl groups on the oxide surface per molecule of phosphate. However, van der Zee and van Riemsdijk (1988) suggested that phosphate adsorption consisted of two distinct mechanisms: one relatively fast, reversible adsorption process and a relatively slow, largely irreversible precipitation mechanism; for example in soils classified texturally as sandy. Goldberg and Sposito (1985) reported that the mechanism for phosphate adsorption is ligand exchange by hydrous Al/Fe oxides of soil minerals. More recently, metal oxides have been investigated to improve phosphate adsorption (Ayoub et al., 2001; Arias et al., 2006; Boujelben et al., 2008). However, while these recent studies have pointed to the role of metal oxides for phosphate adsorption, Liu et al 2005 (a, b) reported that media function and deployment is also influenced by the properties of the media substrate itself such as porosity, pore size distribution, strength and substrate chemistry. To date, research has focused on comparisons of economical substrates such as reuse or waste substrates (Agyei et al., 2002; Oğuz, 2005; Yang et al., 2007) without examining the role of the substrate as compared to substrate combined with an oxide coating for adsorption of phosphate. Additionally, in many of these studies a controlled surrogate aqueous matrix such as the common use of de-ionized water has provided a consistent and reproducible matrix for testing media and facilitating media comparison (Fontes and Weed, 1996; Namasivayam and Sangeetha, 2004; Arias et al., 2006; Georgantas and Grigoopoulou,

2007; Boujelben et al., 2008). However; actual rainfall-runoff or wastewater matrices are much more complex with competitive interactions; and rainfall-runoff is highly variable spatially and temporally (Dean et al. 2005, Sansalone et al. 2005). As a result, studies have either utilized a reproducible surrogate aqueous matrix or separately, an actual environmental matrix without comparison to the surrogate matrix.

Objectives

This study focuses on phosphate (as DP) adsorption equilibria by AlOx as a media-based reactant. Comparisons are made as function of media substrates, and between aqueous matrices of (DI water as a surrogate), wastewater and rainfall-runoff at equal DP concentrations. This study is driven by the following hypotheses. First, a media-based AlOx reactant, as a coating or admixture can significantly increase the adsorption equilibria of a given substrate as compared to the substrate alone. Second, the physical and chemical indices of the substrate impact the adsorption equilibria of the resulting media with AlOx. Third, at the same pH, redox and DP concentration, the chemistry of a actual runoff or wastewater matrix with competing solutes with result in a statistically significant decrease in adsorption equilibria for a given media.

Materials and Methodology

Sorbents and Media Preparation

Clays, pumice and Portland cement concrete are all reported to be effective for removing phosphate ions from water (Fontes and Weed, 1996; Agyei et al., 2002; Ayari et al., 2005; Akbal 2005; Liu et al., 2005). In this study these three materials were used to prepare raw substrates and then coated with Aluminum Oxide. In addition, the raw substrates were tested as control in the experiments. The effective size of the sorbents ranged from 0.85 – 4.75 mm for clay and concrete; 2 – 4.75 mm for pumice.

Raw substrate (UCM) preparation

UCM_c: Bentonite with mineralogical composition of sodium hydrated aluminosilicate was purchased from Halliburton Energy Services, Inc. The clay was first mixed with explosive reagents and water, and then sintered in kiln to remove the moisture and be solidized, following by crushing and sieving to recover the desired gradation. This porous substrate was then soaked in an acid solution (H_2SO_4, 10 - 15%) for 24 h to removal the phosphorus residual. After that, the raw substrate (UCM_c) was rinsed with D.I. water until the pH was higher than 4.5 and then dried at 105 ^oC.

UCM_p: The pumice (2 – 4.75 mm) was purchased as commercials from Hess Pumice Products. The same acid soaking pretreatment was applied to pumice to produce pumice raw substrate (UCM_p).

UCM_{pcc}: The concrete raw substrate was produced using a mass ratio 1:1 (water to cement). This cementitious slurry was then cured and size graded.

Aluminum oxide coated media (AOCM) preparation

$AOCM_c$ and $AOCM_p$: $AOCM_c$ and $AOCM_p$ were prepared by applying aluminum as surface coating. Stock solution of 1M Al (III) was prepared by dissolving $Al(NO_3)_3 \cdot 9H_2O$ in De-ionized (D.I.) water. Al (III) solution was added to the raw substrate contained in a Pyrex tray so that the substrate was just submerged. This Pyrex tray was then put in the oven and temperature was kept at around 200 ^oC. At least 24 hours were needed to fully dry and coat the substrate. Later, the aluminum coated sorbents was washed with D.I. water to remove the surficial fine materials. Then the sorbent was dried at 105 ^oC and finally stored in polypropylene bottles for further use.

$AOCM_{pcc}$: $AOCM_{pcc}$ was prepared by integrating aluminum solution into the cementitious matrix as the “aqueous” admixture. The mass ratio of aqueous $Al(NO_3)_3$

solution (0.5 M) to cement is 1:1. This cementitious slurry was then cured and size graded in the same way as raw substrate preparation.

Chemicals

A phosphorus stock solution was prepared by dissolving anhydrous potassium dihydrogen orthophosphate (KH_2PO_4) powder (Analytical reagent grade, Fisher Scientific) into D.I. water. The stock solution was calibrated to 100 mg/L and 1000 mg/L concentrations, which were utilized as standard solutions as necessary.

Phosphorus concentration was measured by HACH DR/5000 Spectrophotometer using PhosVer 3 Ascorbic Acid Method (Standard Method 1998). All measurements were duplicated and high repeatability was assured by controlling experimental error within ± 5%. Measurements of pH were carried out using a multi-meter (Orion 290A combination electrode), which was preliminary calibrated using a 3-point calibration curve with reference units at a pH of 4, 7, and 10.

Surface Charge and Specific Gravity (ρ_s)

Surface charge for the tested media was measured using a potentiometric titration methodology described by Van Raij and Peech (1972). pH_{pzc} was then calculated by linearly interpolating between the last positive and first negative surface charge values.Specific gravity (ρ_s) measurement utilized a helium gas pycnometer.

Powder X – ray Diffraction (XRD)

XRD analysis was conducted on oxide coating materials and raw clay substrate. The instrument used was XRD Philips APD 3720. Cu K_α was employed, with a tube current of 20 mA and a tube voltage of 40 kV. Scans were conducted from 10 to 120 (°2θ) with a step size of 0.02 (°2θ).

Fourier Transform Infrared Spectrometry (FTIR)

FTIR measurement was performed with a Nicolet Magna IR-760 system. Coating materials were removed from the coated media surface for FTIR analysis. Reynolds Alpha Alumina and Inframat Gamma Alumina were also analyzed as references. 3.5 milligrams of the prepared material were pressed with KBr (1:100) to a pellet. The measurements were carried out in the mid-infrared range from 4000 to 400 cm^{-1}.

Experimental Matrices and Adsorption Equilibria (Isotherm) Study

In order to estimate static or dynamic adsorption capacity, it is essential to have information on adsorption equilibrium to quantify how much phosphorous can be adsorbed. A common way to represent the adsorption equilibrium is the equilibrium isotherm from which the amount of phosphorus species adsorbed under a given set of chemistry conditions can be determined for a given media.

Comparison and evaluation of the engineered media as well as the raw substrates were carried out in three different experimental matrices, including synthetic runoff, filtered rainfall-runoff and wastewater matrix. The chemistry of experimental matrices was summarized in Table 2-1. In present study, the specific working phosphorus concentrations utilized to obtain isotherm data were: 0, 0.05, 0.5, 1.0, 2.5, 10, 25 and 50 mg/L. For the synthetic runoff matrix, the above initial TDP concentrations were obtained by diluting stock phosphorus solution and ionic strength was fixed at 0.01 M using KCl. Solution pH was adjusted to 7 at the beginning of experiments by dropwise addition of HCl or NaOH. For rainfall-runoff and wastewater matrix, the initial concentration of the rainfall-runoff or wastewater was kept to replace one of the eight working phosphorus concentrations, whichever was the closest. Then the others were obtained by diluting the raw sample with D.I. water or adding high concentration

phosphorus stock solution, in such a way that the original chemistry of the matrix was best maintained. In addition, the real rainfall-runoff sample was filtered through 0.7 µm paper filter to remove the coarse solids in the feeding solution before dilution or phosphate-spike.

0.5 g adsorbent and 40 ml of working phosphate solution were added into a 50 ml polyethylene centrifuge tube. The mixture was thoroughly mixed on a horizontal bench shaker at a rate of 100 rpm allowing adsorption to take place at 20°C until equilibrium reached, usually 24 hr. The content in the centrifuge tube was then filtered through 0.45µm syringe filter and the total dissolved phosphate concentration in the filtrate was measured using spectrophotometer (HACH, DR5000). The amount of adsorbate that was adsorbed on the adsorbent was then calculated from the difference between the initial and equilibrium solute concentrations.

Equilibria Model

Equilibria represent one of four fundamental categories of adsorption models; models that quantitatively describe media or soil behavior (Liu et al. 2005b). Although an equilibrium isotherm does not account for temporal mass transfer effects of most transport phenomena; the operating curve of an equilibrium isotherm model represents an asymptotic limit as a function of concentration for adsorption capacity of a given soil or media system. At each unique set of aqueous – solid adsorbent phase conditions there is a unique media or soil capacity, q_e [mg/g].

$$q_e = \frac{(C_0 - C_e)V}{W} \quad (1)$$

C_0 and C_e are the initial and equilibrium solute concentrations [mg/L], respectively; V the volume of the solution [L] and W the mass of the adsorbent [g]. The relationship

between solute adsorbed, q, as a function of the solute concentration in the fluid phase, C, at temperature T is called the adsorption isotherm at T. A singular point for a unique set of aqueous-solid phase conditions cannot represent an isotherm (Sansalone and Ma 2009).

$$q = q(c) \text{ at T} \tag{2}$$

An isotherm model can be represented by a number of mathematical forms that can be combined kinetics and breakthrough representations (Suzuki, 1990). A common isotherm is the Langmuir model.

$$q = \frac{bq_m C}{1 + bC} \tag{3}$$

q is the solute adsorbed per unit mass of adsorbent and q_m is the maximum adsorbed phase concentration where all the adsorption sites are occupied. As identified by Tien,(1994) the assumptions include (1) the solute molecules are adsorbed at localized states; (2) each adsorption site accommodates one solute molecule and all the sites are energetically identical; and (3) there are no lateral interactions between sites. These assumptions result in an idealized adsorbent surface; in contrast to the heterogeneity of actual surfaces. Even across the surface of a perfect crystal, Everett (1993) indicated that the energy of interaction with a solute varies across the surface and such heterogeneity cannot be neglected.

However, the surface heterogeneity can be modeled through an adsorption energy distribution, and mathematically, a heterogeneous surface may be considered to be composed of many homogeneous sites (Tien, 1994; Rocha et al., 1997). Therefore, a heterogeneous adsorption surface can be considered as a summation of simplified homogenous Langmuir surfaces.

$$q = \frac{b_1 q_{m1} C}{1 + b_1 C} + \frac{b_2 q_{m2} C}{1 + b_2 C} + \cdots = \sum_i \frac{C(q_m)_i}{\frac{1}{b_i} + C} \tag{4}$$

q_{mi} and b_i are values of q_m and b for the i^{th} site. With $b' = \frac{1}{b_i}$, eq. (4) can be rewritten.

$$q = \sum_i \frac{C(q_m)_i}{b' + C} \tag{5}$$

Each adsorption site is characterized by specific adsorption energy. By assuming a continuous distribution of the site energy, equation (5) can be written as:

$$q = \int_0^\infty \frac{C}{b' + C} N(b') db' \tag{6}$$

The site frequency distribution N(b') discretizes sites having adsorption energies between b' and b' + db'. Tien (1994) modeled the distribution of N(b'); with A' as a constant.

$$N(b') = A'(b')^{\frac{1}{p}-1} \tag{7}$$

Substitute equation (7) with equation (6) and simplying:

$$q = \int_0^\infty A' \frac{C(b')^{\frac{1}{p}-1}}{b' + C} db' = A' \int_0^\infty \frac{(b')^{\frac{1}{p}-1}}{\frac{b'}{C} + 1} db' \tag{8}$$

When p > 1, solution of the above equation leads to the Freundlich model, where

$$q = A' \frac{(\frac{1}{C})^{-\frac{1}{p}}}{\sin[(1 - \frac{1}{p})\pi] \Big/ \pi} \tag{9}$$

Assuming that $1-\frac{1}{p} \approx 1$, equation (9) can be approximated as:

$$q = A' \cdot \frac{(\frac{1}{C})^{-\frac{1}{p}}}{\frac{\sin \pi}{\pi}} = AC^{\frac{1}{p}}, \left(A = \frac{A'\pi}{\sin \pi}\right) \quad (10)$$

This has the form of the non-linear Freundlich isotherm equation, commonly used to model heterogeneous adsorbent surfaces. The heterogeneous composition and structure of the adsorbent substances and the potential of multiple sorption mechanism contributes to nonlinear isotherms. The commonly utilized form of Freundlich, as used herein is:

$$q = K_F C^n \quad (11)$$

K_F and n are constants incorporating all parameters affecting the adsorption process, i.e. adsorption capacity and intensity respectively. C_e is the concentration of solute in solution at equilibrium [mg/L]. The Freundlich model and experimental data were fit using non-linear regression analysis.

Results and discussion

Physicochemical Characteristics of Sorbents

The major components of pumice are amorphous silicon dioxide (SiO_2) bonded metal oxides such as Al, Ca and Mg etc as reported by Panuccio et al. (2009). The concrete substrate of Type II cement, with major components of C-S-H (Calcium-Silicate-Hydrate, 50 - 60%), $Ca(OH)_2$ (20 - 25%)and CSA (calcium sulfoaluminates, 15-20%). XRD analysis was carried out to determine the mineral composition of raw substrate of clay (after calcination) and α-quartz (SiO_2), Goethite (FeOOH) and Calcite

($CaCO_3$) were identified. The major composition of the three substrates is summarized in Table 2-2.

FTIR combined with XRD was used to analyze the composition and structure of media coating. No aluminum-related crystals were found during the XRD analysis, which may lead to the conclusion that the coating was amorphous, not crystalline. Figure 2-1 illustrates the FTIR spectrum of the media coating. The broad band between 2800 ~ 3700 cm^{-1} is associated with –OH stretch (Klute, 1986; Liu, 1999; Chandrasekharan et al., 2008). More accurately, 3700 cm^{-1} corresponds to free O-H stretch, 3675 ~ 3540 cm^{-1} to O-H stretch and 3390 ~ 2800 cm^{-1} to bonded O-H stretch (Klute, 1986). Bands below 1000 cm^{-1} represent Al-O bonds (Costa et al., 2007). The peak at 1384 cm^{-1} for media coating and γ – alumina is associated with nitrate bond (Smidt E et al., 2005; Garai J. et al., 2006), which originates from the precursor during aluminum oxide preparation. The transformation between different Al_2O_3 phases strongly depends on the precursors and the heat treatment. Usually the spectrum of low temperature phase alumina shows a broader band of –OH group. With increase of treatment temperature, the bands tend to decrease the intensity due to the removal of water molecules. In the mean time, the intensity corresponding to Al-O bond increases. These phenomena were observed, as compared the three spectra shown in Figure 2-1. Since the media coating in this study was prepared with $Al(NO)_3$ and only calcined at 200 °C, broader band of –OH stretch and lower Al-O intensity were identified in FTIR test, and also the nitrate coming from the $Al(NO)_3$ cannot be eliminated.

Table 2-3 summarizes the physical characteristics of the sorbents. Surface area has been regarded as an important indicator of the media capacity in some

circumstances (Colombo et al., 1993; Liu et al., 2001; Arias et al., 2006). Compared with UCM, the SSAs of both $AOCM_c$ and $AOCM_{pcc}$ are higher, while it is opposite for $AOCM_p$ and UCM_p. This may be due to the highly porous nature of pumice substrate, which can be blocked or filled during the coating process. In contrast, for clay and concrete based media, aluminum oxide contributes to the surface roughness and results in a higher SSA. The literature has reported a wide range of specific surface area of aluminum oxide, from < 15 m^2/g to > 200 m^2/g (Goldberg et al., 2001; Genz et al., 2004). Surface area was found to be affected by various factors, such as concentration of the starting reagents, aging, heating and reaction in aqueous solution. Hietela et al. (1989, 1990) interpreted the increase in heating temperature can result in the increase in surface area of low surface material. In their study of surface characterization of amorphous aluminum oxides, Goldberg and her coworkers (2001) found aluminum oxide minerals of widely differing initial surface areas measured in the dry state had the surface areas of comparable magnitude upon reaction in aqueous. Therefore, initial surface area may be a conditional indicator of chemical reactivity of synthetic amorphous aluminum oxide.

For all of the three substrates based media (clay, pumice and concrete), there is not much difference between coated media and corresponding raw substrates in pH_{pzc}. In addition, pH_{pzc} of activated alumina has been reported to be 8.1 ~ 9.1 (Genz et al., 2004), which is much higher than 4 ~ 5 as shown by $AOCM_c$ and $AOCM_p$. This implies that the electrical properties of the underlying material was not masked by the surface aluminum coating, which is also exemplified by the coating efficiency of $AOCM_c$ (33.13 ± 18.32 mg aluminum coating /m^2 UCM_c) and $AOCM_p$ (7.16 ± 0.87 mg aluminum coating

/m^2 UCM_p). Unlike clay and pumice based AOCM, concrete based media has a much higher pH_{pzc}. The high pH value of point of zero charge of $AOCM_{pcc}$ and UCM_{pcc} is due to the presence of large amount of $CaO/Ca(OH)_2$ in the substrate, which can definitely overwhelm the aluminum coating especially when aluminum was integrated into the cementitious matrix and not applied as a surface coating.

Studies in Synthetic Runoff Matrix (Hypothesis (1) and (2))

Hypothesis (1)

Comparison of the performance of AOCM and UCM in synthetic runoff matrix is shown in Figure 2-2. The isotherms rise sharply in the initial stages due to plenty of readily accessible sites and eventually reach a plateau indicating that the adsorbent is saturated at this level. In all three cases (clay based, pumice based and cement concrete based), the coating media showed much better capacity. The Freudlich isotherm was used to describe the sorption equilibria. The model parameters are summarized in Table 2-4. All R^2s are no less than 0.96, indicating a good simulation of experimental data. The values of K_F and n determine the steepness and curvature of the isotherm. Usually n values between 0 and 1 represent beneficial adsorption and indicate that significant adsorption takes place at low concentration but the increase in the amount adsorbed with concentration becomes less significant at higher concentration. Also, the higher the K_F value, the greater the adsorption intensity. Therefore, the higher K_F values for the coated media confirm that the adsorption capacity of AOCM was greater than that of UCM. Since for each pair of media, AOCM and UCM were in the same gradation and both experiments were carried out under the same conditions, this difference can be reasonably ascribed to aluminum coating. Two gradations (0.85 – 2 mm) and (2 – 4.75 mm) were tested for $AOCM_c$/UCM_c and

$AOCM_{pcc}$/UCM_{pcc} in this study. Figure 2-3 depicts the media size effects in synthetic runoff matrix. Not surprisingly, small media size exhibited greater sorption capacity. Since the adsorption experiments were carried out with the same amount of adsorbents (0.5 g), this phenomenon can be easily related to the specific surface area. Although in the earlier discussion the initial SSA of amorphous alumina as a reliable indicator of potential reactivity was questioned, that was stated for the absolute SSA value of one media. Here, SSA of two adsorbents is compared and the trend that higher SSA better reactivity still stays true. The SSA ratio of $AOCM_c$ (0.85 – 2 mm) to $AOCM_c$ (2 – 4.75 mm) is about 8 and that of $AOCM_{pcc}$ (0.85 – 2 mm) to $AOCM_{pcc}$ (2 – 4.75 mm) is about 9. Larger SSA means more active sites could be available for phosphate to attach with and in return higher removal efficiency will be achieved. However, although there was notable increase in percentage of phosphate removal as the adsorbent particle size decreased, the increase was not exactly proportionate to the increased surface area. This indicates the phosphate is removed from the liquid phase mainly by chemisorptions rather than physical adsorption, especially at high P concentration.

The higher removal efficiency of coated media comes from surface reactions between the media coating and aqueous phosphate. Although there are rare direct evidences, it is generally accepted that phosphates are adsorbed on hydrous aluminous oxide through ligand exchange between phosphates and the surface hydroxyl groups (Goldberg and Sposito, 1985; Genz et al., 2004; Kim and Kirkpatrick, 2004; Arias et al. 2006; Yang et al., 2006; Georgants and Grigoropoulou, 2007). When anions have a specific affinity for the metal atoms in the hydrated oxide, ligand exchange can result in formation of surface complexes containing no water molecules between the surface

Lewis acid site and the adsorbed ion, which are referred to as inner sphere. Huang (1975) clearly demonstrated the significance of specific chemical adsorption by calculating free energy for the adsorption of phosphate on γ-Al_2O_3.

A generalized ligand exchange reaction for phosphate ions was summarized by Goldberg and Sposito (1985):

$$aSOH\ (s) + H_bPO_4^{b-3}\ (aq) + cH^+\ (aq) \leftrightarrow S_aH_cPO_4\ (s) + bH_2O\ (l) + (a-b)OH^-\ (aq)$$

Where S refers to a metal ion, OH to a reactive surface hydroxyl and $b \leq 3$ is the degree of protonation of the phosphate ion.

In this study metal ion is Al and at pH of 7, the majority of phosphate ions exist as the form of $H_2PO_4^-$. Therefore, the reaction can be re-written as:

$$2{\equiv}Al\text{-}OH + H_2PO_4^- \leftrightarrow ({\equiv}Al)_2HPO_4 + H_2O + OH^-$$

In spite of controversy arising from the problem of what stereo-chemical configuration a phosphate takes on when it is complexed by a surface Lewis acid site due to the difficulty of probing the structure of the phosphate surface complex in an aqueous environment (Rajan, 1975; Guan et al., 2005), an increase of pH usually accompanies the adsorption reaction, as demonstrated in the above equation (Chang et al., 1997; Kitis et al., 2007). In this study, it was noticed that pH decreased as the working solution got contacted with $AOCM_c$ or $AOCM_p$ and then increased after certain time of reaction. The initial drop of pH may be due to the redundant H^+ from pretreatment of acid soaking. Then following pH increase can be ascribed to the surface reaction, which released OH^- as a result. For $AOCM_{pcc}$, an enhancement of solution pH was always observed and this should be correlated with the dominant influence of alkalinity caused by the concrete media. However, although the ligand exchange is

favored as a major mechanism of phosphate-metal oxide adsorption, many researchers have noted that the whole reaction is a complicated process and more than one mechanism could contribute to the phosphate removal (Johnson et al., 2002; Kim and Kirpatrick, 2004). Additionally, Arias et al. (2006) and Yang et al. (2006) pointed out that phosphorus sorption is a continuous sequence of adsorption and precipitation and is very difficult to make a distinctive quantitative analysis of the amount of adsorption and chemical co-precipitation. The role of each mechanism largely depends on the chemical nature of media and working solution, as discussed later.

Hypothesis (2)

Figure 2-4 compares the isotherm profiles of three AOCMs as well as UCMs in synthetic runoff matrix. In order to exclude particle size effect, all the results were obtained from the same gradation (2 – 4.75 mm). For UCMs, it can be easily noticed that UCM_c and UCM_p almost performed identically while there was a significant difference between those two and UCM_{pcc}. It is believed that the capacity of UCM_c and UCM_p for phosphorus removal from aqueous phase is usually related with the Al or Fe content in the substrate, which is consistent with the literature (Fontes and Weed, 1996; Nooney et al., 1998; Arias et al., 2006; Boujelben et al., 2008). For UCM_{pcc}, positive charge on the adsorbent surface (at pH 7) increased its affinity for the negatively charged phosphate ions and the phosphate was removed from solution via deprotonation and subsequent precipitation as $Ca_3(PO_4)_2$. Due to the high content of Calcium, UCM_{pcc} exhibited a much higher removal capacity compared with UCM_c and UCM_p.

The isotherm profile of AOCMs in synthetic runoff matrix is very instructive especially in contrast with that of UCMs. Unlike the uncoated counterparts, $AOCM_c$ and $AOCM_{pcc}$ showed similar higher capacity, while $AOCM_p$'s efficiency was relatively low. On the contrary, the SSA of $AOCM_p$ (2 – 4.75 mm) is the highest among the three of them, which should apparently promise a better performance. One reason for this observation is the physical nature of pumice. Pumice is a light, porous igneous volcanic rock. In spite of the highly porous structure of $AOCM_p$, quite percent of the porosity may come from micro pores which could decrease penetrability and hinder the ingress of phosphate ions to active sites. As discussed earlier, aluminum coating on the raw substrates resulted in a higher capacity and for $AOCM_{pcc}$ surface precipitation can also be an important mechanism. Therefore, investigation of the different performance between $AOCM_p$ and $AOCM_c$ logically lead to examination of coating efficiency. As reported earlier, less than ¼ aluminum coating (in mass) was contained on $AOCM_p$ compared with $AOCM_c$, which can be the direct cause for the low capacity of $AOCM_p$.

Even though exactly same methods were employed for $AOCM_c$ and $AOCM_p$, the coating efficiency can be varied due to different physical and chemical nature of the raw substrates. For example, it is very possible that not all of the aluminum on $AOCM_p$ serves as a specific surface functional group since part of them may just penetrate and fill into the pumice pores. This speculation is supported by the surface area change of pumice media after aluminum coating, as shown in 2-3. The raw substrate surface chemistry can also impact the interactions among surfaces and aluminum oxide during binding. Bentonite has a 2:1 layer clay mineral with two silica tetrahedral sheets bonded to a central alumina octahedral sheet The isomorphic substitution of Al^{3+} with Fe^{2+} and

Mg^{2+} and Si^{4+} with Al^{3+} results in net negative charge, which is balanced by the cations such as Na^{+} and Ca^{2+} located between the layers and surrounding edges ((Önal and Sarıkaya, 2007). The clay mineral used in this study is NaB (Na-bentonite) with Na^{+} being the exchangeable cation. During the pretreatment of acid soaking, quite amount of the alkali metal ions (Na^{+}) contained in the clay are exchanged for the hydrogen and create Brönsted acid centres. Furthermore, these H^{+} protons can migrate, disrupt the bonds between Si, O and Al, and lead to the formation of new groups (Christidis et al., 1997). These new groups may be bound in a less cohesive manner and thus leave a lower energy barrier for the interaction of aluminum coating with the substrate surface, resulting in a higher coating efficiency. On the other hand, pumice is mainly formed by SiO_2^{4-} tetrahedral networks, where approximately one in ten Si atoms is randomly replaced by Al atoms, maintaining the same coordination (Floriano, 1994). The substitution of Al^{3+} for Si^{4+} also involves the addition of monovalent cations, usually sodium and potassium to balance the net charge. It can be assumed that the charge-balanced cations in pumice is mainly located within the network and not as easily and largely exchanged with H^{+} as for bentonite, thus the coating efficiency for pumice substrate is lower.

Studies in Rainfall-runoff and Wastewater Matrices (Hypothesis (3))

As has been proved a better performance in synthetic runoff matrix, AOCM was further tested in rainfall-runoff and wastewater (after advanced treatment) matrices. The results are illustrated in Figure 2-5 and 2-6. The model parameters were summarized in Table 2-5. Figures 2-7 to 2-9 elucidate effect of matrices on the performance of $AOCM_c$, $AOCM_{pcc}$ and $AOCM_p$ respectively.

Although capacity of the three AOCMs followed the same order as in synthetic runoff matrix (Figure 2-4), much more significant difference was observed between $AOCM_{pcc}$ and the other two media. Meanwhile, less divergence between the isotherm profiles was shown between $AOCM_c$ and $AOCM_p$. In fact, it can be seen from Figure 2-5 and Figure 2-6 that the isotherm curvature for $AOCM_{pcc}$ has shifted from convex to concave as the matrix changed from synthetic runoff to rainfall-runoff/wastewater matrix. This noticeable change along with more than 99% phosphate removal efficiency even under the condition of 50 mg/L initial concentration clearly indicates an inherent mechanism transit. On the other hand, the “anomalies” in the results can also be perceived through Freundlich model parameter evaluation. In Table 2-5, abnormal large K_F are reported and the values of n are greater than 1 which has actually violated the monolayer surface coverage assumption ($n < 1$). In this case, Freundlich model can only be regarded as an empirical model mathematically simulating the experimental results, but not an adsorption model with the key parameter of the maximum surface coverage. All these evidences have shown that the major mechanism of phosphorus removal for $AOCM_{pcc}$ transited from adsorption to surface precipitation as the working matrix changed. Agyei et al. (2002) studied the removal of phosphate ions from aqueous solution by fly ash, slag, ordinary Portland cement and found that removal efficiency of PO_4^{3-} increased in such an order that mimicking the order of increasing percent CaO in the adsorbents, clearly indicating the affinity of phosphate for CaO. It has been a consensus that the formation of insoluble calcium phosphate and consequently the Ca-P precipitation is a significant mechanism for P removal using furnace slag or cement (Agyei et al., 2002; Lu et al., 2008).

In this study, the water chemistry of rainfall-runoff and wastewater has promoted the precipitation of phosphate ion greatly and changed surface precipitation to the dominant mechanism. This transition should be attributed to the high content of $CaO/Ca(OH)_2$ in concrete substrate as well as the water chemistry of rainfall-runoff and wastewater matrices. Some suspended and settleable solids may be present in runoff and wastewater and it has been recognized that phosphorus has an affinity to react with solid particles (Appan and Wang, 2000; Georgantas and Grigoropoulou, 2007). Therefore, the suspended/settleable solids in samples may serve as nuclei and promote the aggregation and precipitation of phosphorus on $AOCM_{pcc}$. It is also believed the high concentration of Ca^{2+} in runoff (25.45 mg/L) and wastewater matrix (51.32 mg/L) could also contribute to the enhancement of phosphate surface precipitation, in addition to those coming from dissolution of the solid $AOCM_{pcc}$. Visual MINTEQ ver. 2.61 has been used to predict the potential P-precipitates for $AOCM_{pcc}$ in all of the three matrices under both natural and phosphate spiked conditions. Solution conditions were based on the results from the final equilibrium state where 0.5 g of $AOCM_{pcc}$ were added to 40 mL working solutions of synthetic runoff, rainfall runoff and wastewater, respectively. The saturation index (SI) representing the tendency of a mineral will be dissolved or precipitated. It can be seen from Table 2-6 that most of the SIs are well above 0, which reinforce the occurrence of surface precipitation.

Contrary to $AOCM_{pcc}$, from Figure 2-7 and 2-9 it can be found that adsorption capacity of $AOCM_c$ and $AOCM_p$ severely decreased in rainfall-runoff and wastewater matrices as no major removal mechanism transition occurred. In their study of rainfall-runoff mental element speciation, Dean et al. (2005) detected that different anions and

cations were transported into the dissolved phase in urban rainfall-runoff. Besides PO_4^{3-}, the anions included NO_3^-, SO_4^{2-} and CO_3^{2-}. In this study, similar results were obtained as shown in Table 2-1. Since the presence of multi-anions, simultaneous adsorption may occur and cause direct competition for adsorption sites. Ma (2005) found SO_4^{2-} showed apparent competition on P adsorption. Here, SO_4^{2-} concentration in rainfall-runoff was found to be 10 mg/L, about 40 times more than that of synthetic runoff and an even higher SO_4^{2-} concentration (106 mg/L) was detected in wastewater samples. The result of competitive effects could be a dramatic decrease in the adsorption capacity of PO_4^{3-}. In addition, although the presence of Ca^{2+} could increase the phosphorus adsorption through formation of ternary complex (Sansalone and Ma, 2009), it was found the effect can only be significant in base conditions. Therefore, SO_4^{2-} competition should be a primary reason for weaker $AOCM_c$ and $AOCM_p$ isotherms in runoff and wastewater matrices.

Summary

This research investigated equilibria between aqueous phosphorus species (as total dissolved phosphorus, TDP) and aluminum oxide-based (AlOx) media consisting of three separate substrates; clayey soil, pumice and Portland cement concrete. Equilibrium was modeled as Freundlich isotherms for three matrices: rainfall-runoff, wastewater and de-ionized (DI) water as a surrogate runoff matrix. The pH of each aqueous matrix was 7.0.

When comparing the suite of media; results demonstrated that each AOCM exhibited significantly higher capacities than the corresponding UCM substrate in synthetic runoff matrix. With the exception of the concrete-based substrate the uncoated clay or pumice had relatively small equilibria capacity across the entire TDP

range from 0.05 to 50 mg/L in comparison to AOCM of the same substrate. This result supports the studies hypothesis that the inclusion of AlOx either as an admixture or coating will statistically significantly increase adsorption capacity. Previous studies have demonstrated ligand exchange as a mechanism for phosphate adsorption onto hydrous metal oxide surfaces. In addition to ligand exchange, results of this study indicate that additional mechanisms, for example surface precipitation for the concrete-based substrate ($AOCM_{pcc}$), occur. $AOCM_c$ and $AOCM_{pcc}$ both provided similar high equilibrium capacity as compared to $AOCM_p$. In constrast, the equilibrium capacity of the UCM_{pcc} dominated the uncoated clay and pumice substrates due to surface precipitation. The smaller media size range of 0.85 to 2.0 mm generated higher equilibrium capacity as compared to the 2.0 to 4.75 mm size range on a dry media mass basis; but the increase was not as quantitatively large as inclusion of AlOx to each substrate.

While a controlled reproducible DI surrogate matrix was utilized to compare isotherms for each AOCM and companion substrate; isotherm results from this surrogate matrix were compared to uncontrolled environmental rainfall-runoff and wastewater matrices. While the DI surrogate matrix generated the highest equilibrium capacity across the range of TDP concentrations examined for $AOCM_c$ and $AOCM_p$, this surrogate matrix generated the lowest equilibrium capacity for $AOCM_{pcc}$ as compared to the actual environmental matrices. Examining each AOCM type separately, the rainfall-runoff and wastewater matrices generated isotherms that were similar for each matrix across the range of concentrations examined. With ligand exchange as the primary adsorption mechanisms, the decreased equilibrium capacity of $AOCM_c$ and $AOCM_p$

loaded by rainfall-runoff and wastewater matrices can be attributed to multiple anion competition, such as SO_4^{2-} competing with phosphate for media exchange sites. In contrast, $AOCM_{pcc}$ capacity combines the dominant mechanism of surface precipitation, ternary complexation with Ca^{2+} (Sansalone and Ma 2009) and ligand exchange to generate nearly identical equilibrium capacity across the entire TDP concentration range which was significantly greater than the surrogate DI matrix.

Nomenclature

AOCM: Alumina oxide coated media

$AOCM_c$: Alumina oxide coated media with clay as raw substrate

$AOCM_p$: Alumina oxide coated media with pumice as raw substrate

$AOCM_{pcc}$: Alumina oxide media with Portland cement concrete as raw substrate

AlOx: Aluminum oxide

b: The Langmuir constant (L/mg)

C: The concentration in the fluid phase (mg/L)

C_0: The initial phosphate concentration (mg/L)

C_e: The phosphate concentration at equilibrium (mg/L)

DI water: De-ionized water

DP: Dissolved phosphorus

K_F: The Freundlich constant

N(b'): The site energy distribution

n: The Freundlich exponent

pH_{pzc}: pH of point of zero charge

q: The amount adsorbed (mg/g)

q_e: The amount of adsorption at equilibrium (mg/g)

q_m: The maximum adsorbed phase concentration (mg/g)

R^2: Coefficient of determination

SI: Saturation index

SSA: Specific surface area (m^2/g)

T Temperature

V: The volume of the solution (L);

W: The weight of adsorbent used (g);

UCM: Uncoated media

UCM_c: Uncoated media with clay as raw substrate

UCM_p: Uncoated media with pumice as raw substrate

UCM_{pcc}: Uncoated media with Portland cement concrete as raw substrate

ρ_s: Specific gravity

Table 2-1. Water chemistry of experimental matrix

Matrix		Synthetic runoff	Filtered rainfall-runoff (Event on 05/16/08)	Wastewater (Secondary effluent)
pH		7.00 ± 0.05	7.11 ± 0.07	7.14 ± 0.10
Conductivity [µs/cm]		1525 ± 37	218 ± 12	780 ± 14
Turbidity [NTU]		2.75 ± 0.56	2.80 ± 1.02	4.40 ± 0.64
Alkalinity [mg/L] as $CaCO_3$		7 ± 1	74 ± 2	77 ± 3
Ionic Strength [M]		0.010 ± 0.002	0.004 ± 0.002	0.012 ± 0.003
DOC [mg/L]		0.3 ± 0.1	28.9 ± 3.6	10.3 ± 2.2
Cation [mg/L]	K^{+} [a]	388 ± 2	4.68 ± 0.07	12.83 ± 0.14
	Ca^{2+}	0.021 ± 0.003	25.45 ± 1.26	51.32 ± 1.90
	Mg^{2+}		3.04 ± 0.12	30.56 ± 1.07
	Pb^{2+}		0.018 ± 0.036	0.098 ± 0.044
	Cu^{2+}		0.049 ± 0.02	1.16 ± 0.03
	Zn^{2+}	BML[b]	0.107 ± 0.15	14.89 ± 0.33
	Cr^{2+}		0.673 ± 0.013	4.01 ± 0.04
	Mn^{2+}		0.127 ± 0.001	0.734 ± 0.015
	Al^{3+}		0.212 ± 0.032	5.56 ± 0.090
	Fe^{3+}		0.128 ± 0.038	6.34 ± 0.11
Sum of cation charge [mmol]		9.95	1.71	7.10
Anion [mg/L]	NO_3^--N	0.81 ± 0.13	3.08 ± 0.15	3.14 ± 0.17
	SO_4^{2-}	0.23 ± 0.09	10.06 ± 1.08	106 ± 1
	Cl^- [a]	363 ± 13	8.05 ± 0.15	146 ± 1
	HCO_3^-	4.2 ± 0.6	45.1 ± 1.2	46.9 ± 1.7
	PO_4^{3-}	0 ~ 50 (n=8)	1.13 ± 0.17	9.15 ± 0.43
Sum of anion charge[b] [mmol]		10.36	1.43	7.46

* Data are mean ± standard deviation

[a] 0.01M KCl was used to adjust the ionic strength of synthetic runoff.

[b] In synthetic runoff, PO_4^{3-} was added as KH_2PO_4 and not included in the charge summation.

Table 2-2. Major composition of raw substrates

Raw substrate	Major compositions
Clay	SiO_2 (48 – 70%); FeOOH (9 – 17 %); $CaCO_3$ (3 – 6%) *(Measured by XRD analysis)*
Portland cement concrete	C-S-H (50 – 60 %); $Ca(OH)_2$ (20-25%) CSA (Calcium sulfoaluminates, 15-20%) (Mehta, 1987)
Pumice	SiO_2 (72%); Al_2O_3 (12%); K2O (5%); Fe_2O_3 (2%) *(Panuccio et al., J. Environ. Manage., 2009)*

Table 2-3. Media characteristics

Media	Substrate	Size [mm]	Specific gravity	pH_{pzc}
$AOCM_c$	Clay	0.85 – 2.0 2.0 – 4.75	2.29 ± 0.04	4.61 ± 0.06
UCM_c	Clay	0.85 – 2.0 2.0 – 4.75	2.31 ± 0.05	4.20 ± 0.08
$AOCM_{pcc}$	Concrete	0.85 – 2.0 2.0 - 4.75	2.67 ± 0.04	11.84 ± 0.16
UCM_{pcc}	Concrete	0.85 – 2.0 2.0 - 4.75	2.67 ± 0.03	11.98 ± 0.12
$AOCM_p$	Pumice	2.0 - 4.75	2.27 ± 0.01	4.59 ± 0.10
UCM_p	Pumice	2.0 - 4.75	2.29 ± 0.02	4.61 ± 0.10

pH_{pzc} = pH of point of zero charge
Data here are mean ± standard deviation (n = 3)

Table 2-4. Freundlich model parameters in synthetic runoff matrix

Media	Size [mm]	K_F	n
$AOCM_c$	0.85 – 2.0	1.35	0.33
	2.0 - 4.75	1.05	0.36
$AOCM_{pcc}$	0.85 – 2.0	1.32	0.58
	2.0 - 4.75	0.89	0.39
$AOCM_p$	2.0 - 4.75	0.39	0.26
UCM_c	0.85 – 2.0	0.018	0.79
	2.0 – 4.75	0.012	0.86
UCM_{pcc}	0.85 – 2.0	0.52	0.53
	2.0 – 4.75	0.49	0.52
UCM_p	2.0 – 4.75	0.012	0.84

*All R^2 values between measured and modeled exceed 0.96.

Table 2-5. Freundlich model parameters in rainfall-runoff and wastewater matrix

Media [mm]	Rainfall-runoff K_F	Rainfall-runoff n	Wastewater K_F	Wastewater n
$AOCM_c$ (0.85 -2.0)	0.32	0.43	0.35	0.31
$AOCM_c$ (2.0 – 4.75)	0.25	0.41	0.33	0.23
$AOCM_p$ (2.0 – 4.75)	0.16	0.33	0.17	0.20
$AOCM_{pcc}$ (0.85 – 2)	998	2.51	995	1.84
$AOCM_{pcc}$ (2 – 4.75)	312	2.29	109	1.93

*All R^2 values between measured and modeled exceed 0.95.

Table 2-6. Predicted Saturation Index (SI) for $AOCM_{pcc}$ in different matrices

Potential precipitates	Actual aqueous matrices* and phosphate spiked matrices [mg/L]								
	Synthetic runoff			Rainfall runoff			Wastewater		
	0*	25	50	1.13*	25	50	9.15*	25	50
$Ca_3(PO_4)_2$ (am1)		2.16	2.72	-0.45	2.19	2.73	1.49	2.33	2.93
$Ca_3(PO_4)_2$ (am2)		4.93	5.49	2.33	4.96	5.50	4.26	5.10	5.68
$Ca_3(PO_4)_2$ (beta)		6.02	6.58	3.42	6.05	6.59	5.35	6.19	6.78
$Ca_4(HPO_4)_3{:}3H_2O$	NA	3.20	4.07	-0.32	3.67	4.51	2.80	4.07	4.94
Hydroxyapatite [HAP, $Ca_5(PO_4)_3OH$]		19.59	20.39	15.29	19.22	20.00	17.98	19.23	20.09

SI = logIAP-logK_{sp}:
-1 < SI < 0, saturated; SI< -1, undersaturated; SI > 0 supersaturated.

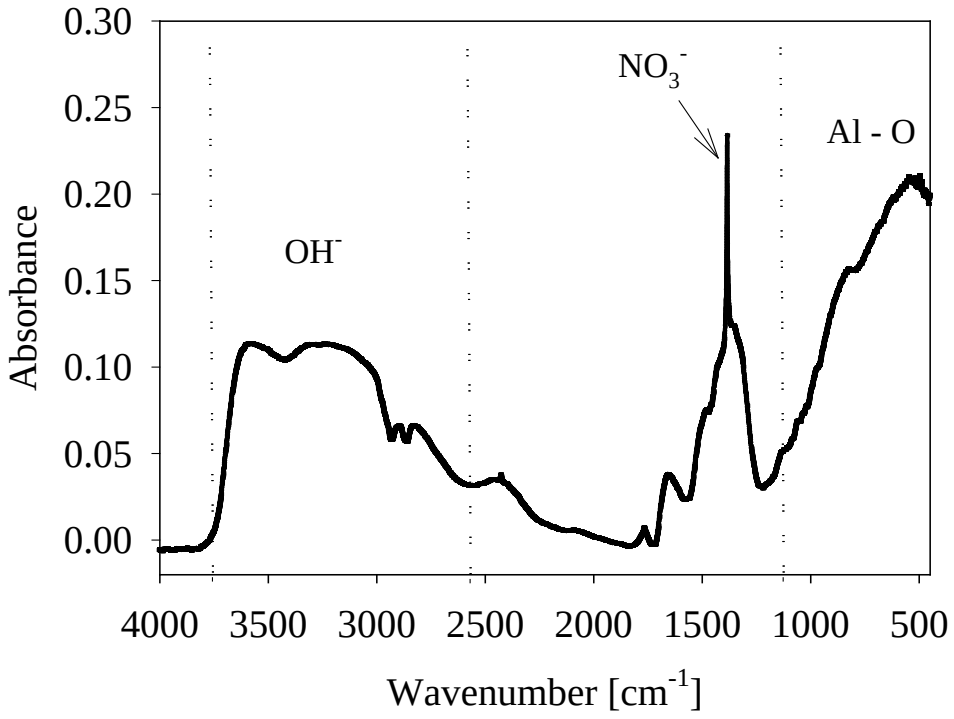

Figure 2-1. FTIR spectra of media coating.

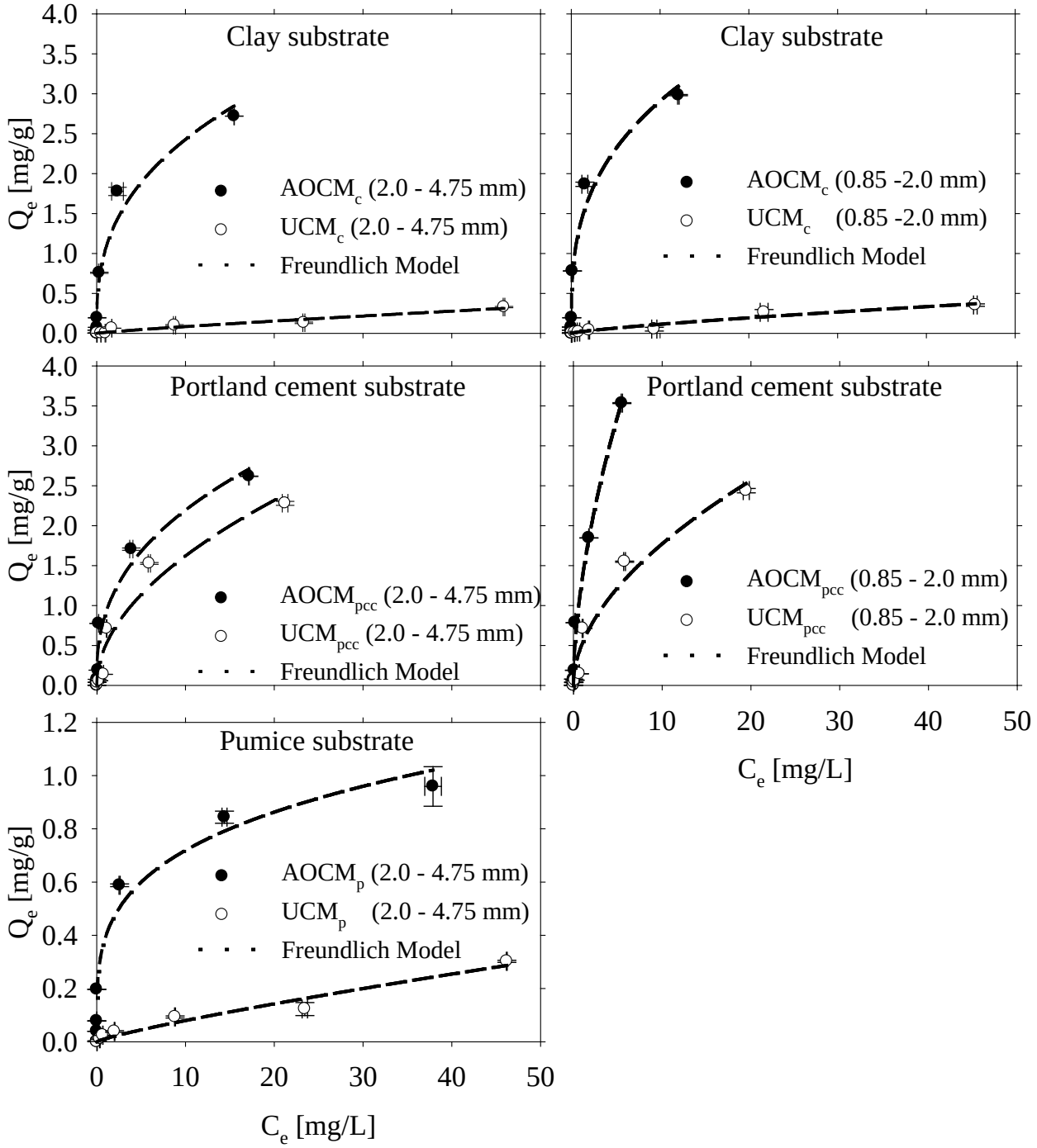

Figure 2-2. Comparison of AOCM and UCM in synthetic runoff matrix.

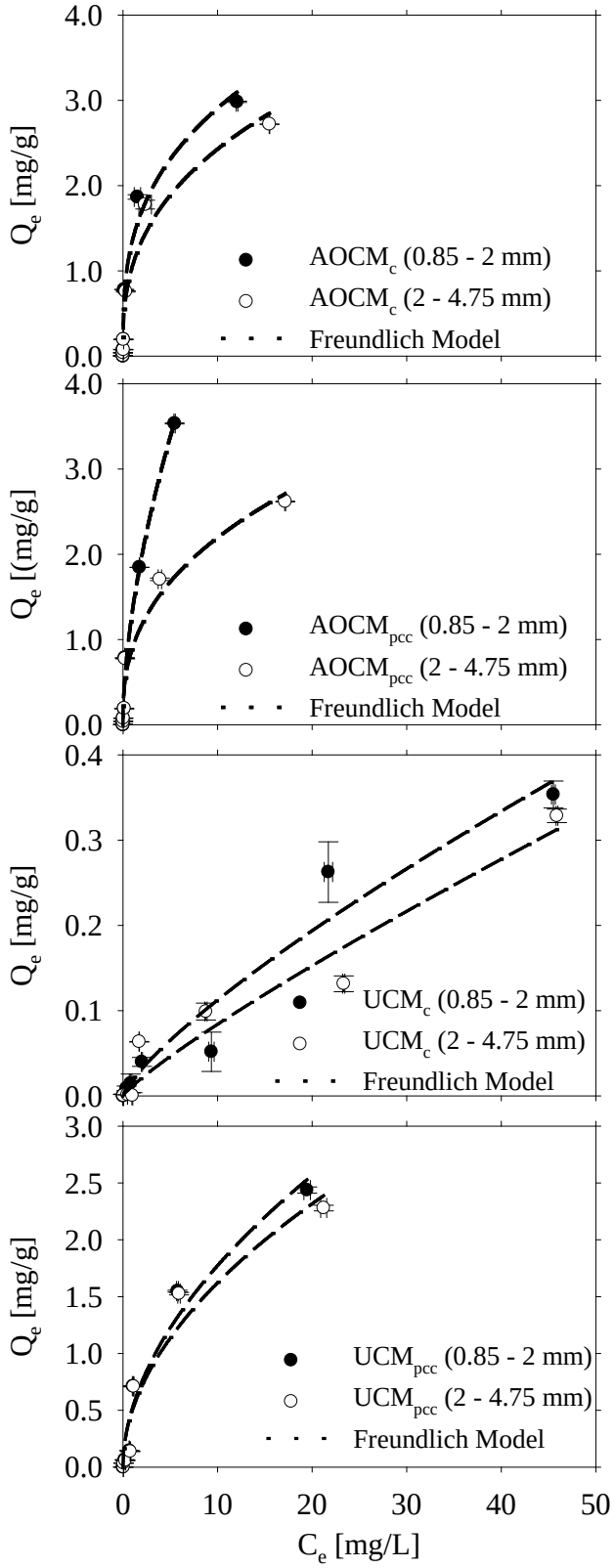

Figure 2-3. Comparison of different media size in synthetic runoff matrix

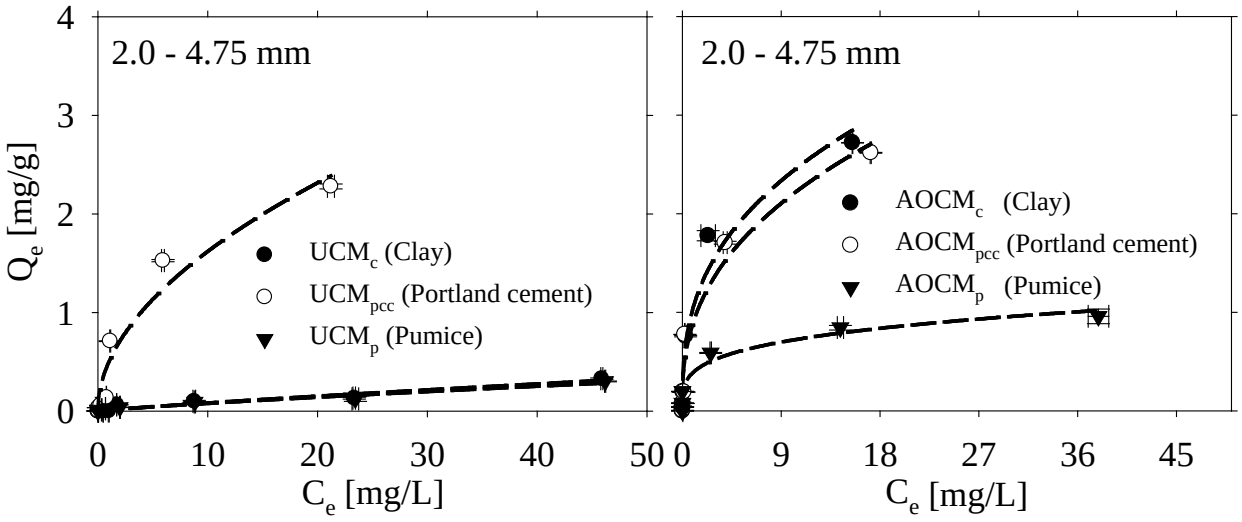

Figure 2-4. Comparison of different AOCM and UCM in synthetic runoff matrix.

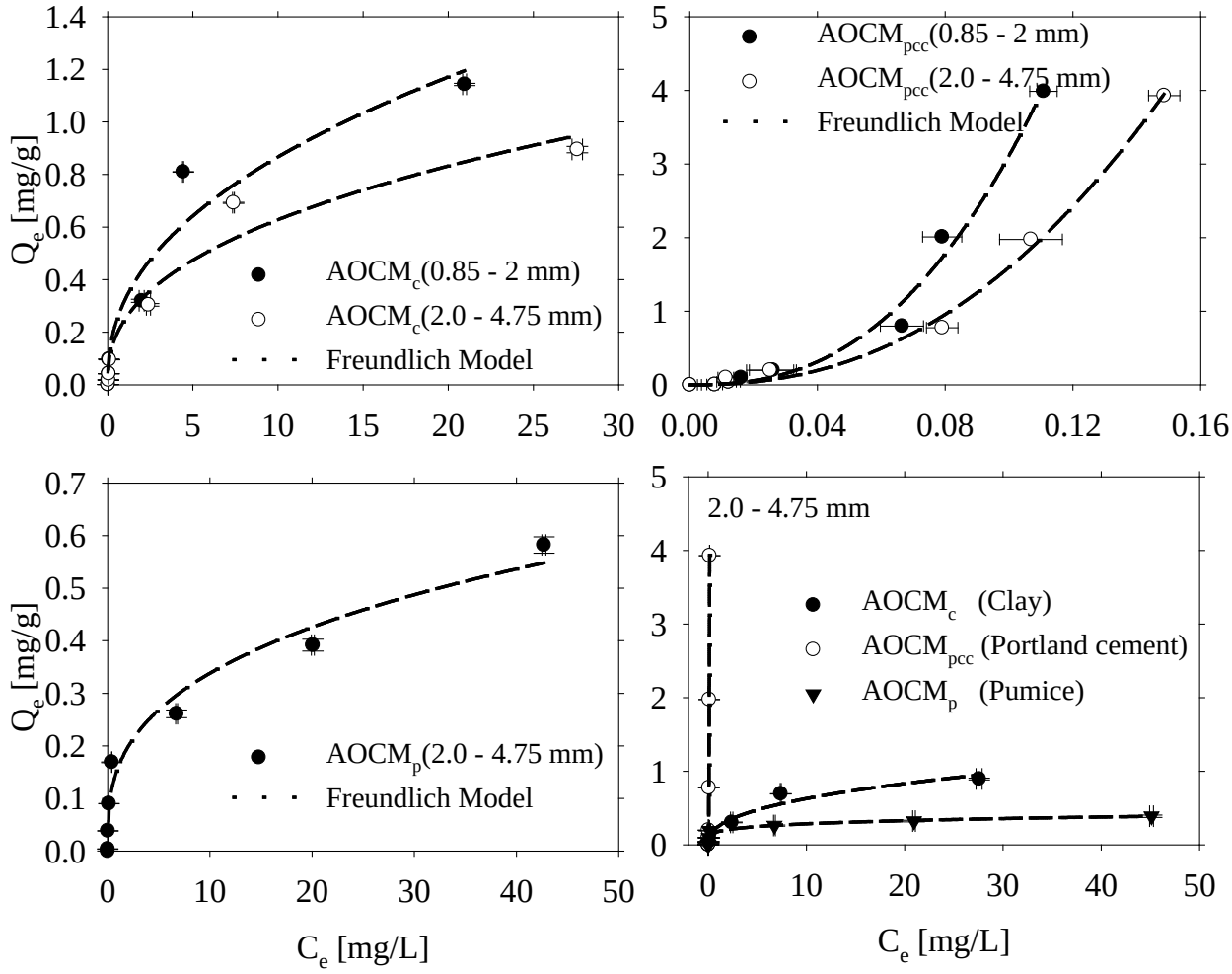

Figure 2-5. Comparison of AOCM in rainfall-runoff matrix.

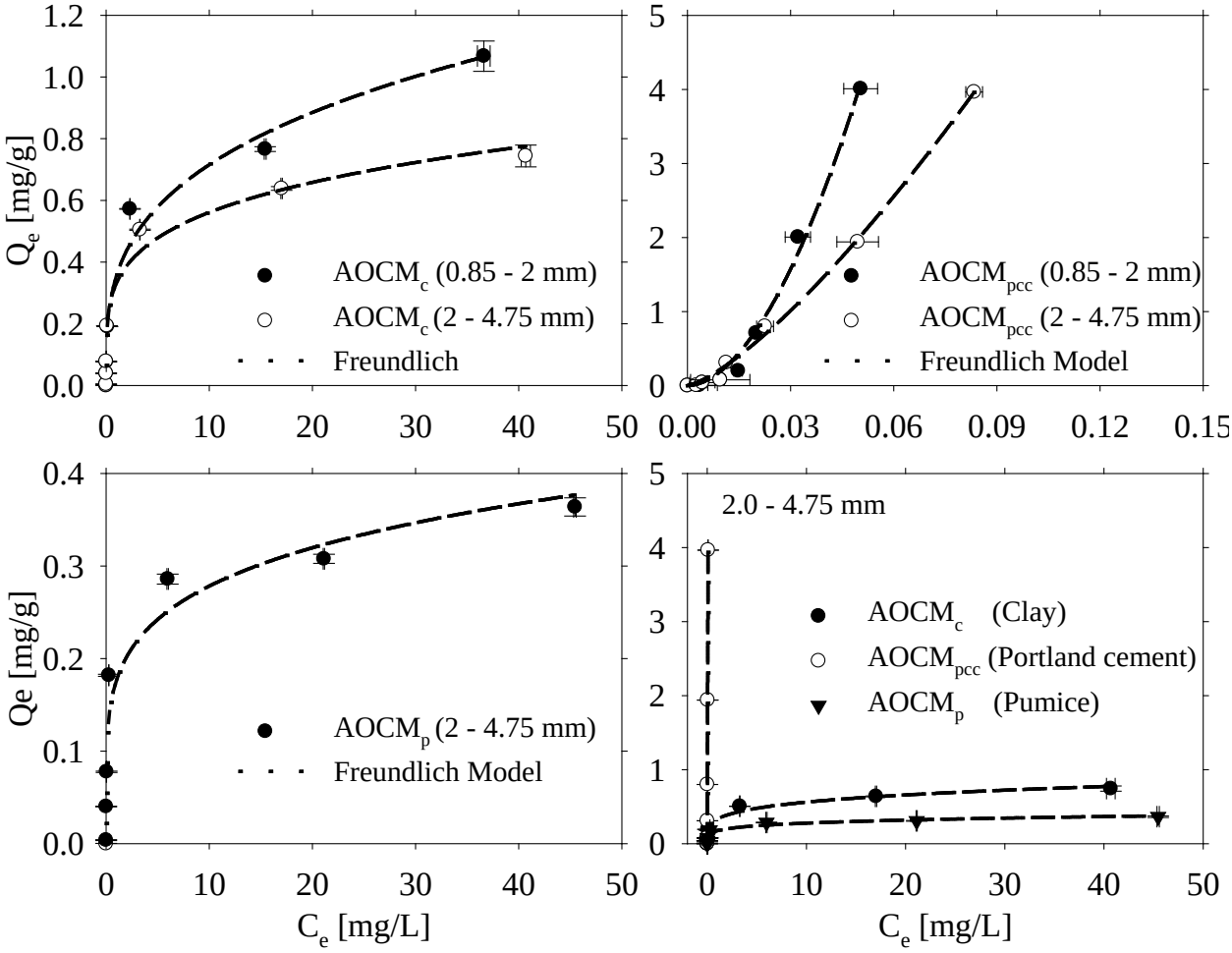

Figure 2-6. Comparison of AOCM in wastewater matrix.

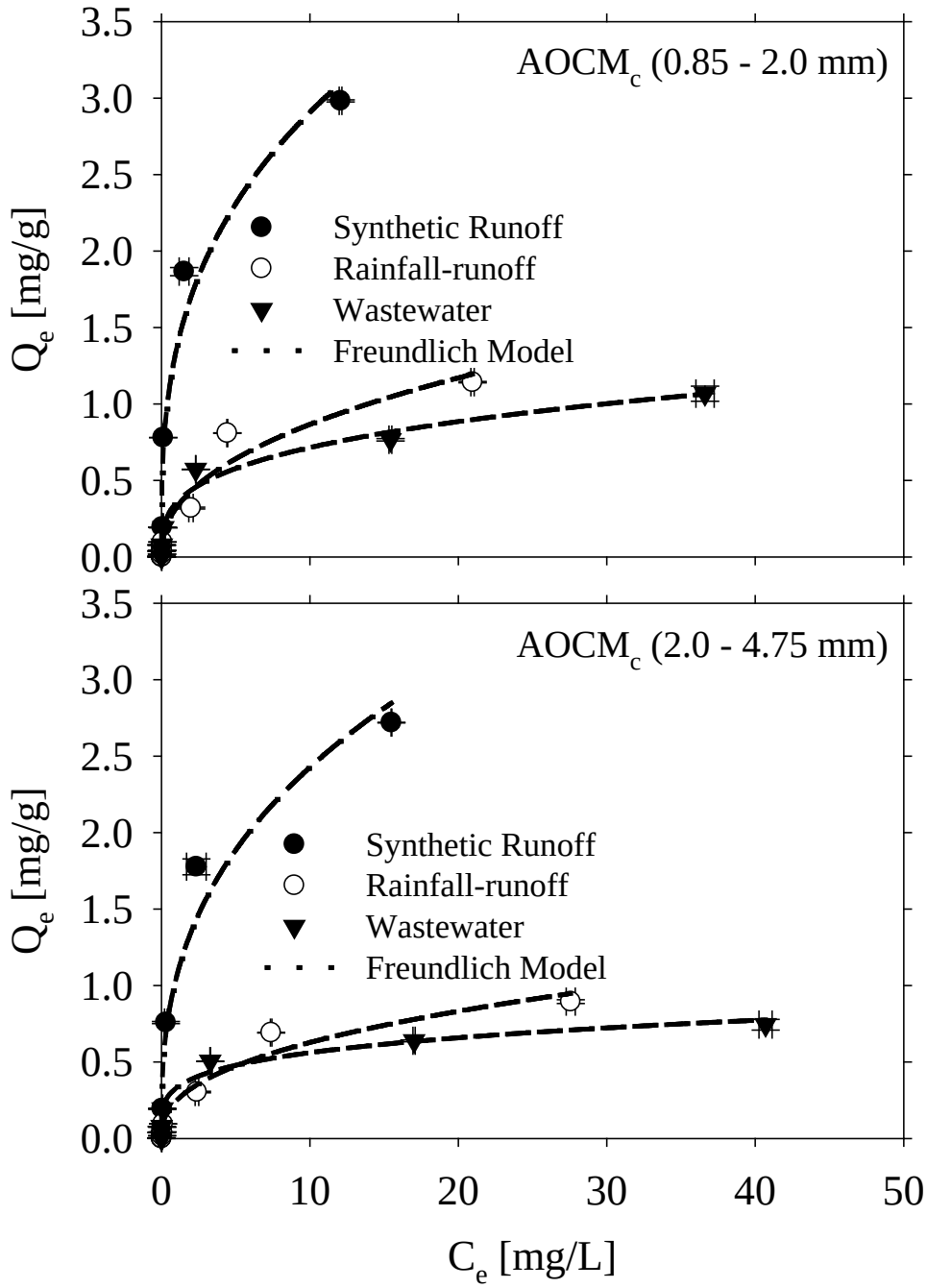

Figure 2-7. Comparison of $AOCM_c$ in synthetic-runoff, rainfall runoff and wastewater matrices.

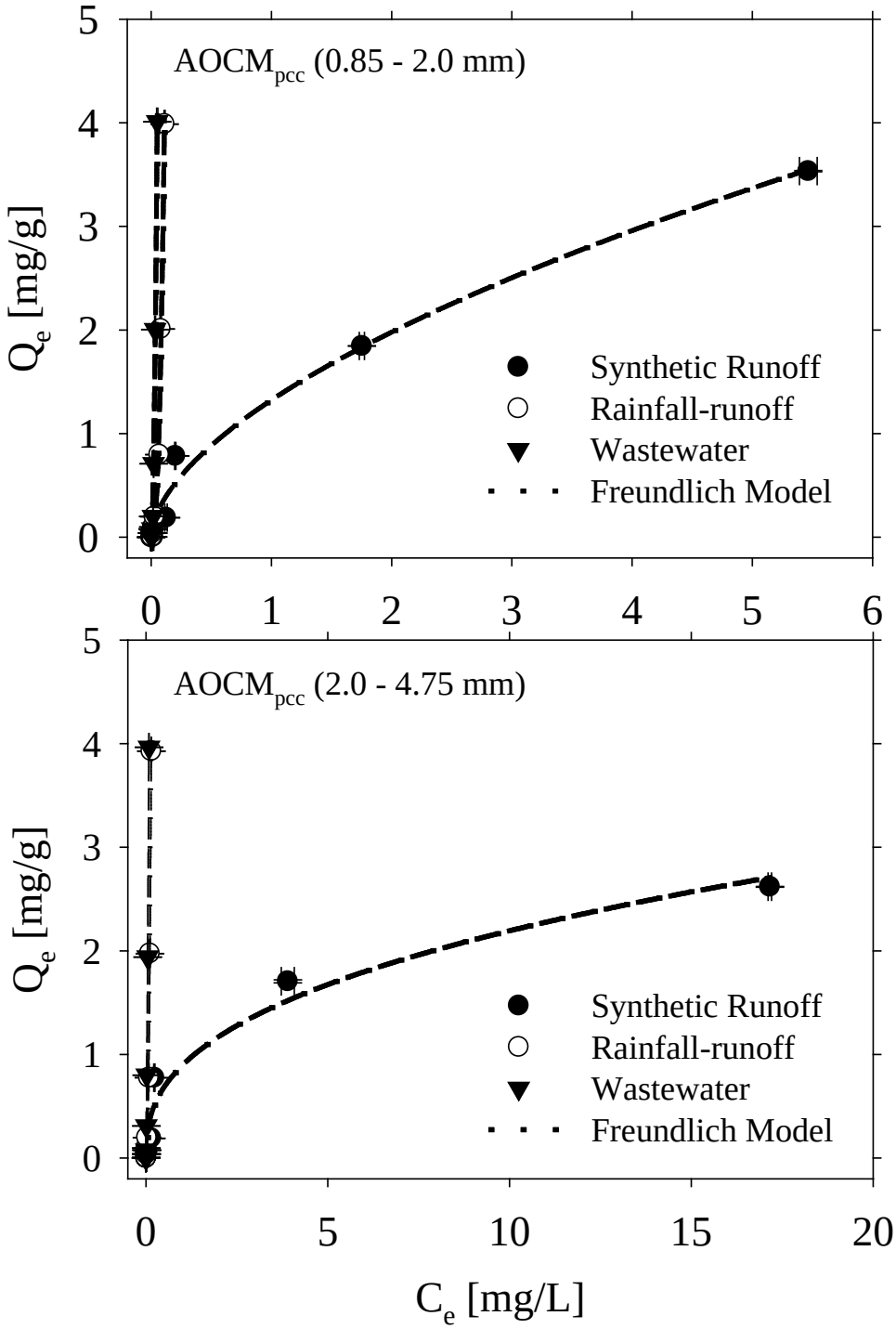

Figure 2-8. Comparison of $AOCM_{pcc}$ in synthetic-runoff, rainfall runoff and wastewater matrices.

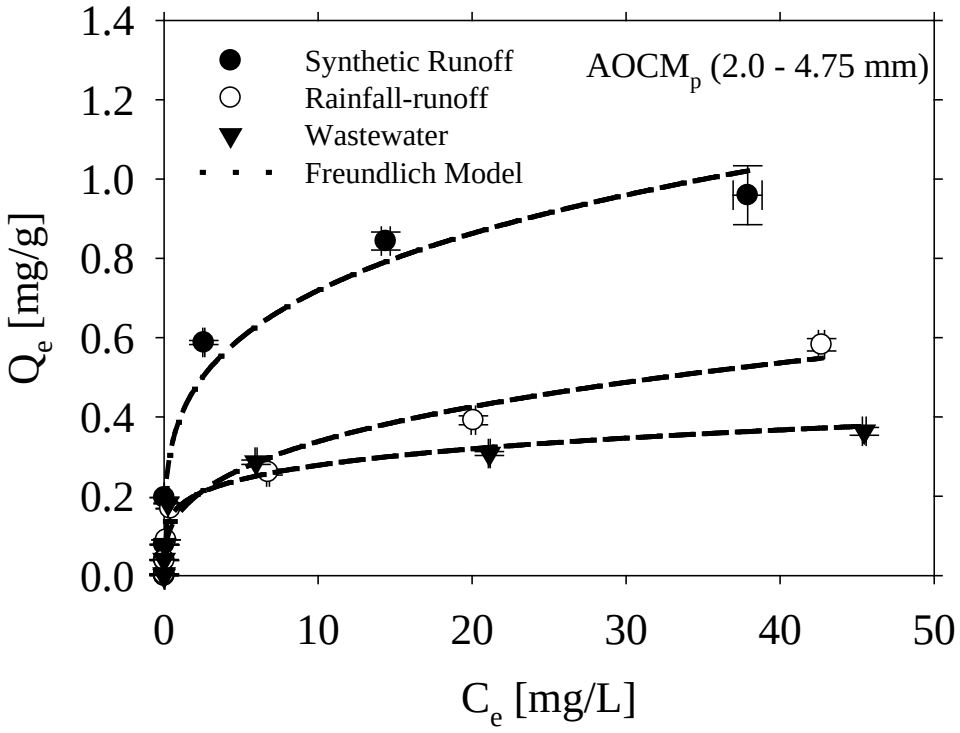

Figure 2- 9. Comparison of $AOCM_p$ in synthetic-runoff, rainfall runoff and wastewater matrices.

CHAPTER 3
BATCH EQUILIBRIA BETWEEN AQUEOUS PHOSPHORUS AND GRANULAR FILTER MATERIALS

Background

It has been well documented that increased phosphorus (P) concentrations in water bodies is a serious pollution concern since P is one of the major limiting factors responsible for eutrophication (U.S. Geological Survey, 1999; Markris et al., 2004; Oleszkiewicz and Barnard, 2006; Endards and Withers, 2007). Consequently, there is increasing pressure and changes in water discharge regulation and legislation for lowering phosphorus concentration in surface water as well as phosphorus total maximum daily load (TMDL) (Read and Fernandes, 2003; USEPA, 2000a; Havens and Schelske, 2001; Walker, 2003). For instance, regulation for P discharge can be as low as 50 µg/L for wastewater and concentrations in excess of 30 µg/L have been established as an indication of excessive nutrients enrichment in lakes and other confined water bodies (Genz et al., 2004; Oguz, 2005). Industrial and municipal wastewater, agriculture and animal feeding operations are well-known phosphorus sources. In recent years, it has also been recognized that urban rainfall-runoff can transport a large amount of nutrients, including phosphorus and nitrogen and severely impair the receiving waters (USEPA, 2002).

Phosphorus occurs in the forms of both dissolved P (DP) and particulate P (PP) and mainly exists as phosphate in aqua-systems and secondary wastewater effluents (Wei et al., 2008; Ma, 2005; Chitrakar et al., 2006). P can be generated from both point sources like domestic and industrial discharge and diffuse source such as urban rainfall runoff. P can be effectively treated via settling and filtration, chemical precipitation, biological method and constructed wetland. However, these technologies are either

more effective for PP removal or constrained from diffuse sources control. For example, the traditional chemical coagulants and biological methods suffer the drawbacks of considerable capital investment, maintenance cost for infrastructure, reagents and sludge disposal.

A feasible process for P control from diffuse sources is adsorptive filtration with employment of low-cost filter media. Diverse solids with regarding to P removal capacity have been tested and evaluated, including natural materials, industrial by-product/waste, active filter substrates, engineered media etc. To exempt form a tedious enumeration here, the author summarizes the recent studies in Table 3-1.

Generally P is bound to the media as a result of adsorption and precipitation reactions with Ca, Al and Fe in the media substrate and the P adsorption capacity of a material represents a central parameter for comparing and selecting candidate materials to be used as P removal media (Seo et al., 2005). However, although lots of materials have been tested, there are still some media applications without proper evaluation and suffering a low efficiency. Moreover, although lot of quantitative information of various adsorbents is available in literature, comparisons and material selections can still be problematic. One reason is that usually these media were tested under different experimental conditions and thus lost the equal base. Even within comparable laboratory control, selections are still not straightforward due to the lack of proper quantitative parameters. The P adsorption capacity is frequently estimated using Langmuir or Freundlich isotherm equations because of the simple form and satisfactory goodness of fit with the experimental data. However, it has been demonstrated that the Langmuir equation can lead to biased and unrealistic estimates of the adsorption

parameters (Seo et al., 2005). As a non-linear adsorption isotherm, Freundlich model has been favored due to the mathematical simplicity as well as the characteristic of heterogeneous surface of the media materials and the diversity of sorption mechanisms. But some researchers have noticed that neither of the two Freundlich parameters can independently represent the media capacity and comparisons among different adsorbents must be taken with caution due to the hidden complexities of K_F (Bowman, 1981, 1982; Chen et al., 1999).

Furthermore, the P adsorption capacity as the first and most important criteria in media selection is intuitive and indubitable; but it is not the only requirement that needs to be satisfied. In addition to P removal capability, the candidate media should also be low cost with steady supply and not contain or release hazardous pollutants into environment. While economical efficiency has drawn enough attention since a variety of low cost materials and industrial by-product/waste are investigated as P adsorbents (Table 3-1), potential environment contaminations caused by the media materials are frequently overlooked.

Objectives

In this paper, seven granular filter materials, including Tire crumb B&G (2 gradations), Expanded shale (2 gradations), Bioretention soil media, Zeolite-Perlite-GAC, Activated alumina, Fe-coated perlite and clay based Aluminum Oxide Coated Media ($AOCM_c$) were chosen and tested through equilibrium isotherm approach. Studies are carried out to validate the following hypotheses: Under consistent surrogate matrix and identical experimental conditions, the suite of media examined can exhibit large variance in aspect of P removal capacity, which can be quantitatively characterized by utilization of Freunlich model. Furthermore, media comparison can be

facilitated by a newly defined unified sorption variable K_u developed by Chen et al. (1999). Finally, deployment of some high capacity media may be constrained by unfavorable metal leaching.

Materials and Methods

Media

$AOCM_c$ (Aluminum Oxide Coated Media with expanded clay as substrate)

An engineered media, $AOCM_c$ was developed and tested in this study. Bentonite with mineralogical composition of sodium hydrated aluminosilicate was purchased from Halliburton Energy Services, Inc. The raw substrate was then prepared through procedures of mixing with explosive reagents and water, sintering in kiln, crushing and sieving, acid washing, DI rinsing and drying. $AOCM_c$ was prepared by applying aluminum oxide as surface coating. Stock solution of 1M Al (III) was prepared by dissolving $Al(NO_3)_3 \cdot 9H_2O$ in DI water. Al (III) solution was added to the raw substrate and the mixture was then put in the oven at a temperature around 200 ^oC for at least 24 hours. Later, the aluminum coated sorbents was washed with DI water to remove the surficial fine materials. Then the sorbent was dried at 105 ^oC and stored in polypropylene bottles for further use. The effective gradation utilized here are 0.85 to 2 mm

Activated alumina

Activated alumina was purchased as a commercial filter media from Schoofs Inc., CA, U. S. A. The alumina is primarily composed of Al_2O_3 (91.5%), SiO_2 (0.02%), Fe_2O_3 (0.03%) and Na_2O (0.35%). The particle size is within the range of 1.4 – 2.41 mm.

Bioretention soil media

Bioretention soil media tested in this study is commercial mixtures for Prince George's County, Maryland with P-index of 25. Soil mixtures include sand, loamy sand, and sandy loam.

Expanded shale

Expanded shale is another commercial filter media. It is a porous material and usually manufactured by firing shale at a high temperature (2000 °F, Forbes et al., 2004). Little research has been undertaken to examine the applicability of expanded shale for phosphorus removal. In this study, the expanded shale was sorted by two size gradation: 2 – 10 mm and 0.45 – 4.5 mm.

Fe-coated perlite

Fe-coated perlite used in this research was collected from Imbrium Systems, Inc. Ferric oxide was coated on perlite to develop a light weighted engineered media. The size ranges from 0.3 to 0.85 mm.

Tire crumb B&G

Tire crumb is a waste material and has been historically stockpiled due to limited economic and environmental feasibility of tire regeneration. As part of resources recovery with sustainable implication, tire crumb B&G has been used as construction materials and roadbed support and fills (Yoon et al., 2006; Liu et al., 2000). Lisi et al. (2004) also studied the use of granulated tires as a subsurface drainage layer to mitigate nutrient leaching. However, more information and tests are needed to evaluate the potential of tire crumb as a phosphorus adsorptive material. In this study, green roof mixture of mainly tire crumb B&G was tested to assess its phosphorus removal ability with two gradations: 0.5 – 4.75 mm and 0.85 – 10 mm.

Zeolite-Perlite-GAC

Zeolite-Perlite-GAC is a commercial mixture of zeolite, perlite and granulated activated carbon with the volume ratio of … and size range of 2.29 – 9.65 mm.
A brief description of the media utilized in this study is summarized in Table 3-2.

Physical Characteristics

Specific surface area measurements were conducted using a modified ethylene glycol monoethyl ether method described by Sansalone et al. (1998). Surface charge for the tested media was measured using a potentiometric titration methodology described by Van Raij and Peech (1972). pH_{pzc} was then calculated by linearly interpolating between the last positive and first negative surface charge values. Specific gravity (ρ_s) measurement utilized a helium gas pycnometer.

Chemicals

A phosphorus stock solution was prepared by dissolving anhydrous potassium dihydrogen orthophosphate (KH_2PO_4) powder (Analytical reagent grade, Fisher Scientific) into D.I. water. The stock solution was calibrated to 100 mg/L and 1000 mg/L concentrations, which were utilized as standard solutions as necessary.

Batch Adsorption Study

Batch studies were performed to examine phosphate adsorption onto the different media. 40 mL of synthetic runoff dosed with predetermined amount of phosphate (0, 0.05, 0.5, 1.0, 2.5, 10, 25 and 50 mg/L) and 0.5 g of the tested media were agitated on a horizontal bench shaker at a rate of 100 rpm allowing adsorption to take place at 20°C until equilibrium reached, usually 24 hr. Ionic strength was fixed at 0.01 M using KCl and solution pH was adjusted to 7 at the beginning of experiments by dropwise addition of HCl or NaOH. Measurements of pH were carried out using a multi-meter (Orion 290A

combination electrode), which was preliminary calibrated using a 3-point calibration curve with reference units at a pH of 4, 7, and 10.

Phosphorus Analysis

After adsorption equilibrium reached, samples were taken and filtered through 0.45µm syringe filter. The total dissolved phosphorus concentration in the filtrate was measured by HACH DR/5000 Spectrophotometer using PhosVer 3 Ascorbic Acid Method (Standard Method 1998). All measurements were duplicated and high repeatability was assured by controlling experimental error within ± 5%. The amount of adsorbate that was adsorbed on the adsorbent q_e [mg/g], was then calculated from the difference between the initial and equilibrium solute concentrations.

$$q_e = \frac{(C_0 - C_e)V}{W} \quad (1)$$

C_0 and C_e are the initial and equilibrium solute concentrations [mg/L], respectively; V the volume of the solution [L] and W the dry mass of the adsorbent [g].

Metal Leaching Tests

Metal leaching experiments were carried out to verify if the treated water quality may be contaminated with soluble metals leaching from the treatment media materials during adsorption. The possibility of metal leaching was examined by mixing deionized water samples with each of the media tested, mostly mimicking the experimental conditions in batch equilibrium study, followed by analysis of the water. Specifically, 0.5 g of each media was added to 40 mL of deionized water in a 50 mL centrifuge tube and then shaken for 24 hours at 100 rpm at 20 °C. Ionic strength was maintained at 0.01 M with KCl. Water samples were then filtered into a sample vial and acidified prior to analysis. The samples were analyzed for dissolved metal content using ICP

instrumentation (Perkin-Elmer Plasma 3200). Similar experimental approach was reported in the literature by Sibrell et al. (2009).

The Freundlich Isotherm and Unified Sorption Variable, K_u

Equilibrium isotherm is a graphical representation showing the relationship between the amount adsorbed by a unit weight of adsorbent and the amount of adsorbate remaining at equilibrium. The operating curve of an equilibrium isotherm model represents an asymptotic limit as a function of concentration for adsorption capacity of a given soil or media system. An isotherm model can be represented by a number of mathematical forms that can be combined kinetics and breakthrough representations. As the isotherm maps the distribution of adsorbate between the liquid and solid phases, a critical parameter is the concentration ratio of solid phase to aqueous phase. Usually, this ratio is described by partitioning coefficient, K_d. Specifically to this study, K_d can be represented as:

$$K_d = \frac{q_e}{C_e} \tag{2}$$

where K_d is the partitioning coefficient [L/g]; q_e is the concentration of solids adsorbed on the solid phase [mg/g] and C_e is the concentration of P in the aqueous phase at equilibrium [mg/L].

The partitioning process can be fundamentally understood from a thermodynamics point of view, such as free energy and chemical potential, and be expressed on a mole fraction basis as following (Schwarzenbach, 2002);

$$K_d = \exp[\frac{-\Delta G}{R \bullet T}] \tag{3}$$

ΔG is the free energy transfer between two phases; R is the general gas constant; T is the absolute temperature.

When a linear isotherm is assumed, K_d is conastant. However, in most of the media adsorption system, the heterogeneous composition and structure of the media substances and the potential of multiple sorption mechanism contributes to the variation of ΔG from site to site. Consequently, linear isotherm is inadequate and the nonlinear Freundlich isotherm equation is commonly used to model heterogeneous adsorbent surfaces (Coles and Yong, 2006).

The equation for Freundlich isotherm is:

$$q_e = K_F C_e^{\,n} \tag{4}$$

K_F is the Freundlich constant and n is the adsorption intensity and depends on the linearity of the isotherm, usually between 0 and 1. Thus K_F represents the sorption capacity of the media when the equilibrium solution concentration is 1.0 mg/L. When n = 1, the isotherm becomes linear and $K_F = K_d$.

The nonlinearity of Freundlich isotherm accommodates the heterogeneous composition and structure of different media materials and diverse sorption mechanisms, resulting in a widely application in many sorption systems (Chitrakar et al., 2006; Kim et al., 2006; Mortula et al., 2007; Wei, et al., 2008; Sibrell et al., 2009). Usually the mathematical modeling facilitates quantitative comparison among different media with model parameters and such comparison and evaluation are often imperative when a variety of media are available. However, in Freundlich isotherm the units of K_F depend on the value of n, whenever n values are different among media, the K_F values are not directly comparable. To address this limitation and make the model parameter

more amenable to media comparison, Cheng et al (1999) proposed a unified sorption variable, K_u, which has the same units as K_d.

The expression of K_u was derived as following:

$$K_F C_e^{\,n} = K_u C_e \tag{5}$$

$$K_u = K_F C_e^{\,n} / C_e = K_F C_e^{\,(n-1)} \tag{6}$$

If C_e has the unit of mg/L and q_e of mg/g as in this study, then the unit of K_u is g/L. Actually in contrast to linear isotherm system where the partitioning coefficient of sorbate between the aqueous and solid phase is a constant, K_u represents the distribution of the coefficients in nonlinear system. Plot of K_u vs C_0 (or C_e) can be a instructive illustration of the dynamic mass transfer of the sorbate between the two phases and provide a more reliable and predictive estimation of media capacity.

Additionally, single-point adsorption isotherm approach is frequently employed in researches (Gao et al., 2004; Penn et al., 2005; Raposo et al., 2009; Karathanasis Shumaker, 2009). However, Eq (6) clearly demonstrates that partitioning coefficient is a function of equilibrium concentration and a single-point isotherm can only represent one point of the whole distribution. Moreover, real situations such as rainfall-runoff events are dynamic processes that exhibit changes not only in constituent concentration (can vary by 1 order of magnitude) but also the speciation and partitioning. In that case, partitioning coefficient is also a function of the immediate environment chemistry.

Results

Physical Characteristics

Table 3-2 summarizes the physical properties of all the media utilized in this study. Two size gradations of expanded shale and tire crumb B&G were tested. Bioretention

soil media has the widest size range, partially due to the miscellaneous constitutes of soil samples. The high specific surface area of activated alumina and $AOCM_c$ should be ascribed to the highly porous structure of alumina and the presence of GAC contributes to the high SSA of Zeolite-Perlite-GAC. The third highest SSA of Fe-coated perlite mostly stems from the fine particle sizes (0.35 -0.85). The variety of specific gravity reflects the diverse materials that constitute the media. Also, pH_{pzc} ranges widely from 4.61 to 9.84.

P Removal Efficiency and Sorption Isotherm

The percent of P removed based on different initial P concentrations is depicted in Figure 3-1. The initial DP (dissolved phosphorus) concentration varied from 0.05 to 10 mg/L. It can be seen generally the percent removed decreased with the increase of initial P concentrations, indicating saturation of the media sorption capacity. However, activated alumina and Fe-coated perlite maintained a removal efficiency of more than 90% within the tested concentration range and $AOCM_c$ also achieved more than 70% removal at C_0 of 50 mg/L, exhibiting high capability with respect to P removal.

Futhermore, P removal efficiency was presented in the form of mass of P removed per media mass [mg/g] as a function of the equilibrium concentration of P in the aqueous phase and the Freundlich equation was applied to model the sorption isotherms. Figure 3-2 compares the performance of two size gradations of tire crumb B&G and expanded shale. It can be found that tire crumb B&G b and expanded shale b showed better capacities, corresponding to a smaller particle size and higher SSA. Therefore, only tire crumb B&G b and expanded shale b were plotted in Figure 3-3, which illustrates the comparison of sorption capacities among all the media tested in this study. It is easily noticed that in Figure 3-3, the eight filter media can be divided into

two groups according to the P removal capacity. Activated alumina, Fe-coated perlite and $AOCM_c$ constituted one group whose capability of P sorption was far superior to those of the rest. Especially for activated alumina and Fe-coated perlite, the isotherm profiles are almost parallel with the Q_e axis within the concentration range used in this study. On the contrast, tire crumb B&G b exhibited very limited capacity with an isotherm curve nearly parallel with C_e axis.

The Freundlich model parameters are summarized in Table 3-3 and the high value of correlation coefficient indicates a good fitting between the experimental and calculated data. The heterogeneity of media materials and variety of sorption mechanisms make Freundlich isotherm an appropriated equation to describe the process involving P mass transfer between aqueous and solid phase. Although the nonlinear Freundlich isotherm is widely used, comparison of model parameters K_F of different media is constrained by the unit. The unit of K_F is determined by n and cannot be compared directly between different sorbents even when the experiments are carried out under identical condtions. For this reason, Chen et al. (1999) proposed a unified sorption variable K_u with the same unit as distribution coefficient, K_d. In this study, the unit of mg/L was assigned to C_e and mg/g to q_e, therefore, K_u has a unit of g/L. K_u was calculated from equation (6) and Figure 3-4 plotted K_u as function of C_e. An approximately L-shape curve was obtained for all the media tested, showing an initially rapid decrease in K_u followed by a more moderate decrease. This result is consistent with those of Chen et al. (1999) and Marchi et al. (2006). Here the values of K_u ranged from >20 L/g to < 0.2 L/g. Two orders of magnitude variation indicates significant differences of the media capacity, therefore in Figure 3-4 a log scale of K_u was

employed for a better demonstration of the comparison. One reason that Freundlich equation has been widely favored is its simple mathematical form with only two parameters. However, as was pointed out by Bowman (1981), the hidden complexities in K_F provide no rational basis for comparing sorption capacities among different sorbents. By employing the unified sorption variable of K_u, the media capacity can be reasonably quantitatively evaluated and compared.

Metal Leaching from Media

Besides a satisfactory efficiency, it is very important that the water treatment process must not impair the treated water quality by contamination of the water with soluble salts or metals from the treatment media material (Sibrell et al., 2009). 13 metals in the filtrate from metal leaching tests, including Al, As, Ba, Ca, Cd, Cr, Cu, Fe, Mg, Mn, Ni, Pb and Zn, were measured as described previously. All the results were summarized in Table 3-4, expressed as milligram of metal leached per gram of media. It can be noted that the concentration of As was below Method Detection Limit (0.05 mg/L) for all the media and so were the concentrations of Cr (MDL: 0.002 mg/L) and Ni (MDL: 0.005 mg/L) for most media. Generally, these media contained Al, Ca, Fe and Mg and other metals measured in this study were mostly in trace level. Previous studies have shown that phosphorus sorption is often positively related to media properties of Al, Fe, and Ca content (Kang et al. 2003; Karageorgiou et al., 2007; Mortuna et al., 2007). Figure 3-5 illustrates the amount of Al, Fe and Ca leached out of each media in contrast with the unified sorption coefficient K_u at C_e of 0.03 mg/L which was generally accepted as an indication of excessive nutrient enrichment in confined water bodies (Genz et al., 2004; Oguz, 2005) and at C_e of 0.1 mg/L (USEPA, 1986). It can be seen from Figure 3-5 that Fe-coated perlite leached significant amount of Fe as compared

with the other media. Activated alumina, and bioretention soil media were the two adsorbents that released most Al among all the media. Most media leached certain amount of Ca. Comparing expanded shale a and expanded shale b, it can be found that the smaller gradation resulted in a higher metal concentrations in the filtrate. The same result was obtained for tire crumb B&G a and b, indicating that particle size impacted on metal leaching quantities as well. In addition, if the amount of metal leached could be positively related to the content of metal in each media, Figure 3-5 implies it is not necessarily true that higher content of Al/Fe/Ca results in higher removal efficiency. The media capacity is determined by many factors, such as physical characteristics, chemical properties and the form and activity of metal content.

Discussions and Implications

As summarized in Table 3-1, alumina related residuals, by-products and sludge have been extensively studied as potential adsorbent for P removal. In many soils Al and Fe-oxides are present making soil a reactive substrate, specifically for phosphate species (Fontes and Weed, 1996; Nooney et al., 1998; Arias et al., 2006; Boujelben et al., 2008). It has been reported that aluminum hydroxide is formed on the surface of activated aluminum oxide in water and then reacts with phosphate ions through ligand exchange as shown in the following equations (Urano and Tachikawa, 1991):

$$Al_2O_3 + 3H_2O \rightarrow 2Al(OH)_3$$

$$Al(OH)_3 + H_2PO_4^- \rightarrow AlPO_4 + OH^- + 2H_2O$$

Analogous mechanism accounted for the reaction between phosphate ion and surface alumina coating on $AOCM_c$.

Similarly, Fe-oxide tailings, blast furnace slag, steel slag and granulated ferric hydroxide were tested for removal of P due to the richness of Fe in the materials (Genz

et al., 2004; Zeng et al., 2004; Drizo et al., 2006; Mortula et al., 2007.) It is generally agreed that the mechanism of phosphate removal involved the formation of inner-sphere complexes on Fe-oxide surfaces (Genz et al., 2004). Hence, along with the fine particle size (therefore, relatively higher SSA), high P removal efficiency was achieved by Fe-coated perlite in this study. Additionally, here the batch equilibrium experiments were carried out at pH of 7, which was lower than pH_{pzc} (7.91) of Fe-coated perlite and two mechanisms including electrostatic attraction and ligand exchange (inner-sphere complexes) could be involved for P removal(Chitrakar et al., 2006).

The moderate P uptake capability of expanded shale was possibly ascribed to the major content of calcite. It has been proved that the P removal of Ca-containing materials was through the formation of insoluble Ca-P compounds and consequently surface precipitation (Oğuz et al., 2003; Karageorgiou et al., 2007).

Zeolite-perlite-GAC is a mixture of three filtration media: zeolite, perlite and GAC with volume ratio of 5:4:1. The major component zeolite is a family of natural and synthetic aluminosilicate minerals. It is the main absorptive material used in agricultural and industrial situations. Perlite is a naturally occurring volcanic product characterizing with lightweight, chemically inert, coarse, and granular. It is an effective physical filtration media. GAC is a highly porous adsorbent material, but not usually used for P removal (Mortula et al., 2002). The zeolite-perlite-GAC mixture may be more effective as filtration media and the limited capacity of DP adsorption can be ascribed to the Al and Ca oxides contained (Sakadevan andBavor, 1998).

As a relatively novel best management practice for urban storm water, bioretention has been studied and employed to minimize the impact of urban runoff during storm

events (Hsieh and Davis, 2005; Li and Davis, 2008). Generally, bioretention consists of porous media layers of mixes of soil, sand and organic matters and utilizes the chemical, biological and physical properties of plants, microbes and soils for removal of pollutants from storm water runoff. It appeared that phosphorus removal was the most variable of six pollutants examined in column and grab filed studies (-240% ~ over 80%, Davis et al., 2009). The bioretention soil media tested in this study is commercial mixtures for Prince George's County, Maryland with P-index of 25. As a result, very low DP uptake capacity was achieved. In one aspect, soil sorption of P could be long term process, which may not take place and finish within the time scale of this study; in another aspect, the complexity of the chemistry of these species as well as the soil characteristic accounts for the capacity variety. It has been recognized that treatment of dissolved phosphorus species is much more sensitive to media characteristics and proper media selection is critical for effective DP removal (Davis et al., 2009; Hunt et al., 2006).

Another media tested in this study which was also known to be utilized in BMPs for stormwater treatment was tire crumb B&G, the main composition of a commercial green roof mixture. Green roofs offer an aesthetically pleasing treatment solution that utilizes unused space to treat and store stormwater runoff and pollutants may be removed via several processes, such as sedimentation, adsorption, filtration, bioremediation etc. The efficiency of the system will be determined from the total precipitation and the total overflow. Actually, it has been reported that the green roof should be irrigated with recycled stormwater runoff, which will contain suspended and dissolved nutrients that are repeatedly recycled in order to maximize the natural nutrient utilization capabilities

of the biological processes taking place (Hardin, 2006). In this study, very limited DP uptake capacity was achieved for these media. As it has been shown the media chemical characteristics were correlated with pollutant removals (Hsieh and Davis, 2005), results obtained here indicate that further modification of the filter media should be conducted, more effectively designed process should be applied or other practices/techniques should be conjunct with to achieve favorable DP removal efficiency.

It has been reported that phosphorus sorption is often positively related to media properties such as Al, Fe, and Ca content (Kang et al. 2003; Karageorgiou et al., 2007; Mortuna et al., 2007). In order to improve the media capacity, efforts have been put to modify the natural adsorbents and develop engineered media, usually by applying Al or Fe coating (Ayoub et al., 2001; Arias et al., 2006; Boujelben et al., 2008). On one hand higher content of Al/Fe in media should be desirable from the efficiency point of view; on the other hand, unfavorable metal leaching could be an environmental concern associated with the application of such engineered media. These two apparently contradictions not only result in more challenges in media preparation but also require more discretion in media evaluation. Among the media tested in this study, Fe-coated perlite and activated alumina showed best P removal capacity. However, at the same time 3.49 ± 0.05 mg Fe/ g Fe-coated perlite and 1.09 ± 0.02 mg Al / g activated alumina were released, respectively. Moreover, it should be noticed that these results were obtained at pH of 7. Much more acidic condition could be encountered in the actual environment and may result in higher amount of metal leaching. Therefore, albeit the high sorption capacity of activated alumina and Fe-coated perlite, caution should be

taken with the selection of these media since quite amount of Al and/or Fe leaches into the treated water. Comparatively, a satisfactory P removal efficiency can be achieved with $AOCM_c$ but without the compromise of significant metal leaching, which indicates $AOCM_c$ can be a promising adsorptive-filtration media for P control.

Summary

In this study, batch equilibria between dissolved P (DP) and 9 adsorptive media were tested and evaluated. Results demonstrated a significant capacity variation among different media. The unified sorption coefficient K_u developed by Chen et al. (1999), which illustrates the distribution of partitioning coefficient of sorbate between the aqueous and solid phase at various equilibrium concentrations, was adopted as a quantitative index to facilitate the comparison of media capacity. Results indicated that activated alumina, Fe-coated perlite and $AOCM_c$ were the three media with good equilibrium capacity while the rest including tire crumb B&G, expanded shale, Zeolite-Perlite-GAC and bioretention soil media exhibited very limited capabilities. The possible treated water contamination due to media application was examined through metal leaching tests. Al, Ca, Fe and Mg were found to be the major metals released into the water sample. It was also found the high P removal efficiency of activated alumina and Fe-coated perlite was accompanied by a significant amount of Al and Fe leaching, imposing an environmental concern of these media application. On the contrary, $AOCM_c$ seemed to be able to satisfy both P removal and minimal contamination requirement and thus it is considered as a promising cost effective adsorptive filtration media for P treatment.

Nomenclature

$AOCM_c$:	Alumina oxide coated media with clay as raw substrate
T	Temperature
C_0:	The initial phosphate concentration (mg/L)
C_e:	The phosphate concentration at equilibrium [mg/L]
DP:	Dissolved phosphorus
DI water:	De-ionized water
ΔG	Free energy transfer between two phases
K_d,	Partitioning coefficient [L/g].
K_F:	The Freundlich constant
K_u	Unified sorption variable [L/g]
n:	The Freundlich exponent
pH_{pzc}:	pH of point of zero charge
PP	Particulate phosphorus
q:	The amount adsorbed (mg/g)
q_e:	The amount of adsorption at equilibrium [mg/g]
q_m:	The maximum adsorbed phase concentration [mg/g]
R	The general gas constant
R^2:	Coefficient of determination
SSA:	Specific surface area [m^2/g]
T	The absolute temperature
TMDL	Total maximum daily load
V:	The volume of the solution (L);

W: The weight of adsorbent used (g);

ρ_s: Specific gravity

Table 3-1. Summary of sorption media used in short-term isotherm batch experiments to remove P

Media	Aqueous Matrix	Matrix P [mg/L]	pH (s.u.)	Capacity [mg/g]	Reference
Alum sludge	DI wastewater	2.5 3.7	7 6 .5-7	0.674 0.185	Mortula et al., 2007
Acid mine drain sludge	DI	20	7	9.89 ~ 31.97	Wei et al., 2008
Acid mine drain sludge	DI	1.0	---	1.82 – 23.9	Sibrell et al., 2009
AlOx	MBR Filtrate	4	7.9 - 8.7	12.0 – 13.8	Genz et al., 2004
AlOx media	DI	0 – 8.16	7	2.1	Sansalone & Ma, 2009
Al residual	DI	0 -100	---	1.33 – 48.7	Dayton et al., 2003
Alum sludge	DI	5	4.3 - 9	0.7 – 3.5	Yang et al., 2006
Bioretention media	DI	3	7	0.081	Hsieh and Davis, 2005
Blast furnace slag	DI	16.3 - 163	9.8 - 11.7	3.2 – 18.9	Kostura et al., 2005
Blast furnace slag	DI	326.3	6.7 – 6.8	46.5	Lu et al., 2008
Calcite	Tap water	32.63	7.6 - 12	3.1	Karageorgiou et al 2007
Coal bottom ash	Landfill leachate	0.05 – 0.09	7	0.008 – 0.034	Lin and Yang, 2002
Double hydroxides	DI	16.3	6	44.3	Das et al., 2006
Expanded shale	DI	0.5 – 3.0	7	0.97	Forbes et al., 2004
$Fe_5HO_8 4H_2O$	WWTP effluent	2.7	7	5	Kang et al., 2003
FeOx	MBR Filtrate	4	7.9 - 8.7	16.9 – 23.3	Genz et al., 2004
FeOOH	seawater	0.3-1.0	7.8	10	Chitrakar et al., 2006
Fly ash	DI	26.1	11.5	71.87	Oguz 2005
Iron oxide tailings	DI	20	6.7 -6.8	7	Zeng et al., 2004
$KAl_3(SO_4)_2(OH)_6$	DI	62	5	145.6	Özacar, 2003
Lignocellulose-media	DI	50 -1000	---	16.4 – 80.9	Kim et al., 2006
Masonry sand	DI	0.5 – 3.0	7	0.59	Forbes et al., 2004
Mineral–based sorbent	DI	5	8	1.9 – 19	Gustafsson et al., 2008
Powered alum sludge	DI	4.8	4.2	0.98	Fu et al., 2008
Recovered ochre	DI	100	---	2.5	Heal et al., 2004
Sands	DI	2.5 - 320	7.6 – 9.6	0.004 – 1.19	Bubba et al., 2003
Steel furnace slag	DI	326.3	6.7 – 6.8	33.3	Lu et al., 2008
Synthetic hydrotalcite	DI	200	8.6	47.3	Kuzawa et al.,2006
Zirconium hydroxide	DI Seawater wastewater	1 10 0.30 2	5.0 7.7 8.8	30 10 15	Chitrakar et al., 2006
$ZnCl_2$ activated coir pith carbon	DI	3.3 – 13.01	4	0.47 – 1.35	Namasivayam and Sangeetha, 2004
Suspended PM[a] Settleable PM Sediment PM	Rainfall -runoff	0.082	7 - 8	3.27 0.42 0.22	Sansalone et al., 2010

[a] PM = Particulate matter

Table 3-2. Media characteristics and cost

Media	Size [mm]	SSA [m^2/g]	Specific Gravity	pH_{pzc}	Cost (2010 $/lb)
Activated alumina (commercial alumina)	1.4 – 2.41	571 ± 4	2.67 ± 0.01	8.83 ± 0.04	2 - 4
$AOCM_c$ (clay based aluminum oxide coated media)	0.85 – 2	282 ± 22	2.29 ± 0.04	4.61 ± 0.06	3.5 – 5.5
Bioretention soil media (commercial mixture for Prince Geoge's County, Maryland, P-index = 25)	0.001 – 10	22.2 ± 4.5	2.69 ± 0.03	6.35 ± 0.03	0.10 – 0.25
Expanded shale (commercial expanded shale)	2 – 10 0.45 – 4.5	3.90 ± 1.03 4.71 ± 1.04	1.91 ± 0.02	9.84 ± 0.10	0.75 – 1.00
Iron coated perlite (iron oxide coated perlite)	0.3 – 0.85	41.8 ± 2.2	1.24 ± 0.03	7.91 ± 0.08	1.50 – 2.25
Tire crumb B&G (green roof mixture of mainly tire crumb)	0.85 – 10 0.5 – 4.75	30.5 ± 6.2 35.5 ± 9.2	1.19 ± 0.04	8.58 ± 0.08	0.12 – 1.30
Zeolite-Perlite-GAC (commercial mixture)	2.29 – 9.65	93.7 ± 16.9	2.02 ± 0.01	7.51 ± 0.04	0.65 – 0.95

Table 3-3. Freundlich isotherm parameters

Media	Size [mm]	Matrix	K_F	n	Reference
Activated alumina	1.4 – 2.41	DI	5.49	0.56	This study
$AOCM_c$	0.85 – 2		1.35	0.33	
Bioretention soil media	0.001 – 10		0.18	0.39	
Expanded shale	2 – 10		0.06	0.53	
	0.45 – 4.5		0.15	0.54	
Fe-coated perlite	0.3 – 0.85		6.72	0.64	
Tire crumb	0.85 – 10		0.017	0.51	
	0.5 – 4.75		0.033	0.44	
Zeolite-Perlite-GAC	2.29 – 9.65		0.051	0.59	
Acid mine drain sludge	---	DI	17.0	0.25	Wei et al., 2008
Acid mine drain sludge	0.15 - 4	DI	3.26 – 4.38	0.24 – 0.50	Sibrell et al., 2009
Alum sludge	1.25 (d_{60})	DI	1.03	0.48	Mortula et al., 2007
Blast furnace slag	0 – 0.18	DI	0.29 – 11.11	0.06-0.47	Kostura et al., 2005
Blast furnace slag	0.01 - 15	DI	6.37	1.74	Lu et al., 2008
$Fe_5HO_8 4H_2O$	0.0035	WWTP effluent	19.4	0.05	Kang et al., 2003
$KAl_3(SO_4)_2(OH)_6$	0.09 – 0.15	DI	1.60	0.83	Özacar, 2003
Iron oxide tailings	---	DI	3.59	0.19	Zeng et al., 2004
Lignocellulose-media	---	DI	8.34	0.20	Kim et al., 2006
Recovered ochre	---	DI	3.5	0.48	Heal et al., 2004
Steel furnace slg	0.01 - 15	DI	1.71	1.72	Lu et al., 2008
Zirconium hydroxide	0.15 – 0.23	DI	17.4	0.33	Chitrakar et al., 2006
		Seawater	43.5	1	
		wastewater	14.9	0.09	
$ZnCl_2$ activated coir pith carbon	0.25 - 0.5	DI	1.61	0.33	Namasivayam & Sangeetha, 2004

All R^2 in this study are greater than 0.96.

Table 3-4. Summary of metals leaching capacity of media

Metal [µg/g]	Activated alumina	Bioretention soil media	Expanded shale a	Expanded shale b	Fe-coated perlite	Tire crumb a	Tire crumb b	ZPG	$AOCM_c$
Al	1090 (20)[a]	972 (23)	67 (2)	120 (2)	27 (3)	156 (6)	260 (6)	137 (5)	285 (4)
Ba	0.8 (0.07)	14 (0.1)	2 (0.1)	6 (0.1)	1 (0.1)	7 (0.1)	3 (0.1)	20 (0.1)	4 (0.1)
Ca	22 (1)	456 (7)	1180 (20)	1600 (20)	599 (8)	576 (10)	876 (10)	2790 (20)	78 (0.6)
Cd	0.4 (0.07)	0.4 (0.06)	0.3 (0.08)	0.4 (0.04)	0.6 (0.08)	0.4 (0.01)	0.4 (0.06)	0.4 (0.09)	0.3 (0.06)
Cu	1 (0.1)	0.9 (0.08)	BDL	1 (0.1)	3 (0.1)	0.6 (0.06)	0.6 (0.08)	0.9 (0.08)	1 (0.2)
Fe	BDL	657 (22)	15 (1)	24 (1)	3490 (50)	125 (6)	215 (5)	24 (2)	0.2 (0.1)
Mg	17 (1)	97 (1)	116 (1)	119 (1)	78 (1)	88 (0.5)	258 (4)	328 (4)	6 (0.1)
Mn	0.08 (0.008)	40 (0.4)	0.4 (0.02)	0.8 (0.01)	15 (0.3)	5 (0.1)	3 (0.1)	1 (0.1)	0.5 (0.01)
Pb	10 (2)	9 (2)	6 (3)	3 (2)	12 (5)	5 (0.5)	7 (3)	11 (3)	6 (2)
Zn	BDL	2 (0.2)	7 (0.1)	4 (0.2)	1 (0.1)	17 (0.3)	53 (0.2)	3 (0.1)	13 (0.4)

[a]: Values in parentheses are standard deviations;
[b]: BDL- Below Detection Limit; As, Cr, Ni are BDL.

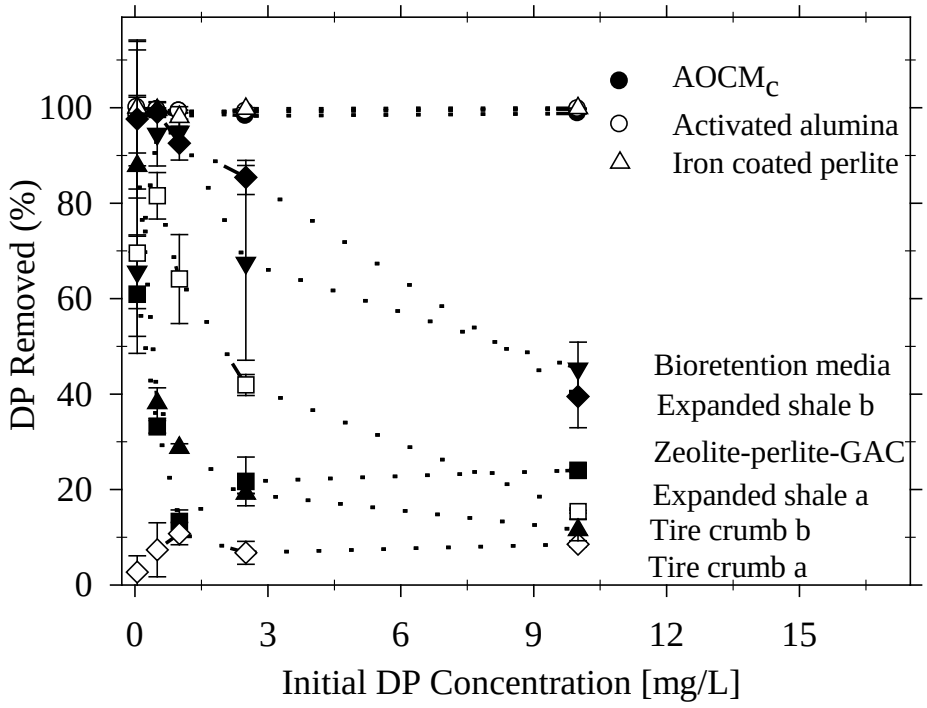

Figure 3-1. Comparison of P reduction by media of granular filter materials.

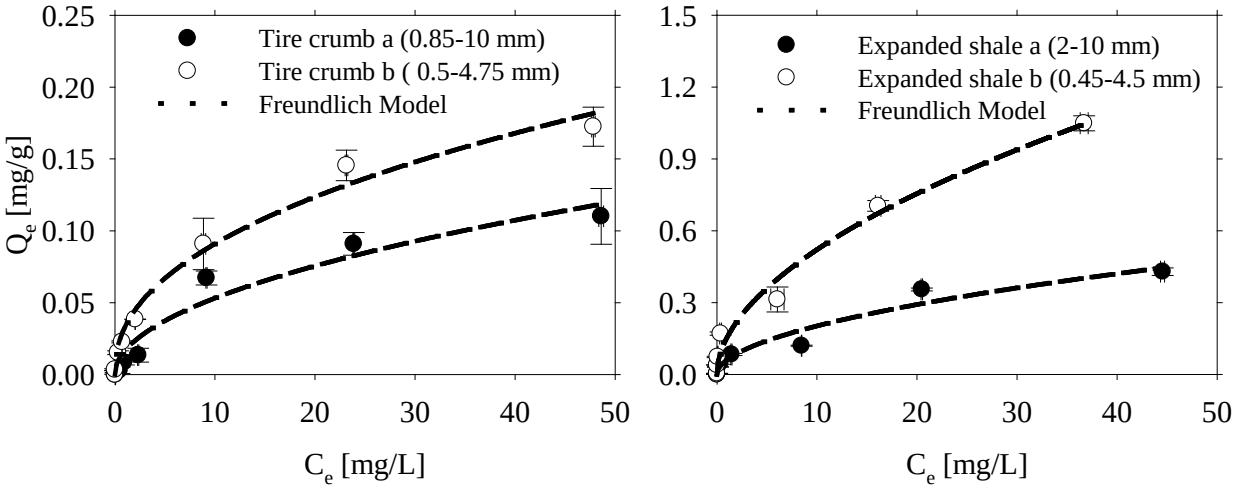

Figure 3-2. Measured and Freundlich modeled isotherms for P removed by Tire crumb B&G and Expanded shale.

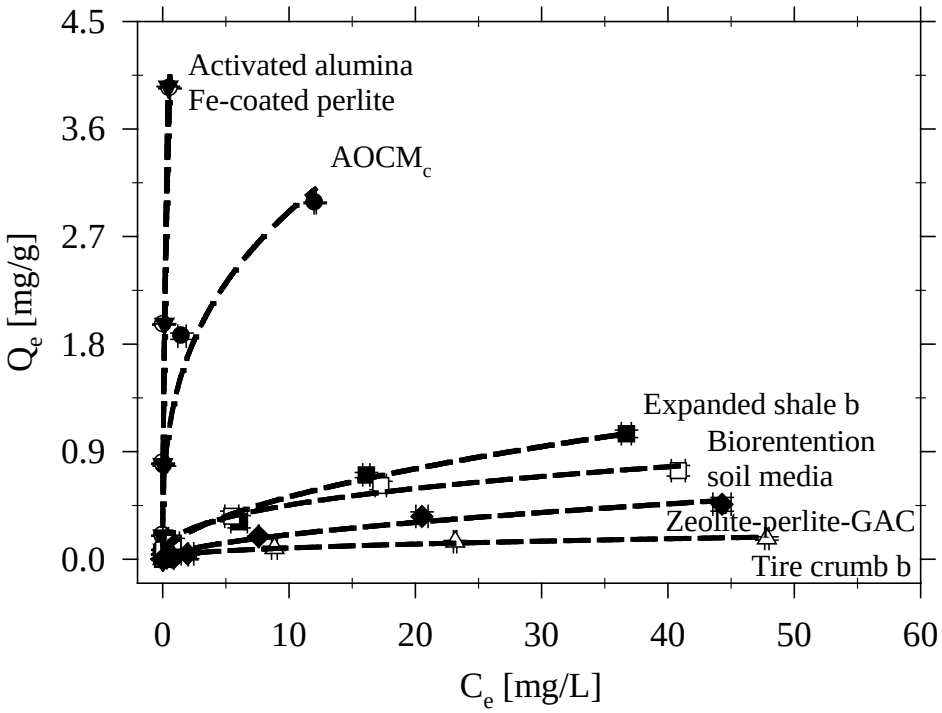

Figure 3-3. Measured and Freundlich modeled isotherms for P removed by each granular filter material.

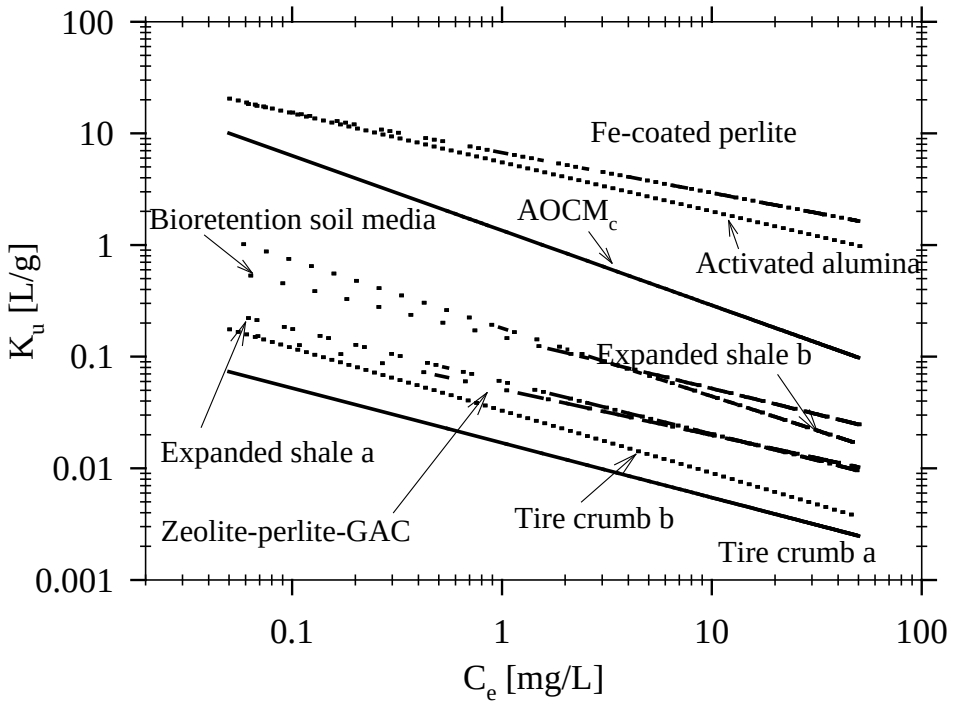

Figure 3-4. Comparison of K_u distribution for media of granular filter materials.

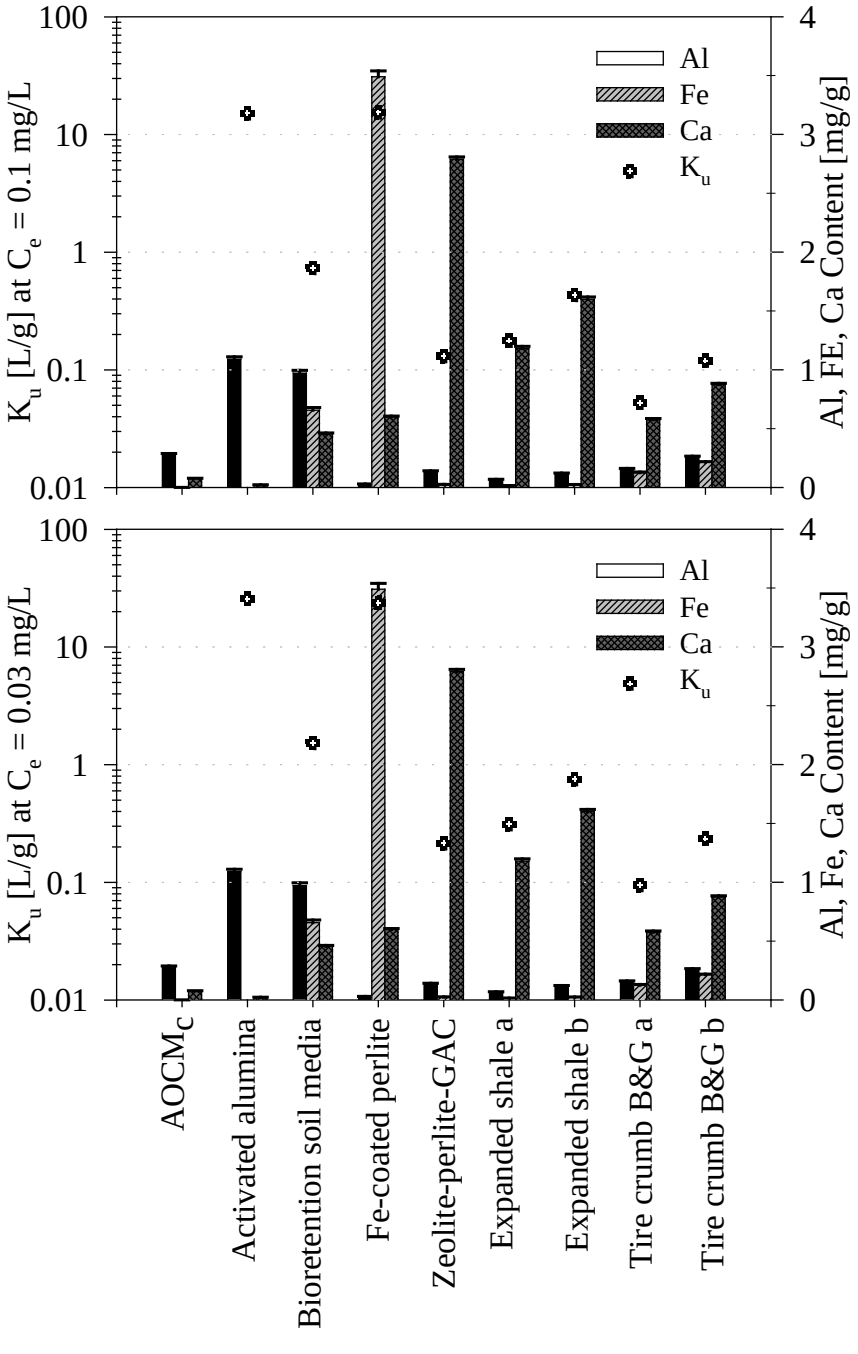

Figure 3-5. Comparison of K_u values at C_e = 0.1 mg/L (USEPA, 1986) and C_e = 0.03 mg/L (Genz et al., 2004; Oguz, 2005) for granular filter materials.

CHAPTER 4
MASS TRANSFER KINETICS OF GRANULAR FILTER MATERIALS FOR PHOSPHORUS IN AQUEOUS MATRICES

Background

Recent studies of P loadings to aquatic systems focused on anthropogenically-induced fluxes to aquatic systems demonstrate that such loadings accelerate eutrophication (Karaca et al., 2004; Ádám et al., 2007; Yu et al., 2008). Point sources such as conventional municipal wastewater treatment plants (WWTP) and nonpoint sources such as urban runoff along with sources from agricultural land uses are sources of nutrients that result in receiving water impairments (USEPA, 1996). While the technology exists (although not always implemented) to identify and treat point sources such as discharges from WWTP, control of nonpoint sources has not kept pace with point source control, in part because of the much greater challenges associated with diffuse, stochastic and variable loadings and with technology that is still developing. Many physical, chemical and biological control technologies applied to nonpoint loads can be disadvantaged by unfavorable cost/benefit relationships, low or variable effectiveness, or restrained by operational instability (for example desorption from media systems or lack of maintenance) and lack of sustainability (Karaca, 2004; Sansalone, 2005; Huang et al., 2008).

One technology that has been deployed to control P in runoff and wastewater is granular filtration media systems for PP; with recent incarnations as adsorptive media to facilitate DP control. A category of the adsorptive media incarnations have included filter substrates that range from common non-engineered materials (Sakadevan and Bavor, 1998; Johansson, 1999; Bubba et al., 2003; Hsieh and Davis, 2005; Davis et al.,

2006; Hsieh et al., 2007) to industrial by-products or wastes (Kostura et al., 2005; Drizo et al., 2006; Lu et al., 2008) in order to provide reduce the initial cost of media systems. These studies have demonstrated that many of these media do not have sufficient capacity for successful deployment to control DP (Bubba et al. 2003; Forbes et al. 2004, Kim et al. 2008, Sansalone and Ma 2009). Recent studies have also demonstrated that engineered coatings and media substrates can significantly improve the adsorptive capacity of granular media as compared to non-engineered media (Ayoub et al., 2001; Arias et al., Liu et al. 2005a; Ko et al., 2007; Boujelben et al., 2008; Sansalone and Ma 2009). While recent studies have illustrated the equilibrium capacity of oxides of Fe and Al for phosphate (Arias et al., 2006; Boujelben et al., 2008; Sansalone and Ma 2009), little research has focused on examining the role of the substrate in combination with the oxide for mass transfer of DP.

Furthermore, if media and media substrates require comparison, testing that allows comparison between media for a given media phenomena are required; specifically overall mass transfer rate for DP. When comparing media phenomena under equivalent conditions a controlled surrogate matrix is required. The most common controlled surrogate aqueous matrix is de-ionized (D.I.) water which provides a consistent and reproducible matrix for media testing and facilitating media comparisons subject to different controlled loadings (Namasivayam and Sangeetha, 2004; Liu et al. 2005b, Arias et al., 2006; Georgantas and Grigoopoulou, 2007; Boujelben et al., 2008). However, while such a consistent and reproducible matrix provides a vehicle for media comparability, studies have also shown that the equilibrium capacity of DP can be non-representative when comparing results from a DI matrix and an actual aqueous matrix

subject to similar pH and DP concentrations (Millero et al., 2001; Chen et al., 2002; Shilton et al., 2005; Ádám et al., 2007, Sansalone and Ma 2009). Specific to this study, a wastewater matrix is more complex than a DI water matrix with competing and synergistic ions. Actual rainfall-runoff subject to advective, diffusive and reactive multi-phase phenomena at much shorter interaction times than wastewater matrices in a WWTP illustrate a higher level of complexity as a result of competitive interactions, variable species and a highly hetero-disperse particulate matter (PM) phase (Dean et al., 2005; Sansalone, 2005). Monitoring and modeling of media phenomena with a surrogate matrix such as DI water can provide a comparative basis for media subject to similar actual matrix chemistry such as pH, redox, and DP concentrations. However, resulting media phenomena and model parameters such as overall mass transfer rates from a DI surrogate matrix may be less than representative of actual aqueous matrices such as rainfall-runoff and wastewater for a given media.

Objectives

Mass transfer processes between the aqueous and solid media phase can be described and quantified macroscopically through equilibria, kinetics, breakthrough and leaching. Equilibria approaches provide distribution coefficients and provide information on the final state of a reaction. However, in order to evaluate the time-dependent profile of mass transfer phenomena, examine mechanisms, and develop design and model parameters for media-based technologies, knowledge of kinetics is needed. There is a significant body of literature on equilibrium capacity for DP and metals for non-engineered and engineered media. However, kinetics and overall mass transfer rates for DP are needed to compare media deployed in control technologies (unit operations and processes) for DP; and are compared herein. Additionally, it is hypothesized that

the role of media substrates for media engineered with oxides for overall mass transfer can be significant yet has not been illustrated in the literature for DP; and this role is examined herein. It is hypothesized that media testing using actual uncontrolled and complex runoff or wastewater matrix, as compared to the potential non-representativeness of a controlled and reproducible DI surrogate matrix, produces disparate overall mass transfer rate parameters. Therefore in addition to comparing media (three of AOCM, three of UCM and six commercially-available media) the role that an aqueous matrix imparts on overall mass transfer rates and capacity is examined.

Materials and Methods

Media

Three aluminum oxide coated media substrates: $AOCM_c$ (fired clay substrate), $AOCM_p$ (pumice substrate), $AOCM_{pcc}$ (Portland cement concrete substrate) and their uncoated media (UCM) substrates are monitored and modeled. Clay and concrete substrates are crushed into two selected size gradations. Activated alumina; bioretention soil media; expanded shale; iron coated perlite; tire crumb (B&G) and zeolite-perlite-GAC (volume ratio: 5:4:1) are also monitored and modeled in this study as supplied or deployed in unit operations and processes. Table 4-1 summarizes the media characteristics.

$AOCM_c$ and $AOCM_p$ were prepared by applying aluminum as surface coating. Al (III) solution was added to the raw substrate contained in a Pyrex tray so that the substrate was just submerged. This Pyrex tray was then put in the oven and temperature was kept at around 200 ^oC. At least 24 hours were needed to fully dry and coat the substrate. Later, the aluminum coated sorbents was washed with D.I. water to remove the surficial fine materials. $AOCM_{pcc}$ was prepared by integrating aluminum

solution into the cementitious matrix as the “aqueous” admixture. The mass ratio of aqueous $Al(NO_3)_3$ solution (0.5 M) to cement is 1:1. This cementitious slurry was then cured and size graded in the same way as raw substrate preparation.

Chemicals

A 1000 mg/L phosphorus stock solution utilized is prepared by dissolving anhydrous potassium dihydrogen orthophosphate (KH_2PO_4) powder (Analytical reagent grade, Fisher Scientific) into DI water for the synthetic runoff. The stock solution is diluted as required for the synthetic runoff. Dilute HCl and NaOH solution (0.02N) were used to adjust the pH. Ionic background was fixed as 0.01M as KCl. All measurements (Eaton et al., 1998, summarized in Table 4-2) are duplicated and repeatability is assured by controlling experimental error within ± 5%.

Experimental Matrices and Strategy

Batch kinetic are carried out utilizing three different aqueous matrices: synthetic runoff, actual rainfall-runoff and secondary wastewater as upflow sand filter effluent from the University of Florida Advanced Wastewater Treatment (AWT) facility. The chemistry of each aqueous matrix is summarized in Table 4-3. Given that a DI aqueous matrix is consistent and reproducible surrogate the entire suite of media is monitored in synthetic runoff, with a DP concentration of 1.0 mg/L. This DP concentration is chosen based on the event-based concentrations of DP during actual rainfall-runoff events (Sansalone and Ma 2009). The AOCM and UCM forms are further examined in actual rainfall-runoff and wastewater with their measured DP concentrations (2.7 mg/L and 11.1 mg/L, respectively). It is noted that the University of Florida catchment (Lake Alice watershed) where field monitoring is conducted is an asphalt-paved surface parking facility with raised vegetated islands and therefore high biogenic loadings including

nutrients. While the wastewater is treated to AWT levels and effluent is reclaimed for campus-wide irrigation, N and P concentrations remain elevated in the effluent. Finally, the role of each aqueous matrix on media mass transfer is investigated. In this objective, the DP concentration of synthetic runoff and wastewater is adjusted to the same level as that of runoff (2.7 mg/L) to eliminate the interference of different driving force. Specifically, a synthetic runoff with initial concentration of 2.7 mg/L was prepared following the same procedure as described above for 1.0 mg/L; wastewater sample with initial P concentration of 11.1 mg/L was pretreated with $AOCM_c$ to remove the excessive phosphorus. It has also been validated that no major chemistry of the wastewater sample which can influence media performances was altered after the pretreatment ($\Delta pH < 3\%$; $\Delta[Ca^{2+}] < 2\%$; $\Delta[SO_4^{2-}] < 8\%$).

Batch Kinetic Study

Batch kinetics is an experimental technique which is considered representative of more realistic conditions and can be conveniently employed to determine the sorption parameters (Liu et al., 2005). In this study, mass transfer rates investigated by the batch kinetics experiments are facilitated using a recirculating flow-through reactor. Here, a short column (40 mm i.d., 90 mm length, Teflon PFA column) packed with test media served as the reactor. The sorbent solution ratio was fixed at 20 g to 2 L for all the tests and comparisons were made on equal mass base. The experimental set-up is illustrated in Figure 4-1. The ionic strength is set at 0.01 M with KCl and pH was adjusted to 7 in synthetic runoff. For the axial filter column the surface loading rate ranges within 20 to 60 L/min-m^2. In this study, surface loading rate of 40 L/min-m^2 are chosen and kept throughout the experiments, based on the database of peak flow of 1-year return event (Sansalone and Teng, 2005).

Duplicate 10 mL samples are collected from the sampling port shown in Figure 4-1. The time intervals of sampling were predetermined according to the preliminary tests of media kinetics. The sampled solution is filtered through 0.45 μm filter. The DP (as phosphate) concentration is determined using a spectrophotometer (HACH, DR5000). DP mass transfer to the media from the aqueous matrix at each time intervals, q_t [mg/g], and at equilibrium q_e [mg/g] is computed.

$$q_t = \frac{V(C_0 - C_t)}{W} \tag{1}$$

$$q_e = \frac{V(C_0 - C_e)}{W} \tag{2}$$

In these expressions C_0 is the initial concentration [mg/L]; C_t and C_e are the solution concentrations at time t and equilibrium [mg/L], respectively; V the volume of the solution [L] and W the dry weight of media used [g].

Overall Mass Transfer Rate Modeling

Modeling of kinetics can be carried out by empirical or fundamental models. In this case a 2nd order potential driving model is illustrated (Liu et al. 2005a). The elementary second-order reaction with different reactants can be generalized.

$$A + B \xrightarrow{k} P \tag{3}$$

The differential equation and analytical solution with initial condition of $[A] = [A]_0$ and $[B] = [B]_0$ at $t = 0$ are as follows.

$$\frac{d[A]}{dt} = -k[A][B] \tag{4}$$

$$[A] = \frac{[A]_0\{[B]_0 - [A]_0\}}{[B]_0 \exp\{kt([B]_0 - [A]_0)\}} \tag{5}$$

In these expressions *k* is the reaction rate constant ($M^{-1}s^{-1}$), *t* is the reaction time (s), and $[A]_0$ and $[B]_0$ are initial concentrations of reactants A and B at t = 0, respectively. For a heterogeneous solution (DP concentration at the near-surface differs from bulk solution), the surface reaction mechanism with a hydrous oxide and may be depicted as surface complexation reactions.

In developing the mathematical description of the overall mass transfer process, certain assumptions are made. There can be various rate limiting steps, such as chemical reaction, film diffusion and intra-particle diffusion. For the kinetic model of this study, an overall rate covering all the processes is utilized to simplify the presentation of kinetics from aqueous solution to media. This overall rate is considered to be related to the sorption potentials (chemical or electrical or other energy forces of the diffusion processes) of surface sites and sorbates. Since only differences in potential are ever physically meaningful, and the differences of potential can be from the variation of space or time, the potential at equilibrium ($t = \infty$) can be set to zero or as a standard potential. Thus the potential for any time, t, is $\rho_t - \rho_\infty$ (ρ_t is the absolute potential at time t, and ρ_∞ is the absolute potential at $t = \infty$). Concentration differences between the bulk solution and media surface sites are utilized at time, t, and at equilibrium for model computations. Potential differences are assumed to be correlated to the difference in bulk solution concentration of DP and number of surface sites. Moreover, equilibria follows the Freundlich isotherm and this has been confirmed previously (Sansalone and Ma 2009). With these assumptions the second order rate, eq. (5) can be correlated to differences in DP concentrations and available surface site number between time *t* and equilibrium. Using a similar hypothesis, kinetics of divalent metal adsorption onto oxide-

coated media is successfully modeled (Liu et al, 2005a). A potential driving rate differential equation based on equation (5) can be represented as follows.

$$\frac{dC_t}{dt} = -k(S_e - S_t)(C_t - C_e) \tag{6}$$

Here S_t is the number of active sites occupied on the media at time t, and S_e is the number of active sites occupied at equilibrium on the media. S_t and S_e can be represented as follows.

$$S_t = \frac{C_0 - C_t}{a} \tag{7}$$

$$S_e = \frac{C_0 - C_e}{a} \tag{8}$$

Here C_0 is the initial DP concentration, C_t is the DP concentration at time t, C_e is the DP concentration at equilibrium, and a is the sorbent/solute ratio. It has been shown that the integrated potential driving model rate equation can be linearized.

$$\frac{t}{C_0 - C_t} = \frac{t}{C_0 - C_e} + \frac{a}{k(C_0 - C_e)^2} \tag{9}$$

The overall mass transfer rate constant k and equilibrium concentration C_e can be determined by plotting $t/(C_0-C_t)$ against t (Liu et al. 2005a).

Additionally, substitute $a = \frac{W}{V}$ and Eq. (1) and (2) into Eq. (9), we can get:

$$\frac{t}{q_t} = \frac{t}{q_e} + \frac{1}{kq_e^2} \tag{10}$$

q_e and q_t [mg/g] is the amount of phosphorus transferred at equilibrium and time t, respectively.

To compare monitored and modeled result, RMSE (Root Mean Square Error) and chi-square tests are utilized and calculated for each kinetics run.

$$RMSE = \sqrt{\frac{\sum_{i=1}^{n}[Q(q_i) - E(q_i)]^2}{n}} \tag{11}$$

In this expression $Q(q_i)$ is the observed (monitored) value and $E(q_i)$ is the expected (modeled) value. The fit between monitored and modeled is also evaluated with a chi-square (χ^2). χ^2 measures the difference between expected and observed values and is a quantitative measure of the relationship. χ^2 is defined in the following manner and a smaller χ^2 indicates a better fit:

$$\chi^2 = \sum_{i=1}^{n} \frac{[O(q_i) - E(q_i)]^2}{E(q_i)} \tag{12}$$

Intra-media diffusion model

While the 2nd order potential driving model is intended to simulate the overall mass transfer rate the model does not separately identify mechanisms. For media that has internal porosity there is intra-media diffusion that occurs during the overall mass transfer process. From a system design and modeling point of view, a lumped or overall mass transfer rate is appropriate (Özacar, 2003) but may not clearly illustrate the mechanism of diffusion that occurs as part of the overall mass transfer. Hence, a intra-media model is also utilized for the purpose of identifying diffusion.

A functional relationship common to most intra-media diffusion (q_t) phenomena is that solute mass transfer rate varies proportionately with the square-root of time (Alvin et al, 2010).

$$q_t = f(t^{0.5}) \tag{13}$$

The rate parameter for intra-particle diffusion (k_p) can be determined.

$$q_t = k_p t^{0.5} \quad (14)$$

k_p is the intra-media diffusion rate constant (mg/g·min$^{0.5}$). A plot of q_t versus $t^{0.5}$ may illustrate multi-linearity, indicating multiple rate controlling steps occur during the overall mass transfer.

Results and Discussions

Tests in Synthetic Runoff (C_0 = 1.0 mg/L)

Kinetics are determined for three AOCM forms and their UCM substrates. AOCM and UCM media parameters and synthetic aqueous parameters are summarized in Table 4-1 and 4-3 respectively. Overall mass transfer kinetics of DP from synthetic runoff to the media are shown in Figure 4-2 illustrating that equilibrium is approached in approximately 90 minutes for AOCM forms and 150 minutes for UCM forms without Al-Ox. The kinetic data are simulated with the 2nd order potential driving model and Table 4-4 lists the model parameters, χ^2 and RMSE for each media form. Results demonstrate that compared with UCM, the mass transfer kinetics for all AOCM forms were much greater. With the exception of the PCC substrate the equilibrium capacity of the Al-Ox media was significantly higher than the UCM substrate indicating that the Al-Ox improves the media capacity. The mass transfer of phosphates to hydrous aluminous oxide is through ligand exchange to surface hydroxyl groups (Goldberg and Sposito, 1985; Genz et al., 2004; Kim and Kirkpatrick, 2004; Arias et al. 2006; Yang et al., 2006; Georgants and Grigoropoulou, 2007). Therefore, it is hypothesized that an increase of pH should be observed during mass transfer given the release of surface hydroxyl groups for all AOCM forms. The higher kinetics and capacity of the AOCM as compared

to the UCM substrate is a result of the Al-Ox ligand exchange and the number of surface sites providing such exchange, and therefore higher equilibrium capacity as compared to UCM of the same substrate.

While $AOCM_{pcc}$ kinetics and capacity were not markedly higher than other AOCM forms, the permeable concrete media substrate (UCM_{pcc}) exhibited much higher kinetics and capacity as compared to the permeable clay substrate (UCM_c) and permeable pumice substrate (UCM_p). This is attributed to the high content of CaO in concrete substrate; as shown for increasing CaO content in fly ash, slag and conventional Portland cement (Agyei et al., 2002). The affinity of phosphate for CaO, and the resulting formation of insoluble Ca-P precipitation indicate that surface precipitation and ligand exchange combine to provide higher kinetics and equilibrium capacity. However, the relative significance of each mechanism is a function of the media composition combined with the aqueous matrix; which will be discussed later in the results. Figure 4-2 and Table 4-4 illustrate that there is not a marked difference between the two size gradations of clay and PCC substrates. Usually, if the mass transfer is chemically rate controlled, the rate constant is independent of particle diameter (Ho and McKay, 1999), suggesting that chemisorption is the dominant mechanism with surface precipitation as a co-mechanism. Since media size (a surrogate for SSA) does not provide a marked difference for kinetics or capacity for $AOCM_c$ and $AOCM_{pcc}$ the balance of this study utilized only the 2 ~ 4.75 mm gradation. Plot f of Figure 4-2 superimposes AOCM (2 ~ 4.75 mm) results from plots a, b and c to illustrate kinetics and equilibrium capacity. Although $AOCM_p$ displayed slower kinetics and lower capacity, no marked variance among $AOCM_c$, $AOCM_p$ and $AOCM_{pcc}$ is observed, in contrast to a UCM comparison

from plots a, b and c. Results with the synthetic matrix illustrate that the Al-Ox coating promoting ligand exchange provides the dominant mass transfer mechanism generating comparable kinetics and capacity results; despite differences illustrated for mass transfer by each individual substrate.

In addition to AOCM, media utilized in stormwater BMP deployments are monitored and modeled for overall mass transfer kinetics using the synthetic runoff matrix. These media as summarized in Table 4-1 include activated alumina, bioretention soil media, expanded shale (a, b), iron coated perlite, tire crumb (a, b) (Black&Gold) and zeolite-perlite-GAC. The kinetics of each media including AOCM (2 - 4.75 mm) is shown in Figure 4-3. Results illustrate a wide range of kinetics; ranging from the highest for AOCM forms to essentially no different from 0 ($p \leq 0.05$) for tire crumb (B&G) and zeolite-perlite-GAC. While the reactivity of the activated alumina and iron contributes to their relatively high kinetics and equilibrium capacity the fine gradation of the iron perlite limits the range of hydraulic applicability and the potential for ferric-ferrous reduction under anaerobic conditions limits applicability to aerobic environments, while the potential for leaching is potentially limiting for both media. Table 4-4 summarizes the 2nd order model parameters for the conditions of the synthetic matrix. The model did not fit the tire crumb or zeolite-perlite-GAC media since the mass transfer rate to, and from, these media were essentially equal resulting in media capacity that is not different from 0 ($p \leq 0.05$).

Intra-media Diffusion

Multiple transport processes or rate-limiting steps can exist with the overall mass transfer process. The overall mass transport process generally involves: (i) mass transfer of sorbate from the bulk phase to media surface; (ii) a reaction mechanism at

the surface site or sites; (iii) intra-media diffusion, which includes diffusion of sorbate occluded in micro-pores (pore diffusion) and along pore-wall surfaces (surface diffusion). The combination of pore and surface diffusion within the immediate region are referred to as intra-media diffusion.

The reaction at the surface (step ii) is usually rapid and not rate-limiting; while usaually step (i) is rate–limiting for a system with poor mixing, low sorbate concentration, high affinity to the adsorbent and small particles (Choy et al., 2004; Alvin et al., 2010). Therefore, the intra-media diffusion is hypothesized as the rate determining step.

According to Eq. (14) if q_t as a function of $t^{1/2}$ is linear then intra-media diffusion is rate limiting. Previous studies have shown that this function will not have a 0-intercept if an external surface adsorption or instantaneous adsorption stage exists (Hameed and Daud, 2008; Khaled et al., 2009). Plotting such a function can therefore illustrate multi-linearity and the mass transfer process can be broken down into two or more steps: the first is the external surface adsorption rate; the second rate is the slower mass transfer stage with intra-media diffusion controlling the rate; and the third stage is the final equilibrium stage. The slope of the second rate is called as intra-media diffusion rate constant, k_p (Özacar, 2003; Karaca et al., 2004; Kostura et al., 2005).

Figure 4-4 illustrates the root time plots for DP mass transfer for the media exhibiting overall kinetics that are not significantly different from zero and tested in synthetic runoff (C_0 = 1.0 mg/L). As can be seen, the external surface adsorption (first step) is completed in less than 5 minutes (when the first sample was taken). The other media of essentially zero capacity did not exhibit this behavior. After 5 minutes the intra-

media diffusion control is attained and continued for times that ranged from 20 to 40 minutes depending on the media, after which the final equilibrium stage is started. Table 4-5 summarizes the rate parameters of k_{p1} and k_{p2}, with k_{p1} as the intra-media diffusion rate constant and k_{p2} as the rate constant of the equilibrium stage. The 2nd order model and intra-media model simulate the monitored data. While the diffusion model illustrates discrete mass transfer stages and mechanisms the 2nd order model simulates the overall mass transfer rate continuum over the entire range of times with a single set of parameters applied to the entire mass transfer process. Since the focus is to illustrate the overall mass transfer rate and rate parameters for modeling the 2nd order potential driving model is utilized for actual rainfall-runoff and wastewater matrices.

Kinetics in Rainfall-Runoff and Wastewater Matrices

Studies have illustrated that water chemistry influences media capacity (Shilton et al., 2005; Ádám et al., 2007, Sansalone and Ma 2009). Hypothesizing that the selection of the aqueous matrix also influences the kinetics as well as equilibrium capacity for a media, AOCM is also tested in actual rainfall-runoff (C_0 = 2.7 mg/L for DP) and secondary effluent from an AWT (C_0 = 11.1 mg/L for DP) with the water chemistry of these matrices listed in Table 4-3. The experimental results are presented in Figure 4-5 and Figure 4-6, respectively. Kinetics data are simulated with the 2nd order model and the rate constants for each media for each aqueous matrix are summarized in Table 4-6. AOCM is compared with UCM in plots a, b, c in Figure 4-5 and 6. While comparative trends between AOCM and the UCM substrate are similar to trends obtained in the synthetic runoff matrix under the same monitored conditions the magnitudes of the model parameters are different. Given that the actual rainfall-runoff had a higher DP concentration (2.7 mg/L) as compared to the synthetic runoff (1.0 mg/L) the equilibrium

capacity is comparably higher, but lower than the initial concentration ratio of 2.7 suggesting the role of competitive interactions on equilibrium capacity. In contrast, when comparing the rate constants in Table 4-4 and 4-6 the results clearly indicate a significant decrease in the overall mass transfer rate constant for actual rainfall-runoff when compared to synthetic runoff despite the DP enrichment in actual rainfall-runoff. Despite a clear influence of the aqueous matrices, Al-Ox coating exhibited a significant influence on media capacity, in particular for clay and pumice substrates with ligand exchange as dominant mechanism and surface precipitation a negligible mechanism as compared to $AOCM_{pcc}$. Similar results are shown for wastewater as summarized in Figure 4-6.

Figure 4-5d and 4-6d overlay each AOCM kinetics profile thereby illustrating the role of the substrate. While the kinetics of $AOCM_c$ and $AOCM_{pcc}$ are still similar to each other, albeit with commensurately different equilibrium capacities and kinetics as compared to the synthetic runoff, there is a marked and significant difference for $AOCM_p$, especially in the wastewater matrix. $AOCM_p$ exhibited slower kinetics and lower equilibrium capacity. These results indicate that although an effective coating is critical to enhance substrate behavior, coupled physico-chemical characteristics of the substrate and imposed water chemistry also impact media capability, as illustrated with these actual and more complex aqueous matrices.

In order to further compare and investigate the influence of the aqueous matrix on overall mass transfer kinetics, synthetic runoff, actual rainfall-runoff and wastewater are batched at the same initial DP concentration of 2.7 mg/L. Thus, the effect of different driving forces for reaction and diffusion caused by different C_0 levels is

excluded. Figure 4-7 illustrates the comparison among various water matrices as well as pH variation along with the contact time for $AOCM_c$, $AOCM_p$ and $AOCM_{pcc}$, respectively. Table 4-7 summarizes the 2nd order model parameters for all aqueous matrices with an equal DP (C_0 = 2.7 mg/L).

As identified earlier, reactions between aqueous phosphate and Al-Ox are ligand exchange between phosphate ions ($H_2PO_4^-$ or HPO_4^{2-}) and the surface hydroxyl group (OH^-), resulting in OH^- release into solution. As shown in Table 4-7, the change in pH (Δ pH) increases across the period of mass transfer yet is different between synthetic and actual matrices (rainfall-runoff and wastewater), with an initial pH of all the matrices in the range of 7.0 as shown in Table 4-3. The differences in the Δ pH between synthetic and actual rainfall-runoff and wastewater matrices is in part a result of higher buffer capacity in these latter two matrices due to the presence of primarily HCO_3^-. Figure 4-7a overlays the kinetics of $AOCM_c$ in each matrix. Kinetic rates follow the order of synthetic runoff, rainfall-runoff and wastewater. The actual matrices introduce the presence of competitive ions such as SO_4^{2-} which compete for the active sites and decrease the media kinetics rates and capacity. However, the impact is insignificant ($p \leq 0.05$) for $AOCM_c$ kinetics and capacity.

Similar increases in pH (as Δ pH) are obtained for $AOCM_p$, as presented in Table 4-7. In contrast to Figure 4-7a, 7b illustrates significantly lower ($p \leq 0.05$) kinetic rates and apparently capacity when comparing synthetic and actual matrices. The time to equilibrium is nearly doubled in the actual matrices compared to $AOCM_c$. The kinetic rates of $AOCM_p$ in these complex matrices are significantly less than $AOCM_c$.

Due to the high content of CaO in cement concrete substrate higher increases in pH (as Δ pH) are obtained for $AOCM_{pcc}$, as presented in Table 4-7. In contrast to Figure 4-7a, and 7b; 7c illustrates lower kinetic rates for $AOCM_{pcc}$ in the actual rainfall-runoff matrix. In contrast to $AOCM_c$ and $AOCM_p$; $AOCM_{pcc}$ exhibits higher kinetic rates in synthetic runoff and wastewater than in rainfall-runoff. It has been reported that both SO_4^{2-} and Ca^{2+} can influence the P removal by AOCM (Sansalone and Ma, 2009). SO_4^{2-} decreases P sorption due to the competitive effect on ligand exchange while Ca^{2+} increases P sorption through promotion of surface precipitation. Thus, the presence of both SO_4^{2-} and Ca^{2+} in one matrix can exert contrary effects on the kinetic rates. The relative significance of each effect is determined by the dominant mechanism involved, i.e., if ligand exchange is the major mechanism, competitive effect will be more evident; if surface precipitation is dominant, promotion effect will be observed. Furthermore, mechanism transition is a function of media composition combined with the aqueous matrix. High concentration of Ca^{2+} in wastewater matrix (56 mg/L), high content of CaO, alkaline condition in the solution all facilitate $Ca_3(PO_4)_2$ precipitation and overwhelm the SO_4^{2-} competition effect. As a result, the surface precipitation of $Ca_3(PO_4)_2$ is enhanced in wastewater as compared to rainfall-runoff.

Summary

Overall mass transfer rates of DP from a series of aqueous solutions by a suite of granular filter media in a re-circulating reactor is monitored and modeled. The media include three Al-Ox coated media: $AOCM_c$ (clay based), $AOCM_p$ (pumice based), $AOCM_{pcc}$ (Portland cement concrete based) and their uncoated media (UCM) substrates; and a series of commercially-available media: activated alumina;

bioretention soil media; expanded shale (a, b); iron coated perlite; tire crumb (a, b) (B&G) and zeolite-perlite-GAC. Kinetic rates are examined in a synthetic runoff matrix, an actual rainfall-runoff matrix, and a secondary effluent wastewater matrix. Kinetics parameters are developed based on simulation of monitored data with a 2^{nd} order potential driving model for overall mass transfer and an empirical model to identify intra-media diffusion as a rate limiting mechanism. Compared to the UCM controls for each AOCM, the Al-Ox coated media achieved significantly higher kinetic rates and equilibrium capacity as irrespective of the aqueous matrix. The role of the AOCM substrates did not illustrate a significant effect in a DI matrix. While the kinetic rates for the commercially available media were all below that of AOCM forms in a DI matrix, these media exhibited varied capacity and decreased in the order from iron coated perlite, activated alumina, expanded shale and bioretention soil media. Tire crumb (B&G) media used for green roof applications and zeolite-perlite-GAC mass transfer rates to and from were equal and therefore net equilibrium capacity was not significantly greater than 0. For the DI matrix the 2^{nd} order potential driving model simulated the overall mass transfer rate and the intra-media diffusion model identified the rate limiting diffusion of the permeable AOCM and other media. The DI matrix is a controlled and reproducible matrix that allows comparison of media on an equivalent basis but a basis that may not represent the complex interactions of actual matrices such as rainfall-runoff and wastewater.

In order to examine the kinetic rates of DP mass transfer for actual aqueous matrices, municipal wet weather flow (rainfall-runoff, C_0 = 2.7 mg/L) and dry weather (secondary wastewater, C_0 = 11.1 mg/L) matrices are tested with AOCM and UCM.

Again each AOCM out-performed the UCM substrate. However, while the type of AOCM substrate had an insignificant effect in the synthetic matrix, $AOCM_p$ kinetics rates and equilibrium capacity are significantly lower than $AOCM_c$ and $AOCM_{pcc}$ in both rainfall-runoff and wastewater matrices.

The choice of an aqueous matrix impacts resulting media parameters as developed from the 2nd order model. Therefore to investigate the effect of the aqueous matrix the DP concentration in each matrix (synthetic and actual) are adjusted to that of actual rainfall-runoff (2.7 mg/L) to eliminate the interference of different driving forces. The presence of SO_4^{2-} and Ca^{2+} in the actual matrices can exert contrary effects on phosphate mass transfer, as SO_4^{2-} competes for the active sites with phosphate ions through ligand exchange and Ca^{2+} enhances the surface precipitation of phosphate as $Ca_3(PO_4)_2$. Results demonstrated that the competition effects of SO_4^{2-} dominates in the rainfall-runoff matrix and decreases the AOCM overall mass transfer rate. While this competitive effect is observed for $AOCM_c$ and $AOCM_p$ in wastewater, surface precipitation overweighed the competition effect for $AOCM_{pcc}$, due to the high concentration of Ca^{2+} (56 mg/L) in the aqueous matrix as well as the alkaline condition in aqueous phase created through contact with concrete-based media, resulting in a faster kinetics.

Nomenclature

$[A]_0$: Boundary condition of reactant A at t = 0

a: Sorbent solution ratio (g/L)

AOCM: Aluminum oxide coated media

$AOCM_c$: Aluminum oxide coated media with clay as raw substrate

$AOCM_p$: Aluminum oxide coated media with pumice as raw substrate

$AOCM_{pcc}$: Aluminum oxide media with Portland cement concrete as raw substrate

AlOx: Aluminum oxide

$[B]_0$: Boundary condition of reactants B at t = 0

B&G: Black & gold

C_0: The initial DP concentration (mg/L)

C_t: DP concentration at time t (mg/L)

C_e: DP concentration at equilibrium (mg/L)

DI water: De-ionized water

DP: Dissolved phosphorus

$E(q_i)$ Expected value

k: Rate constant of 2^{nd} order mass transfer (g/mg·min)

k_p: The intra-media diffusion rate constant ($mg/g \cdot min^{0.5}$)

pH_{pzc}: pH of point of zero charge

PP: Particulate phosphorus

q_e: The amount of mass transfer at equilibrium (mg/g)

q_t: The amount of mass transfer at time t (mg/g)

$Q(q_i)$: Observed value

RMSE: Root Mean Square Error

S_e: Number of active sites occupied at equilibrium

S_t: Number of active sites occupied on media at time t

SSA: Specific surface area (m^2/g)

UCM: Uncoated media

UCM_c: Uncoated media with clay as raw substrate

UCM_p: Uncoated media with pumice as raw substrate

UCM_{pcc}: Uncoated media with Portland cement concrete as raw substrate

V: The volume of the solution (L)

W: The dry mass of media used (g)

WWTP: Wastewater treatment plants

ρ_t: Absolute potential at time t

ρ_∞: Absolute potential at $t = \infty$

χ^2: Chi-square

Table 4-1. Media characteristics

Media substrate		Size [mm]	Specific gravity	pH_{pzc}
AOCM and UCM	$AOCM_c$	0.85 – 2.0 2.0 – 4.75	2.29±0.04	4.61 ± 0.06
	UCM_c	0.85 – 2.0 2.0 – 4.75	2.31±0.05	4.20 ± 0.08
	$AOCM_{pcc}$	0.85 – 2.0 2.0 - 4.75	2.67±0.04	11.84 ± 0.16
	UCM_{pcc}	0.85 – 2.0 2.0 - 4.75	2.67±0.03	11.98 ± 0.12
	$AOCM_p$	0.85 – 2.0	2.27±0.01	4.59 ± 0.10
	UCM_p	2.0 - 4.75	2.29±0.02	4.61 ± 0.10
Activated alumina		1.4 – 2.41	2.67 ± 0.01	8.83 ± 0.04
Bioretention soil media		0.001 – 10	2.69 ± 0.03	6.35 ± 0.03
Fe-coated perlite		0.3 – 0.85	1.24 ± 0.03	7.91 ± 0.08
Zeolite-Perlite-GAC		2.29 – 9.65	2.02 ± 0.01	7.51 ± 0.04
Expanded shale	a	2 – 10	1.91 ± 0.02	9.84 ± 0.10
	b	0.45 – 4.5		
Tire Crumb (Black & Gold)	a	0.85 – 10	1.19 ± 0.04	8.58 ± 0.08
	b	0.5 – 4.75		

AOCM = Aluminum Oxide Coated Media
UCM = Un-Coated Media
c = clay based
PCC = Portland cement concrete based
p = pumice based
pH_{pzc} = pH at point of zero charge
Entries are mean ± standard deviation (n = 3)

Table 4-2. Summary of standard method utilized in the experiments

Measurement	Method
pH	S.M. 4500-H^+ B
Conductivity	S.M.2510
Turbidity	S.M.2130
Alkalinity	S.M.2320
DP	S.M. 4500-P-E:Ascorbic Acid Method
SO_4^{2-}	SulfaVer 4 Method
NO_3^-	Cadmium Reduction Method
Cl^-	Mercuric Thiocyanate Method
Dissolved metal	S.M. 3030 B

S.M.: Standard Method;
DP: dissolved P

Table 4-3. Water chemistry of experimental matrix

Matrix		Synthetic runoff	Rainfall-runoff (Event on 01/21/10)	Wastewater (Secondary effluent)
pH		7.00 ± 0.05	6.98 ± 0.23	7.16 ± 0.10
Conductivity [µs/cm]		1025 ± 56	224 ± 8	782± 12
Turbidity [NTU]		0.83 ± 0.46	24.7 ± 3.8	1.25 ± 0.76
Alkalinity [mg/L] as $CaCO_3$		5.4 ± 0.8	75 ± 1	48 ± 2
Ionic Strength [M]		0.010 ± 0.002	0.003 ± 0.002	0.010 ± 0.004
DOC [mg/L]		0.3 ± 0.1	37.8 ± 4.1	12.4 ± 2.8
Ca^{2+}		BDL[c]	28.67 ± 1.34	55.98 ± 2.10
Sum of Cation Charge [mmol]		10.05	1.83	5.49
Anion [mg/L]	NO_3^--N	0.45 ± 0.08	3.25 ± 0.10	1.45 ± 0.05
	SO_4^{2-}	0	19.0 ± 6.0	95 ± 5
	Cl^- [a]	360 ± 10	9.63 ± 0.54	108 ± 3
	HCO_3^-	3.3 ± 0.7	45.8 ± 1.8	29.3 ± 2.1
	PO_4^{3-} [b]	1.00 ± 0.05	2.71 ± 0.12	11.08 ± 0.21
Sum of Anion Charge[b] [mmol]		10.33	1.73	5.78

* Data are mean ± standard deviation
[a] 0.01M KCl was used to adjust the ionic strength of synthetic runoff.
[b] In synthetic runoff, PO_4^{3-} was added as KH_2PO_4.
[c] BDL: Below Detection Limit

Table 4-4. Parameters of 2nd order potential driving model in synthetic runoff (C_0 = 1.0 ± 0.05 mg/L)

Media Substrate		Size [mm]	q_e [mg/g]	k [g/mg·min]	χ^2	RMSE
AOCM and UCM	$AOCM_c$	0.85 – 2.0	0.13	0.76	0.036	0.009
		2.0 – 4.75	0.12	0.62	0.012	0.009
	UCM_c	0.85 – 2.0	0.03	5.64	0.001	0.001
		2.0 – 4.75	0.03	4.80	0.002	0.002
	$AOCM_{pcc}$	0.85 – 2.0	0.13	0.51	0.006	0.007
		2.0 - 4.75	0.14	0.35	0.016	0.009
	UCM_{pcc}	0.85 – 2.0	0.13	0.26	0.027	0.010
		2.0 - 4.75	0.14	0.21	0.026	0.009
	$AOCM_p$	0.85 – 2.0	0.12	0.45	0.018	0.010
	UCM_p	2.0 - 4.75	0.03	0.70	0.008	0.002
Activated alumina		1.4 – 2.41	0.12	0.40	0.013	0.008
Bioretention soil media		0.001 – 10	0.02	5.08	0.005	0.010
Iron coated perlite		0.3 – 0.85	0.13	0.40	0.005	0.052
Expanded shale	a	2 – 10	0.03	0.85	0.007	0.002
	b	0.45 – 4.5	0.09	0.48	0.016	0.006

χ^2: Chi-square
RMSE: Root Mean Square Error
Insignificant net capacity for Tire crumb (a, b) and Zeolite-Perlite-GAC, for which rate of adsorption/desorption were equal ($P \leq 0.05$).

Table 4-5. The sorption kinetics rate parameters in synthetic runoff (C_0 = 1.0 ± 0.05 mg/L) with water chemistry summarized in Table 4-2.

Media Substrate	Size [mm]	k_{p1} [mg·g·min$^{0.5}$]	$RMSE_1$	k_{p2} [mg·g·min$^{0.5}$]	$RMSE_2$
$AOCM_c$	2 – 4.75	0.034	0.0027	0.005	0.0021
$AOCM_p$	2 – 4.75	0.034	0.0025	0.006	0.0040
$AOCM_{pcc}$	2 – 4.75	0.027	0.0056	0.003	0.0031
Activated alumina	1.4 – 2.41	0.025	0.0043	0.004	0.0024
Bioretention soil media	0.001 – 10	0.002	0.0003	0.0002	0.0002
Iron coated perlite	0.3 – 0.85	0.025	0.0027	0.008	0.0032
Expanded shale a	2 – 10	0.005	0.0013	0.0004	0.0003
Expanded shale b	0.45 – 4.5	0.016	0.0054	0.0009	0.0006

AOCM in the size range of 2 – 4.75 mm
Insignificant net capacity for Tire crumb (a, b) and Zeolite-Perlite-GAC, for which rate of adsorption/desorption were equal ($P \leq 0.05$).

Table 4-6. The sorption kinetics parameters for AOCM and UCM and water chemistry matrices shown in Table 4-2.

Media	Rainfall - Runoff				Wastewater			
	q_e [mg/g]	k [g/mg·min]	χ^2	RMSE	q_e [mg/g]	k [g/mg·min]	χ^2	RMSE
$AOCM_c$	0.28	0.063	0.002	0.003	1.25	0.009	0.221	0.100
UCM_c	0.04	3.56	0.003	0.001	0.05	0.30	0.004	0.003
$AOCM_p$	0.27	0.011	0.013	0.006	0.55	0.007	0.109	0.022
UCM_p	0.024	0.85	0.006	0.002	0.077	0.074	0.009	0.004
$AOCM_{pcc}$	0.30	0.036	0.039	0.007	1.29	0.022	0.200	0.106
UCM_{pcc}	0.24	0.036	0.014	0.009	1.35	0.011	0.122	0.071

AOCM in the size range of 2 – 4.75 mm;
Runoff: $C_0 = 2.7 \pm 0.1$ mg/L;
Wastewater: $C_0 = 11.1 \pm 0.2$ mg/L.

Table 4-7. Parameters of 2nd order potential driving model in synthetic runoff, rainfall-runoff and wastewater with the same C_0 of 2.7 mg/L

Media		$AOCM_c$	$AOCM_p$	$AOCM_{pcc}$
Synthetic runoff	q_e [mg/g]	0.26	0.30	0.31
	k [g/mg·min]	0.18	0.046	0.12
	χ^2	0.010	0.004	0.045
	RMSE	0.009	0.004	0.025
	ΔpH	0.56	0.49	4.18
Rainfall - Runoff	q_e [mg/g]	0.28 (108%)*	0.27 (90%)	0.30 (97%)
	k [g/mg·min]	0.063 (35%)	0.011 (24%)	0.036 (30%)
	χ^2	0.002	0.013	0.039
	RMSE	0.003	0.006	0.007
	ΔpH	0.42	0.40	4.29
Wastewater	q_e [mg/g]	0.25 (96%)	0.26 (87%)	0.37 (119%)
	k [g/mg·min]	0.083 (46%)	0.011 (24%)	0.041 (34%)
	χ^2	0.030	0.027	0.071
	RMSE	0.012	0.009	0.027
	ΔpH	0.49	0.35	3.17

* % as compared to that of synthetic runoff;
AOCM in the size range of 2 – 4.75 mm;
C_0 of synthetic runoff and wastewater was adjusted to the same level as that of rainfall-runoff, i.e. 2.7 mg/L.

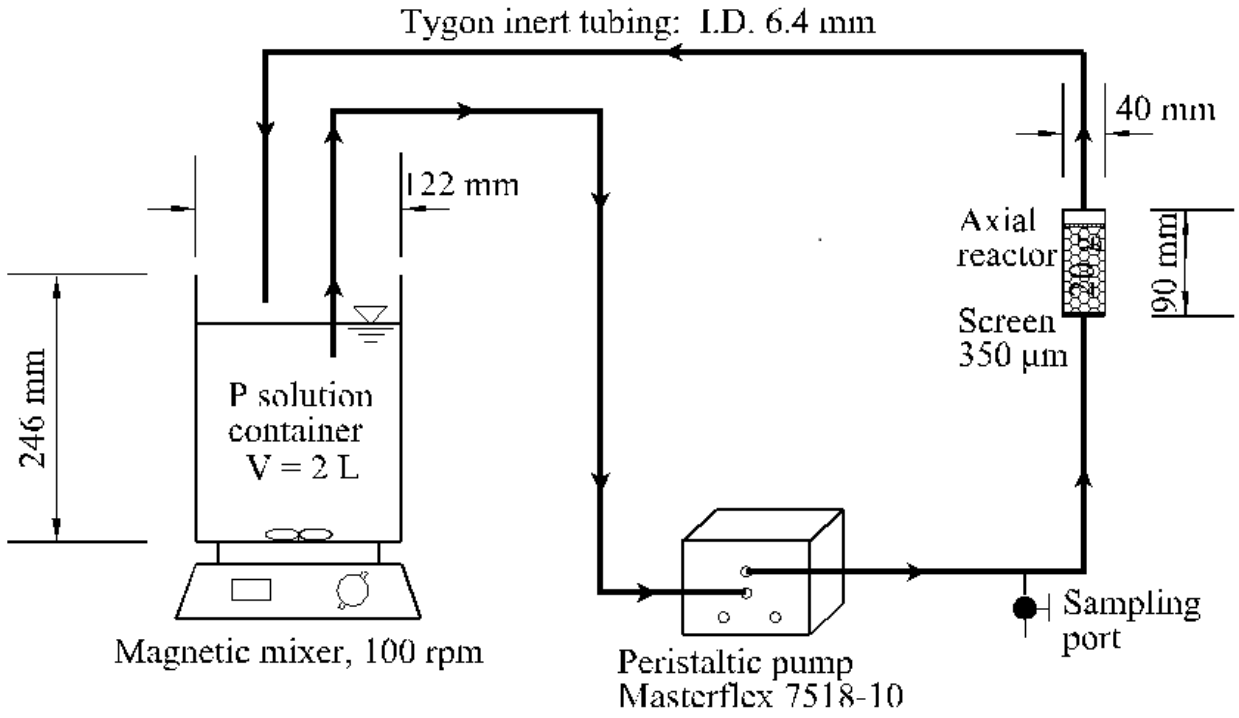

Figure 4-1. Schematic experimental configuration of kinetic tests on media.

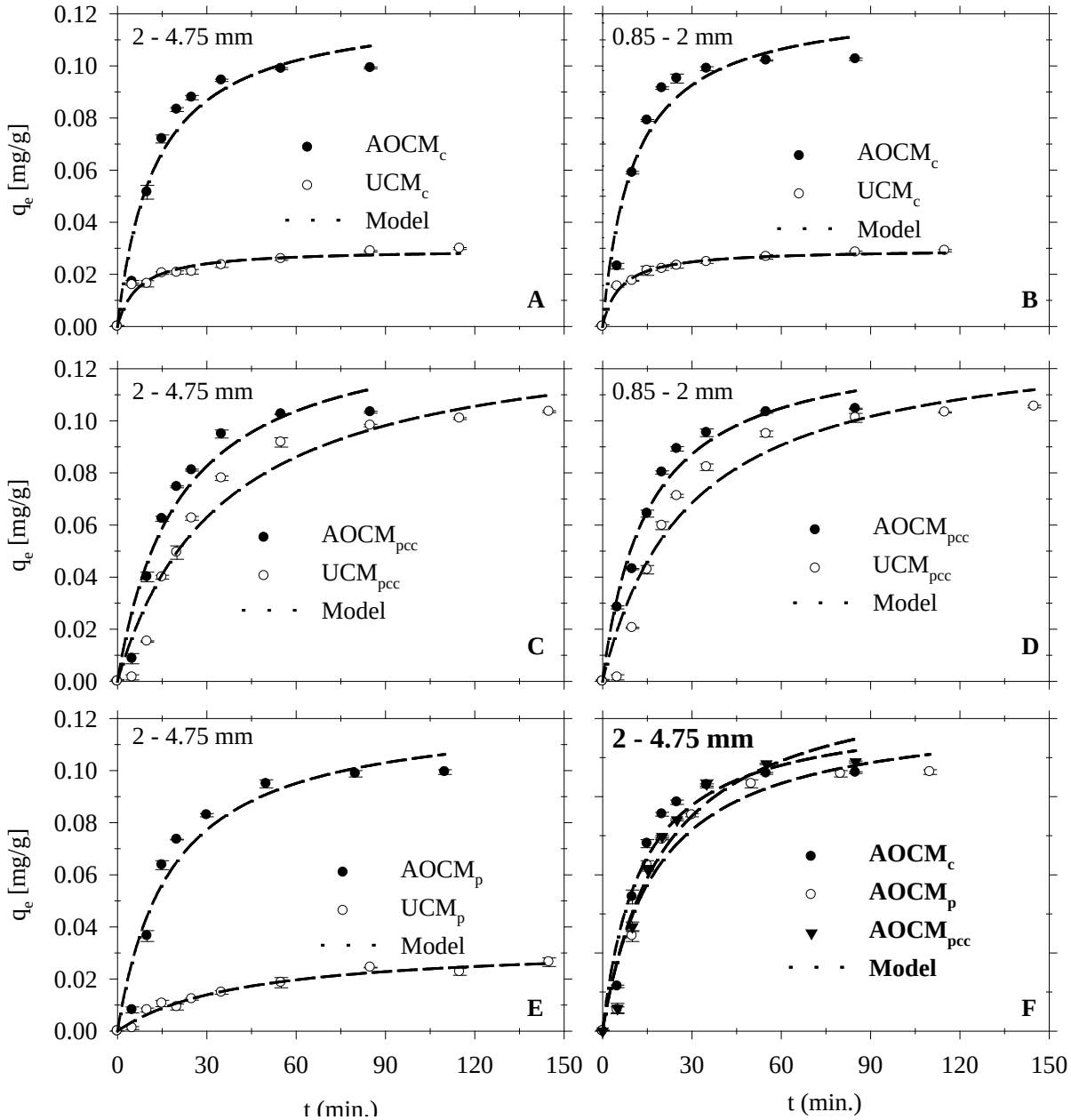

Figure 4-2. A) - E): Kinetics of P mass transfer with AOCM and UCM in synthetic runoff, C_0 = 1.0 mg/L, modeled utilizing a 2nd order potential driving model; F): Kinetics of P mass transfer for different AOCM in synthetic runoff, C_0 = 1.0 mg/L.

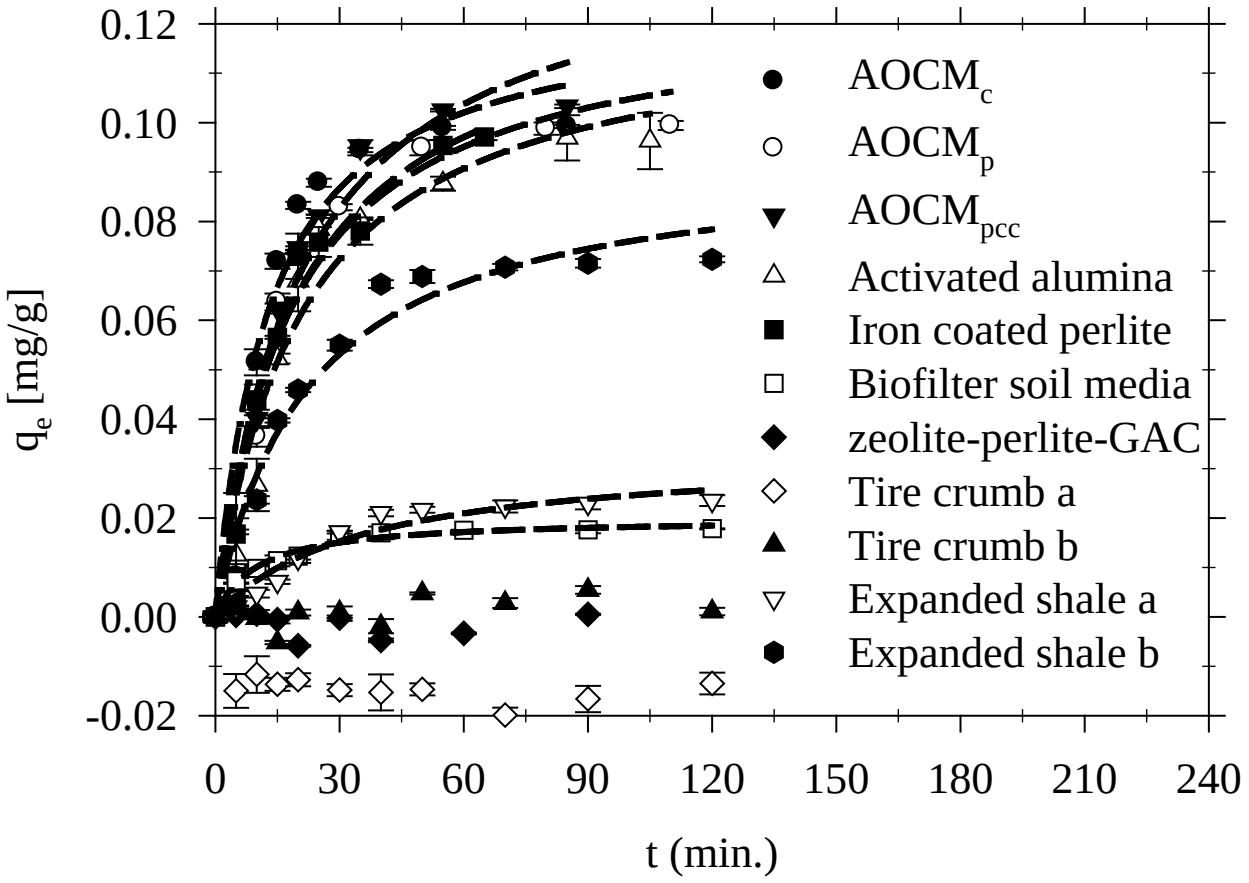

Figure 4-3. Kinetics of P mass transfer for suite of media tested in a synthetic runoff matrix (C_0 = 1.0 mg/L). All kinetics data are modeled using a 2nd order potential driving model; with exception of zeolite-perlite-GAC media and tire crumb (Black & Gold) where net rate of P mass transfer is not significantly different than 0 ($P \leq 0.05$).

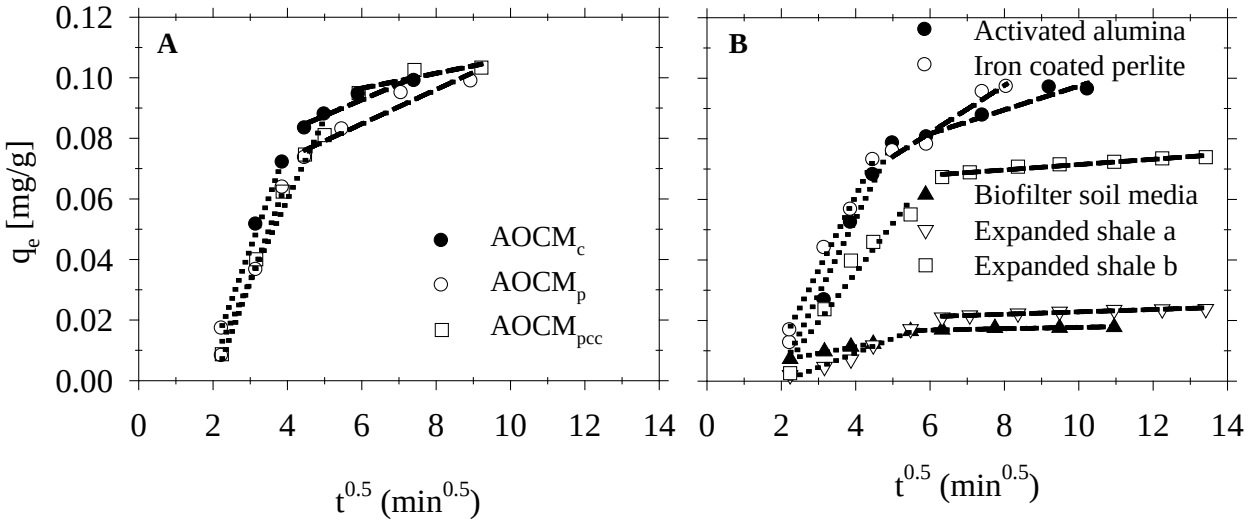

Figure 4-4. Root time plot for P transfer for suite of media tested in a synthetic runoff matrix (C_0 = 1.0 mg/L), with exception of zeolite-perlite-GAC media and tire crumb (Black & Gold) where net rate of P mass transfer is not significantly different than 0 ($P \leq 0.05$).

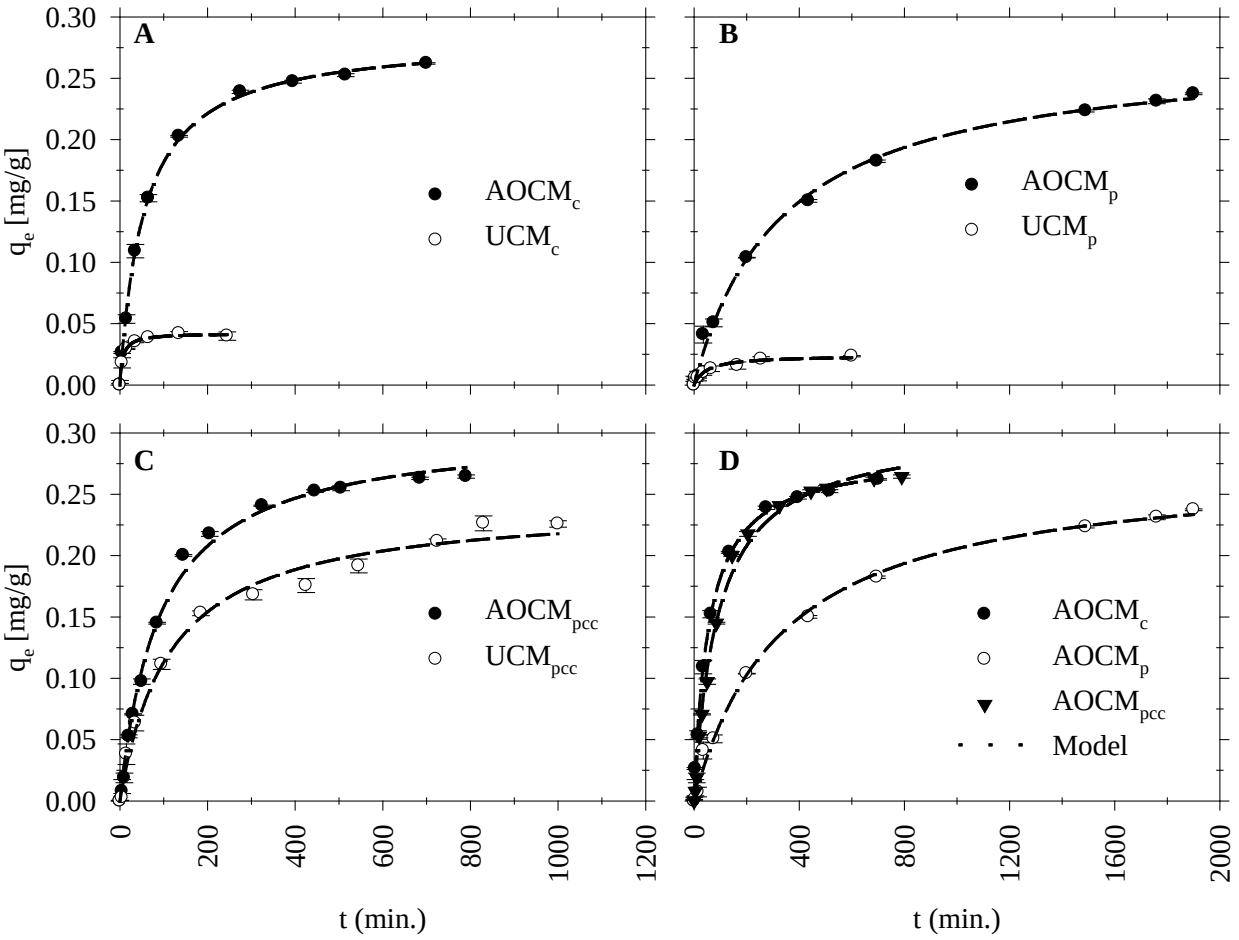

Figure 4-5. Mass transfer kinetics of P onto AOCM and UCM in a Rainfall-runoff matrix with C_0 = 2.7 mg/L utilizing a 2nd order potential driving model.

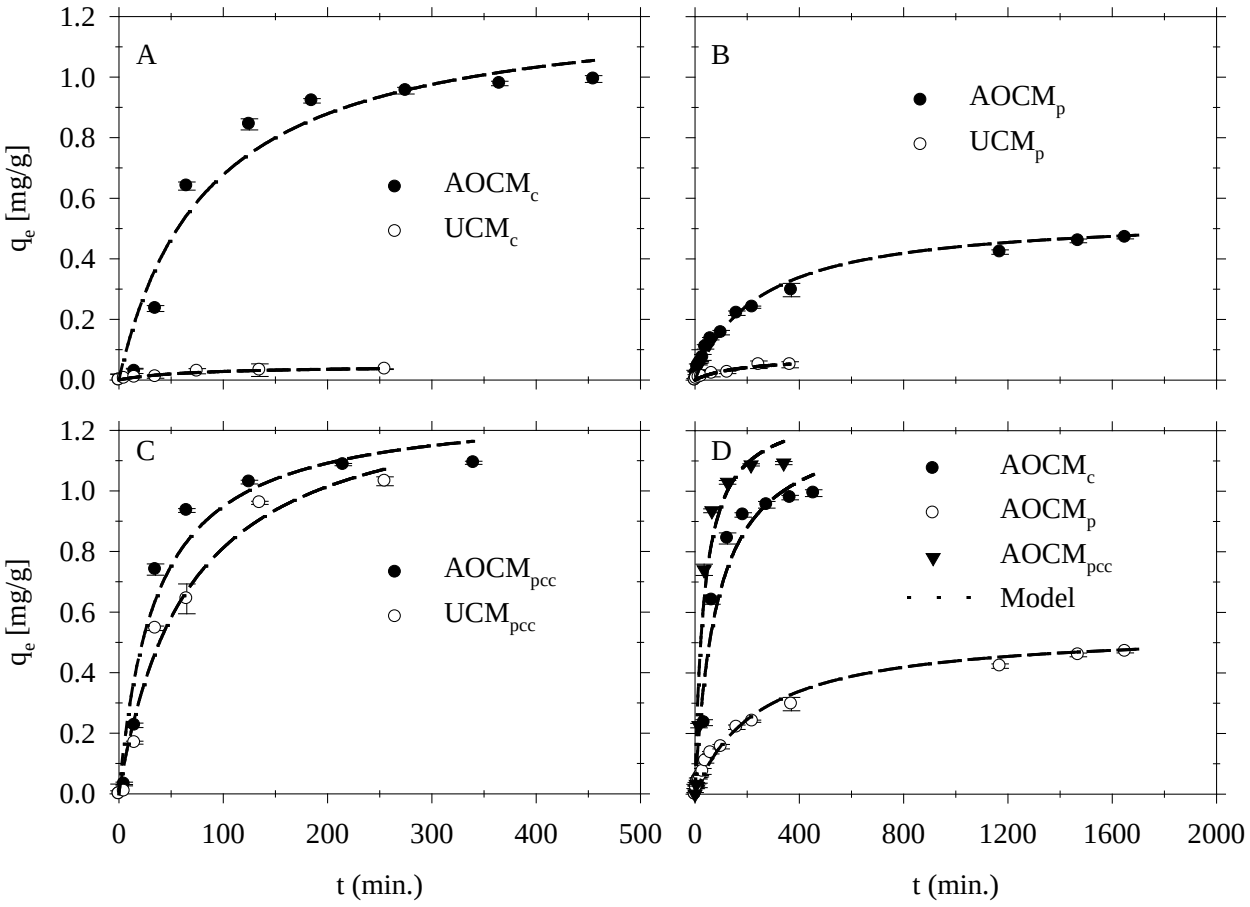

Figure 4-6. Mass transfer kinetics of P onto AOCM and UCM in a wastewater matrix with C_0 = 11.1 mg/L utilizing a 2nd order potential driving model.

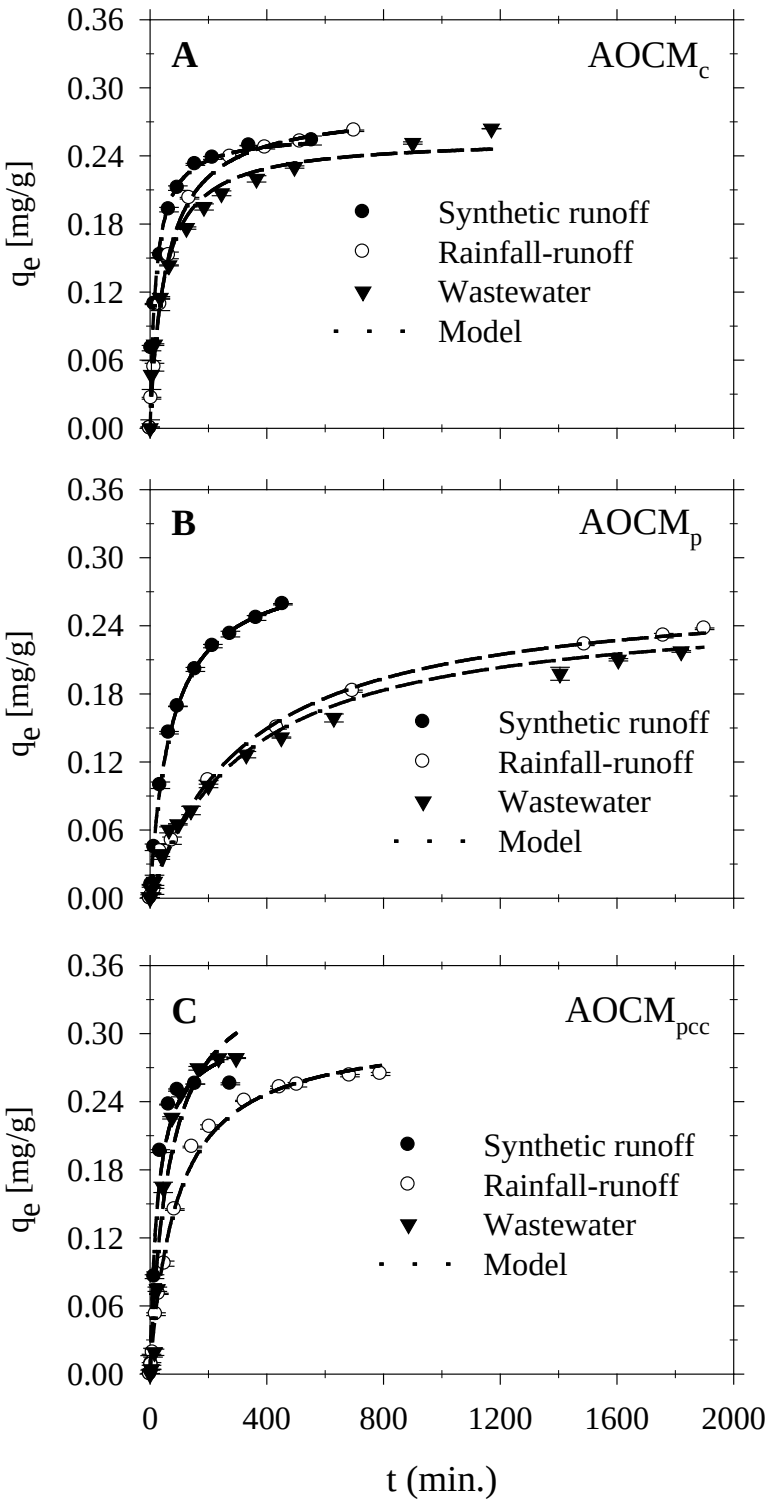

Figure 4-7. Mass transfer kinetics for P onto AOCM comparing kinetics between aqueous matrices. Data are modeled utilizing a 2nd order potential driving model, C_0 = 2.7 mg/L for all aqueous matrices.

CHAPTER 5
BREAKTHROUGH OF PHOSPHORUS FROM GRANULAR FILTER METERIALS

Background

Phosphorus is often identified as the most limiting element and a primary cause of eutrophication (Gomez et al., 1999; Aldridge and Ganf, 2003; Yoshida et al., 2004; Bowes et al. 2005). As an major non-point source and pathway of nutrients, high phosphorus loadings of urban runoff can elevate the tropic level in receiving water (USEPA 1993, Kim et al. 2008). While WEF/ASCE (1998) documented that the event mean concentration (EMC) for total phosphorus (TP) 0.33 mg/L and dissolved phosphorus is 0.12 mg/L; it has been reported that EMC of TP in urban runoff ranged from 0.03 to 5.29 mg/L (Davis, 2007) and for highway runoff the median TP ranged from 0.19 to 1.8 mg/L (Drapper et al., 2000). Dean et al. (2005) reported that urban runoff transported DP from 0.3 to 1.4 mg/L (EMC) in an urban pavement catchment. A desired goal for prevention of plant nuisances in flowing waters not discharging directly to lakes or impoundments is 0.1 mg/L (USEPA, 1986). Oğuz (2005) reported that TP concentration over 0.03 mg/L will likely trigger algal blooms in confined water bodies. Given that runoff discharges of TP from urban land uses can be an order of magnitude higher than levels required to trigger algal blooms, there is a focus on control strategies (after source controls) to separate TP and DP from runoff discharges to receiving waters.

The utilization of filter media as a control strategy for DP has been a long-term interest for wastewater (Pollio and Kumin, 1968; Boari et al., 1976; Yoshida, 1983; Zhao and Sengupta, 1997) and more recently for urban runoff (Gray et al., 2000; Lin and Yang, 2002; Mortula et al., 2007, Sansalone and Ma 2009). While many of these media

have been non-engineered substrates such as sand or perlite with filtration potential but little adsorptive capacity (Bubba et al., 2003; Forbes et al., 2004; Wu et al., 2008); more recent engineered media with Fe or Al coating have shown significantly improved adsorptive capacity in comparison (Ayoub et al., 2001; Arias et al., 2006; Boujelben et al., 2008; Sansalone and Ma 2009). While the most common metric for adsorptive media capacity is the equilibria isotherm (Lee et al., 2003), successful employment of adsorption for phosphorus removal requires breakthrough analysis (Metcalf and Eddy 2003). Application of batch equilibria is often difficult to apply to flowthrough media-based adsorption system without kinetics data and application of so-called single-point "isotherms" represent a further mis-representation of such media-based adsorption (Sperlich et al. 2005, Sansalone and Ma 2009). Breakthrough testing of media utilizing axial bench-scale physical models permits a comparison of media and an economical and controlled method to determine media parameters at a given surface loading rate (SLR). While it is recognized that the most common surrogate aqueous matrix, de-ionized (D.I.) water, does not reproduce the complex interactions of rainfall-runoff, this matrix is a consistent and reproducible matrix for media testing and facilitating media comparisons subject to controlled variations in loading conditions (Namasivayam and Sangeetha, 2004; Arias et al., 2006; Georgantas and Grigoopoulou, 2007; Boujelben et al., 2008). Hence, although studies with a surrogate matrix such as DI water can provide a comparative basis for media, media phenomena and model parameters such as media breakthrough, a comparative assessment utilizing the actual aqueous matrices such as rainfall-runoff and wastewater is needed.

Beyond equilibria, media capacity for a solute can be represented through breakthrough modeling under a known set of loading conditions (Köse and Öztürk, 2008). The time (or more appropriately volume treated) until a set breakthrough or exhaustion level are commonly-reported characteristics of a given media, system and set of loading conditions; while there has been more limited analytical model development to describe breakthrough in time and throughout the media profile (Aksu et al., 2007) unless carried out with an advective-dispersive numerical model (Liu et al. 2005). However, introduction of lumped system parameters and constrained correlations have provided tractable analytical models for one-dimensional flow systems (Lee et al., 2000; Ko et al., 2001; Aksu et al., 2007). One such bed depth service time (BDST) model is the Thomas model that has been widely used in the design of fixed bed adsorption systems (Rao and Viraraghavan, 2002; Thirunavukkarasu et al., 2003; Aksu and Gönen, 2004; Aksu et al., 2007; Köse and Öztürk, 2008; Pokhrel and Viraraghavan, 2008; Sivakumar and Palanisamy, 2009). The main advantages of the Thomas model are simplicity and reasonable accuracy in predicting media breakthrough behavior for adsorptive media. Additionally the kinetics coefficient and adsorption capacity from the model can be determined from monitored data. Typically examined for a single SLR, examination across a range of SLRs can extend the use of the Thomas model to incorporate behavior subject to unsteady phenomena, for example for a fixed bed media absorber utilized after an equalizing or primary treatment operation of runoff (Erickson et al., 2007). While there have been many studies regarding the use of such models (Koh et al., 1998; Aksu and Gönen, 2004; Mantovaneli et al., 2004; Aksu

et al., 2007; Köse and Öztürk, 2008), illustrating the relationship between these Thomas model parameters and SLR has not been demonstrated through a physical model.

In this study, an axial media reactor is utilized for treatment of DP in aqueous matrices: surrogate runoff, rainfall-runoff and wastewater. The study hypothesizes that filter media adsorption behavior is significantly different subject to the same controlled loadings. It is further hypothesized that for the AlOx-coated media that media breakthrough behavior is a function of the substrates for the same diameter substrates. Given that a media intended for DP control should not act as a source of DP, desorption behavior is also quantified for each media. For the media tested that illustrate adsorptive capacity, SLR is hypothesized to have a quantifiable impact on breakthrough behavior. Furthermore it is hypothesized that correlations between SLR and Thomas model parameters can be developed for adsorptive media and a comparison of these correlations can illustrate the differing influence of the media substrate.

Materials and Methods

This study examines AlOx-coated engineered media: $AOCM_c$ (clay based), $AOCM_p$ (pumice based), $AOCM_{pcc}$ (Portland cement concrete based) as well as non-engineered media: tire crumb (a, b), expanded shale (a, b), bioretention soil media and Zeolite-perlite-GAC (volumetric ratio: 5:4:1). $AOCM_c$ and $AOCM_p$ is prepared by applying aluminum as surface coating (Sansalone and Ma 2009). $AOCM_{pcc}$ is prepared by adding aqueous $Al(NO_3)_3$ solution (0.5 M) to produce a water:cement ratio of 0.5. This slurry is cured, crused and size-graded. Specific gravity analysis is conducted with a pycnometer (Quantachrome Ultrapycnometer 1000). Bulk density is determined by measuring the dry mass and corresponding volume of the media bed in the column. Surface charge for the media is measured using a potentiometric titration methodology

of Van Raij and Peech (1972). A constant head test is used to determine the hydraulic conductivity as described by Braja (2001). Media characteristics are summarized in Table 5-1.

DP adsorption subject to continuous flow-through loading is investigated in an axial flow with length of 267 mm and internal diameter of 45 mm. With a fixed bed volume of 350 mL, the ratio of packed media length to the reactor internal diameter (L/D) is fixed at 5. The mass of media utilized is dependent on the media. The constant influent flow is supplied by a peristaltic pump. Samples are collected at regular time intervals and effluent DP concentration (C_e) is determined. The axial column configuration is shown in Figure 5-1.

In this study the breakthrough level (V_b) is set to $C_e/C_0 = 0.1$ (effluent $C_e = 0.05$ mg/L) and exhaustion level (V_{exh}) is set to $C_e/C_0 = 0.9$. Breakthrough curve are presented as a function of the number of bed volumes (N_{BV}) treated.

Three aqueous matrices are utilized: (1) synthetic runoff to compare media and develop Thomas model parameters as a function of SLR, (2) primary rainfall-runoff influent, and (3) secondary wastewater sand filter effluent from a local Advanced Wastewater Treatment (AWT) facility. The chemistry of each aqueous matrix is summarized in Table 5-2. All media are tested in synthetic runoff with a constant influent DP (C_0) of 0.5 mg/L and pH of 7 (controlled throughout the experiment) and a SLR fixed at 40 L/min-m^2 based on the SLR data for a paved urban Cincinnati catchment (Sansalone and Teng, 2005). The breakthrough behavior of $AOCM_c$ and $AOCM_{pcc}$ are further examined in a rainfall-runoff and wastewater matrix, respectively.

A phosphorus stock solution is prepared by dissolving anhydrous potassium dihydrogen orthophosphate (KH_2PO_4) powder (Analytical reagent grade, Fisher Scientific) into D.I. water. The stock solution is calibrated to 1000 mg/L concentration, and utilized as standard solution as necessary. Phosphate concentration is measured by a HACH DR/5000 Spectrophotometer using PhosVer 3 Ascorbic Acid Method (Eaton et al., 1998). All measurements are duplicated and repeatability is within ± 5%. Measurements of pH, conductivity and redox are carried out using a calibrated Thermo Scientific Orion 5-Star multi-meter.

The influence of SLR is varied from 10 to 160 L/min-m^2 for the synthetic runoff matrix. This loading range covers the typical SLR of source areas where unit operation and process are applied for in situ treatment (Sansalone and Buchberger, 1997; Liu et al., 2005). Since hydrology and SLR are variable under event-based conditions, a range of EBCT is experienced for the media. EBCT is the entire volume of packed media bed divided by Q, the volumetric flow rate [L/min]. The flow is volumetrically calibrated periodically and any measured variance is less than ±2%. The dry media mass utilized, SLR, and EBCT for each run are summarized in Table 5-3.

After the media reaches exhaustion in axial column adsorption experiments, the solution in the reactor is drained and desorption study is conducted after 24 hours of gravitational drainage so that only residual moisture content remains in the media bed. In desorption tests, the DP solution is replaced with D.I. water and the media loaded at the 40 L/min-m^2. Media bed effluent samples are filtered and analyzed for DP leached from the media bed.

The Thomas model widely used for fixed bed adsorption systems (Viraraghavan and Rao, 2002; Thirunavukkarasu, 2003; Sivakumar and Palanisamy, 2009) has the following form.

$$\frac{C_e}{C_0} = \frac{1}{1 + \exp[\frac{K_T(q_0 m - C_0 V)}{Q}]} \quad (1)$$

C_e is the effluent DP concentration [mg/L], C_0 the influent DP concentration [mg/L], K_T the Thomas rate constant [L/min-mg], q_0 media phase concentration of the solute [mg/g], m the mass of the adsorbent [g], V the throughput volume [L], and Q is the volumetric flow rate [L/min]. Thomas model results are compared to monitored data utilizing the Root Mean Square Error (RMSE). In this expression $Q(q_i)$ is the monitored value and $E(q_i)$ is the modeled value.

$$RMSE = \sqrt{\frac{\sum_{i=1}^{n}[Q(q_i) - E(q_i)]^2}{n}} \quad (2)$$

The fit is also evaluated with a chi-square (χ^2) test. χ^2 measures differences between the modeled and monitored relationship; the smaller the χ^2 the better the fit between monitored and modeled.

$$\chi^2 = \sum_{i=1}^{n} \frac{[O(q_i) - E(q_i)]^2}{E(q_i)} \quad (3)$$

The relationship between the model parameters, K_T (rate parameter) and q_0 (capacity parameter) are examined as a function of SLR for two adsorptive media (media for which adsorption >> desorption). $AOCM_C$ and $AOCM_P$ are chosen since the mass transfer phenomena are primary ligand exchange and do not include surface precipitation that may dominate $AOCM_{pcc}$

Results and Discussions

Phosphorus Breakthrough Profiles in Synthetic Runoff Matrix for Each Media System

Breakthrough profiles are presented by plotting the ratio of effluent P concentration (C_e) to the initial concentration (C_0), C_e/C_0, against time elapsed or N_{BV} treated. Here, 1 BV is fixed at 350 mL for all media tested. Therefore:

$$N_{BV} = \frac{(1000 mL/\mathrm{L})(Q)(t)}{(350\ mL)} \tag{4}$$

In this expression Q [L/min] is the volumetric flow rate and t is elapsed time (min.). The breakthrough curves for AOCM forms and common non-engineered media are shown in Figure 5-2 and 5-3, respectively. Breakthrough curves shown in Figure 5-2 and 5-3 are conducted in synthetic runoff matrix at surface loading rate = 40 L/min-m^2 (EBCT = 5.7 min) with C_0 = 0.5 mg/L.

From Figure 5-2, results indicate that $AOCM_c$ breakthrough occurred at 900 BV and exhaustion is at greater than 4000 BV. In contrast, breakthrough for $AOCM_p$ and $AOCM_{pcc}$ are approximately 90 and 120 BV, respectively. The N_{BV} of exhaustion for $AOCM_p$ is greater than 2000 and 800 for $AOCM_{pcc}$. These results indicate that besides the active AlOx coating the physio-chemical properties of substrates can also impact the engineered media capacity. The effectiveness of AlOx coating for DP removal promotion has been reported in literature and mass transfer of phosphates to hydrous aluminous oxide is through ligand exchange to surface hydroxyl groups, resulting in OH^- release into solution (Genz et al., 2004; Kim and Kirkpatrick, 2004; Arias et al. 2006; Yang et al., 2006; Georgants and Grigoropoulou, 2007; Sansalone and Ma, 2009). In this study, pH of the feeding P solution is fixed at 7 and ionic strength is adjusted to

0.01M with 2 mol/L KCl solution. An increase of effluent pH is observed for $AOCM_c$ and $AOCM_p$ as a result of ligand exchange between surface hydroxyl groups and phosphate ions. A greater pH increase from $AOCM_{pcc}$ is difficult to discern for ligand exchange due to the CaO in the cement concrete substrate. The conductivity of the first 2 or 3 samples were usually higher in the effluent than in the feed solution; and became relatively constant and similar to the influent. The initial enhancement of conductivity can be attributed to the minerals dissolved from the media surface. The amount of such minerals varied with substrates and was more evident for concrete based media ($AOCM_{pcc}$). The redox ranged between 200 to 300 mV and decreased to below 100 mV at the end of each run. Similar redox decline was reported in literature (Onar et al., 1996).

For media with adsorptive capacity (rate of adsorption >> desorption) the Thomas model is used to simulate adsorption breakthrough behavior as shown in Figure 5-2. The model parameters q_0 and K_T are estimated and summarized in Table 5-4. The small values of χ^2 and RMSE indicate that Thomas model predicts the entire breakthrough behavior.

In addition to the engineered media of AOCM, the commonly available media utilized in unit operation and process media deployments, including bioretention soil media, expanded shale (a, b), tire crumb (a, b) and zeolite-perlite-GAC are also tested in the flow-through column reactor using the synthetic runoff matrix. The resulting breakthrough curves are shown in Figure 5-3. While variability does exist; tire crumb, expanded shale, bioretention soil media and zeolite-perlite-GAC are exhausted within a small number of bed volumes, indicating very limited media capacity. With adsorption ≈

desorption such media could not be modeled with the Thomas model. The media breakthrough and exhaustion capacity are summarized in Table 5-3 for each run.

Desorption Experiments

Desorption study with D.I. water are shown in Figure 5-4. Figure 5-4a and 5-4b summarize the DP effluent profiles. Figure 5-4c and 5-4d compares the total amount of DP adsorbed and desorbed per gram of media used. Results indicate that for $AOCM_c$ and $AOCM_p$ little adsorbed phosphorus is released. After the first one to two samples the DP concentration in the effluent is below the detection limit (0.02 mg/L), suggesting strong adsorption bond between adsorbate and adsorbents. However, $AOCM_{pcc}$ did release phosphorus. Due to the high surface pH of $AOCM_{pcc,}$ phosphorus is removed through surface precipitation (Agyei et al., 2002) and adsorption. The results obtained from this study suggested the temporary physical capture and sloughing of the precipitate deposits from the media. Studies have demonstrated that the the age of calcium precipitate is the factor that affects the P mobility. The aging process may take months to form the stable Ca-P (Gomez et al., 1999). Given that the contact time of P with media is less than 6 minutes; and the whole adsorption-desorption test is conducted in 48 hours the precipitated phosphorus can potentially be weakly desorbed as compared to clay and pumice substrates. Figure 5-4b and 5-4d indicates that the very limited DP adsorbed by the commercially available media is a result of weak physical bonds media such as Tire crumb a and Zeolite-perlite-GAC; the amount of DP desorbed is more than adsorbed.

Phosphorus Breakthrough Profiles in Actual Matrix for $AOCM_c$ and $AOCM_{pcc}$

Although tests with a surrogate matrix of D.I. water provide reproducible comparative data on media capacity, water chemistry influences media adsorption

(Shilton et al., 2005; Ádám et al., 2007, Sansalone and Ma 2009). In order to evaluate media behavior in actual aqueous matrices, $AOCM_c$ and $AOCM_{pcc}$ are also tested in rainfall-runoff and wastewater at a SLR of 40 L/min-m^2.. Results are presented in Figure 5-5. Breakthrough and Thomas model results and parameters along with χ^2 and RMSE are summarized in Table 5-4. As shown in Figure 5-5, breakthrough initiated at approximately 390 BVs for $AOCM_c$ in rainfall-runoff and 1200 BVs for $AOCM_{pcc}$ in wastewater. When comparing the media capacity at breakthrough (X/M_b) of $AOCM_c$ in Table 5-3, the results indicate that media capacity when loaded by rainfall-runoff decreased more than 50% with an X/M_b (0.41 mg/g) as compared to the synthetic matrix (0.94 mg/g), while the inlet DP concentration were the same as 0.5 mg/L. Results suggest the role of competitive interactions, primarily SO_4^{2-} (Sansalone and Ma, 2009), have a significant effect on $AOCM_c$ breakthrough behavior. In contrast, wastewater chemistry and a Ca-rich substrate increased both breakthrough (X/M_b, 0.79 mg/g) and exhaustion (X/M_{exh}, 2.35 mg/g) capacity of $AOCM_{pcc}$ as compared to synthetic runoff matrix (X/M_b, 0.06 mg/g; X/M_{exh}, 0.23 mg/g). Additionally, $AOCM_{pcc}$ did not reach breakthrough until 1200 BVs and exhaustion occurred at greater than 7000 BVs. This breakthrough phenomena exhibited by $AOCM_{pcc}$ in wastewater, along with the desorption results; strongly indicate the occurrence of surface precipitation. Unlike clay and pumice substrates with ligand exchange as dominant mechanism, surface precipitation is important for $AOCM_{pcc}$ due to the high content of CaO. Furthermore, surface precipitation is promoted by the high concentration of Ca^{2+} in wastewater, resulting in the high capacity as shown in Figure 5-5b.

Effect of Flow Rate/Surface Loading Rate on Media Breakthrough Curves

The effect of SLR on DP adsorption of $AOCM_c$ and $AOCM_p$ is examined by varying the surface loading rate from 10 to 160 L/min-m^2, while the influent DP concentration is held constant at 0.5 mg/L. The plots of comparative normalized DP concentration versus number of bed volume treated at different SLR are given in Figure 5-6. SLR has a direct impact on contact time with media and hence influences removal efficiency, especially when the adsorption is diffusion controlled (Genç-Fuhrman et al., 2005). The EBCT ranged from 22.6 to 1.4 min as SLR is varied from 10 to 160 L/min-m^2. As shown in Figure 5-6, the breakthrough curves became steeper and shifted towards the origin with increasing SLR while both the media breakthrough and exhaustion time decreased. As a result, the solute does not have enough time to interact with the sorbate and diffuse into the pores. For example, at a surface loading rate of 10 L/min-m^2, more than 2000 bed volumes of solution can be treated before $AOCM_c$ breakthrough. When the surface loading rate increased to 160 L/min-m^2, the breakthrough occurred at less than 500 bed volumes. Table 5-3 summarizes breakthrough and exhaustion capacity of $AOCM_c$ and $AOCM_p$ at different SLRs and both X/M_b and X/M_{exh} decreased with increasing loading rates. Similar results were obtained from other adsorption studies (Aksu and Gönen, 2004; Genç-Fuhrman et al., 2005; Malkoc and Nuhoglu, 2006; Aksu et al., 2007).

The data at various SLRs are also fit to the Thomas model to determine the Thomas rate constant (K_T) and maximum media concentration (q_0). All the parameter values are listed in Table 5-4. The goodness of fit is evaluated with χ^2 and RMSE. Breakthrough curves modeled at all SLRs reproduce monitored data. As SLR increases,

the value of K_T increases and q_0 decreases. These results are in agreement with the literature (Mantovaneli et al., 2004; Malkoc and Nuhoglu, 2006; Aksu et al., 2007).

Correlations between SLR and Thomas Model Parameters

DP mass transfer processes from an aqueous solution to media is dynamic involving external mass transfer, film diffusion, and intra-particle diffusion. Given that these multiple processes occur simultaneously, simulating every process will require a numerical solution unless these processes can be lumped as a function of a primary system parameter for a given media.

It is hypothesized that volumetric flow rate (as SLR) is the primary system parameter that influences external mass transfer mechanisms, such as axial dispersion and film diffusion, but may be less significant for intra-particle (media) mass transport at small contact times; for example intra-event runoff loadings times as compared to longer inter-event times (Koh et la., 1998; Lee et al., 2003, Liu et al. 2005). The intra-event significant of intra-particle diffusion at a given SLR is also dependent on the pore size distribution in the media. In the Thomas model, the rate constant (K_T), characterizing the rate of solute transfer from liquid to media phase, increases with SLR, indicating the influence of external mass transfer on system kinetics. It is further hypothesized that this relationship is a function of the adsorptive media. Results indicate that in a 1-dimensional flow system with adsorptive media ($AOCM_C$ or $AOCM_P$) that K_T is proportional to SLR; and the following relationship is proposed across the flow rate range.

$$K_T = \lambda * SLR \tag{5}$$

In this expression SLR is the surface loading rate [L/min-m^2] and λ is a proportionality coefficient [m^2/mg] which is a function of the system and the adsorptive media. λ is determined from K_T values at different SLRs using Equation 5 and is presented in Table 5-5. Results in Figure 5-7 illustrate the proportionality of the relationship between K_T and SLR as described in Equation 7. Results also indicate that the slopes (λ) of each relationship for $AOCM_p$ and $AOCM_c$ are statistically significantly different (at p = 0.05)

The second parameter examined in the Thomas model, q_0 [mg/g], is an index for the media phase capacity for a solute, in this case DP. Ideally, in a 1-dimensional flow system of fixed depth the SLR and contact time with the media are directly related, hence it is hypothesized that not only is the mass transfer rate a function of SLR but so is the media capacity. Both intra-particle and external film resistance play an important role in the adsorption process and the surface reaction (ligand exchange) is not the rate-limiting step. Intra-particle (media) mass transfer rate is positively related with flow contact time (Liu et al. 2005) and there should be an inverse relationship, albeit non-linear, between intra-particle mass transfer rate and SLR. In contrast, a higher SLR will decrease the film resistance and result in an increase in the external mass transfer (Ko et al., 2000). Given the separate and divergent influence of these two mechanisms in response to SLR the following equation is proposed.

$$q_0 = q_m (SLR)^{-n} \quad (6)$$

Here, q_m [mg/g] can be regarded as the theoretical maximum media capacity with infinite contact time, while n represents the influence of SLR. Higher values of n represent a greater influence of SLR on q_0. Both q_m and n are hypothesized to be a

function of the adsorptive media. Therefore an adsorptive media with a high mass transfer rate and equilibrium capacity is expected to have a lower n-exponent as compared to another adsorptive media of a lower mass transfer rate and capacity. The q_0 (determined from monitored data) as a function of SLR is fit with Equation 6 and q_m and n are determined. The results are summarized in Table 5-5. Figure 5-7 illustrates that the relationship provided by Equation 6 predicts q_0. Results also indicate that the n-exponent of each relationship (plotted as log-transformed axes) for $AOCM_p$ and $AOCM_c$ are statistically significantly different (at $p = 0.05$) The relationships of Equation 5 and 6 as a function of the primary operating parameter, SLR can represent the breakthrough of $AOCM_c$ and $AOCM_p$, both adsorptive media with a primary mechanism of ligand exchange.

Summary

The breakthrough of influent DP feed at 0.5 mg/L from engineered granular filter media deployed in axial reactors (1 BV = 350 mL and L/D of 5.0), adsorptive media represented by three substrates supporting aluminum oxide, is examined as a function of SLR ranging from 10 to 160 L/min-m^2 with SLR as a surrogate for flow rate. These adsorptive media are compared to common non-engineered media at a fixed SLR of 40 L/min-m^2 with respect to breakthrough and exhaustion capacity and desorption. In these breakthrough and desorption examinations the aqueous matrix utilized is a controlled synthetic runoff matrix of D.I. water, recognizing that while this matrix does not provide the complexity of rainfall-runoff or wastewater, the matrix is consistently reproducible for comparative or parameterization studies.

Results indicate that $AOCM_c$ had higher breakthrough (X/M_b) and exhaustion (X/M_{exh}) capacity as compared to $AOCM_{pcc}$ and $AOCM_p$; $AOCM_c$ largely as a function of the substrate providing higher specific surface area for the AlOx. While $AOCM_{pcc}$ has a higher breakthrough capacity than $AOCM_p$ the exhaustion capacity is lower; both of these results a function of surface precipitates and the instability thereof at the $AOCM_{pcc}$ surface, in addition to ligand exchange generated by the AlOx. In contrast the primary adsorption mechanism of $AOCM_c$ and $AOCM_p$ is ligand exchange.

Results indicate the non-engineered media has very limited DP breakthrough capacity (adsorption rate ≈ desorption rate) compared to the AlOx adsorptive media. Leaching results using D.I. water at a pH of 7.0 and an SLR of 40 L/min-m^2 indicate that a significant, in some cases a predominant fraction of DP adsorbed, is subsequently leached despite a 24 hour inter-event time providing for intra-particle mass transfer. In contrast, all of the three AOCM exhibit low desorption with $AOCM_c$ providing the lowest leaching concentrations and $AOCM_{pcc}$ providing a higher but nominal level of leaching from surface precipitates. Comparing breakthrough results between the synthetic matrix and rainfall-runoff or wastewater matrices for $AOCM_c$ and $AOCM_{pcc}$ respectively; results illustrate differing behavior. Competing solutes reduce the breakthrough capacity of $AOCM_c$ primarily functioning through ligand exchange. In contrast, the additional mechanism of calcium-based precipitation by $AOCM_{pcc}$ generated by the CaO on the hydrated cementitious surface and the higher Ca concentrations in solution results in an increase in breakthrough capacity for $AOCM_{pcc}$ in wastewater. Results indicate that the surface properties of the media whether providing ligand exchange or a separate

mechanism such as chemical precipitation must be considered in conjunction with the aqueous matrix.

SLR ranging from 10 to 160 L/min-m^2, typical of SLRs to runoff filter systems, is a primary explanatory variable for DP breakthrough from adsorptive media. Increasing SLR results in consistently lower BVs at breakthrough and exhaustion levels. The Thomas model reproduced physical model data across all SLRs. The Thomas model rate constant (K_T) and media-phase capacity (q_0) are a function of SLR for a given adsorptive media; media where the adsorption rate >> desorption rate or media that did not include a significant surface precipitation mechanism in addition to an exchange reaction. Mathematical relationships (linear and power law) to SLR are demonstrated for K_T and q_0, respectively. The proportionality constants relating K_T and SLR are significantly different ($p = 0.05$) as are the power law exponent relating q_0 and SLR for the adsorptive media tested.

Nomenclature

AOCM: Aluminum oxide coated media

$AOCM_c$: Aluminum oxide coated media with clay as raw substrate

$AOCM_p$: Aluminum oxide coated media with pumice as raw substrate

$AOCM_{pcc}$: Aluminum oxide media with Portland cement concrete as raw substrate

B&G: Black & gold

BV Bed volume (mL)

C_0: The initial DP concentration (mg/L)

C_e: DP concentration at equilibrium (mg/L)

DI water: De-ionized water

DP: Dissolved phosphorus

EBCT	Empty Bed Contact Time (min)
$E(q_i)$	Expected value
K_T	Thomas rate constant (L/min-mg)
m:	The dry mass of media used (g)
n	Capacity coefficient of surface loading rate
N_{BV}	Number of bed volume
pH_{pzc}:	pH of point of zero charge
q_0	Solid media phase concentration of DP (mg/g)
q_m	Maximum media capacity with infinite contact time (mg/g)
Q	Volumetric flow rate (L/min)
$Q(q_i)$:	Observed value
RMSE:	Root Mean Square Error
SLR	Surface Loading Rate (L/min-m^2)
V	Throughput volume (L)
V_0:	The packed media volume (L)
V_b	number of bed volume (N_{BV}) treated at breakthrough level of $C/C_0 = 0.1$
V_{exh}	number of bed volume (N_{BV}) treated at exhaustion level of $C/C_0 = 0.9$
X/M_b	Breakthrough capacity at $C/C_0 = 0.1$
X/M_{exh}	Exhaustion capacity at $C/C_0 = 0.9$
χ^2:	Chi-square
λ	Proportionality coefficient [m^2/mg], representing conversion constant between surface loading rate and Thomas rate constant

Table 5-1. Media characteristics

Media		Size [mm]	Specific gravity (at 20°)	Bulk density [g/cm^3]	Hydraulic conductivity [cm/s]	pH_{pzc}
$AOCM_c$		2.0 – 4.75	2.29 ± 0.04	0.43 ± 0.04	882 ± 24	4.61 ± 0.06
$AOCM_p$		2.0 – 4.75	2.27 ± 0.01	0.66 ± 0.06	936 ± 18	4.59 ± 0.10
$AOCM_{pcc}$		2.0 - 4.75	2.67 ± 0.04	0.89 ± 0.03	912 ± 14	11.84 ± 0.16
Bioretention soil media		0.001 – 10	2.69 ± 0.03	1.35 ± 0.12	6 ± 1	6.35 ± 0.03
Zeolite-Perlite-GAC		2.29 – 9.65	2.02 ± 0.01	0.71 ± 0.08	864 ± 12	7.51 ± 0.04
Expanded shale	a	2 – 10	1.91 ± 0.02	0.81 ± 0.06	1098 ± 12	9.84 ± 0.10
	b	0.45 – 4.5		0.86 ± 0.05	384 ± 6	
Tire Crumb (B & G)	a	0.85 – 10	1.19 ± 0.04	0.53 ± 0.07	138 ± 3	8.58 ± 0.08
	b	0.5 – 4.75		0.65 ± 0.06	30 ± 6	

$AOCM_c$ = Aluminum Oxide Coated Media, clay based
$AOCM_p$ = Aluminum Oxide Coated Media, pumice based
$AOCM_{pcc}$ = Aluminum Oxide Coated Media, Portland cement concrete based
pH_{pzc} = pH at point of zero charge
Entries are mean ± standard deviation (n = 3)

Table 5-2. Water chemistry of experimental matrix

Matrix	Synthetic runoff	Rainfall-runoff (Event on 05/16/08)	Wastewater (Secondary effluent)
pH	7.00 ± 0.05	7.11 ± 0.07	7.13 ± 0.08
Conductivity [µs/cm]	1025 ± 56	218 ± 12	812 ± 6
Turbidity [NTU]	0.83 ± 0.46	2.80 ± 1.02	3.24 ± 0.22
Alkalinity [mg/L] as $CaCO_3$	5.4 ± 0.8	74 ± 2	66 ± 1
Ionic Strength [M]	0.010 ± 0.002	0.004 ± 0.002	0.013 ± 0.001
DOC [mg/L]	0.3 ± 0.1	28.9 ± 3.6	12.4 ± 2.8
Ca^{2+}	BDL[a]	25.45 ± 1.26	60.52 ± 7.36
NO_3^--N	0.45 ± 0.08	3.08 ± 0.15	1.52 ± 0.08
SO_4^{2-}	0	10.06 ± 1.08	118 ± 2
Cl^- [b]	360 ± 10	8.05 ± 0.15	92 ± 7
HCO_3^-	3.3 ± 0.7	45.1 ± 1.2	29.3 ± 2.1

* Data are mean ± standard deviation
[a] BDL: Below Detection Limit ()
[b] 0.01M KCl was used to adjust the ionic strength of synthetic runoff

Table 5-3. Load-response parameters for a suite of media utilizing water chemistry matrices shown in Table 5-2 and an axial reactor

Media	Matrix	Mass (g)	SLR [L/min-m^2]	EBCT (min.)	X/M_b [mg/g]	X/M_{exh} [mg/g]	V_b	V_{exh}
			10	22.6	2.38	>4.17	2300	>5800
			20	11.3	1.24	>2.83	1200	>4000
$AOCM_c$		160	40	5.7	0.94	>2.45	900	>3500
			80	2.8	0.85	>2.33	860	>3500
			160	1.4	0.53	>1.93	400	>3200
			10	22.6	0.58	1.71	830	4600
			20	11.3	0.32	>0.96	480	>2200
$AOCM_p$		240	40	5.7	0.06	>0.69	90	>1200
			80	2.8	0.03	>0.52	60	>1600
			160	1.4	0.005	>0.32	5	>1000
$AOCM_{pcc}$	Synthetic runoff	313			0.06	0.23	120	800
Bioretention soil media		470			<0.001	0.0031	<1	25
ZPG		200			<0.001	0.0013	<1	5
Tire Crumb (B & G) a		186			<0.001	0.0012	<1	5
Tire Crumb (B & G) b		227	40	5.7	<0.001	0.0024	<1	10
Expanded Shale a		284			<0.001	0.0021	<1	8
Expanded Shale b		302			<0.001	0.0073	1	35
$AOCM_c$	Rainfall-runoff	160			0.41	1.09	390	1800
$AOCM_{pcc}$	Wastewater	313			0.79	> 2.35	1200	> 7300

Axial reactor: L/D = 5;
D (internal diameter of column) = 4.5 cm;
1 bed volume = 350 mL (pore volume equivalent varies with media);
$pH_{influent}$ = 7.0 ± 0.2;
C = Effluent DP concentration, [mg/L]
C_0 = Influent DP concentration, 0.5 mg/L
SLR = Surface Loading Rate [L/min-m^2]
EBCT = Empty Bed Contact Time;
X/M_b = breakthrough capacity at $C/C_0 = 0.1$;
X/M_{exh} = exhaustion capacity at $C/C_0 = 0.9$;
V_b = number of bed volume (N_{BV}) treated at breakthrough level of $C/C_0 = 0.1$;
V_{exh} = number of bed volume (N_{BV}) treated at exhaustion level of $C/C_0 = 0.9$;
> breakthrough capacity is larger than the stated values(the experiment terminated before $C/C_0 = 0.9$)

Table 5-4. Thomas model parameters for AOCM forms utilizing water chemistry matrices shown in Table 5-2 and goodness-of- fit indices between modeled and monitored results

Media	Matrix	SLR [L/min-m^2]	q_0 [mg/g]	K_T ($\times 10^{-3}$) [L/min-mg]	χ^2	RMSE
		10	4.21	0.107	0.497	0.026
		20	2.93	0.236	0.169	0.021
$AOCM_c$		40	2.59	0.480	0.168	0.030
		80	2.37	0.939	0.479	0.058
		160	1.95	1.850	0.192	0.041
	Synthetic runoff	10	1.66	0.108	0.729	0.043
		20	0.97	0.365	0.408	0.049
$AOCM_p$		40	0.69	0.763	0.391	0.049
		80	0.51	1.956	0.243	0.054
		160	0.33	4.555	0.073	0.049
$AOCM_{pcc}$		40	0.24	2.293	0.048	0.035
$AOCM_c$	Rainfall-runoff	40	1.08	1.174	0.063	0.017
$AOCM_{pcc}$	Wastewater	40	2.88	0.184	0.318	0.053

RMSE = Root Mean Square Error;
χ^2 = chi-square.

Table 5-5. Relationships between Thomas model parameters and surface loading rate

Media	q_0 [mg/g] ($q_0 = q_m(SLR)^{-n}$)				K_T [L/min-mg] ($K_T = \lambda * SLR$)		
	q_m [mg/g]	n	χ^2	RMSE	λ ($\times 10^{-5}$)	χ^2 ($\times 10^{-6}$)	RMSE ($\times 10^{-5}$)
$AOCM_c$	7.55	0.278	0.072	0.211	1.16	1.46	1.02
$AOCM_p$	6.64	0.614	0.021	0.053	2.71	272	22.1

SLR = surface loading rate, [L/min-m^2];
q_0 = solid media phase concentration of DP, [mg/g];
q_m = maximum media capacity with infinite contact time;
n = capacity coefficient of surface loading rate;
K_T = Thomas rate constant [L/min-mg];
λ = proportionality coefficient [m^2/mg], representing conversion constant between surface loading rate and Thomas rate constant.

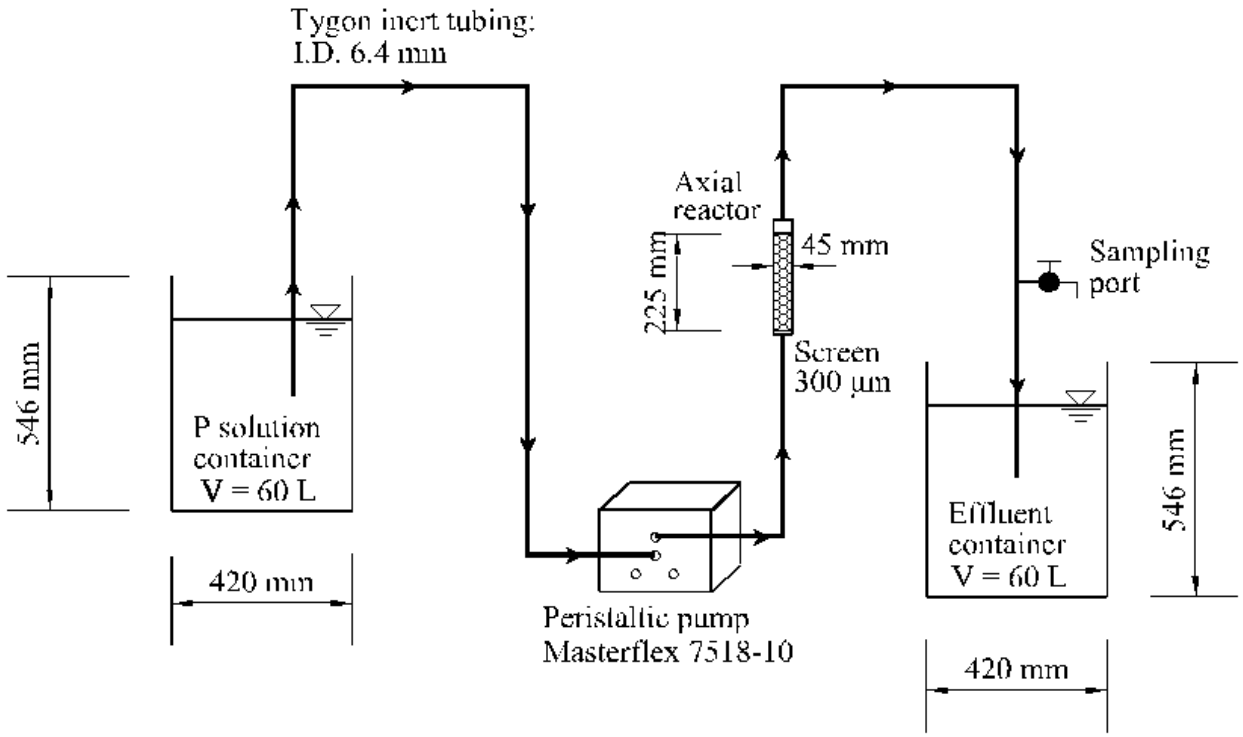

Figure 5-1. Schematic experimental configuration of column breakthrough experiments.

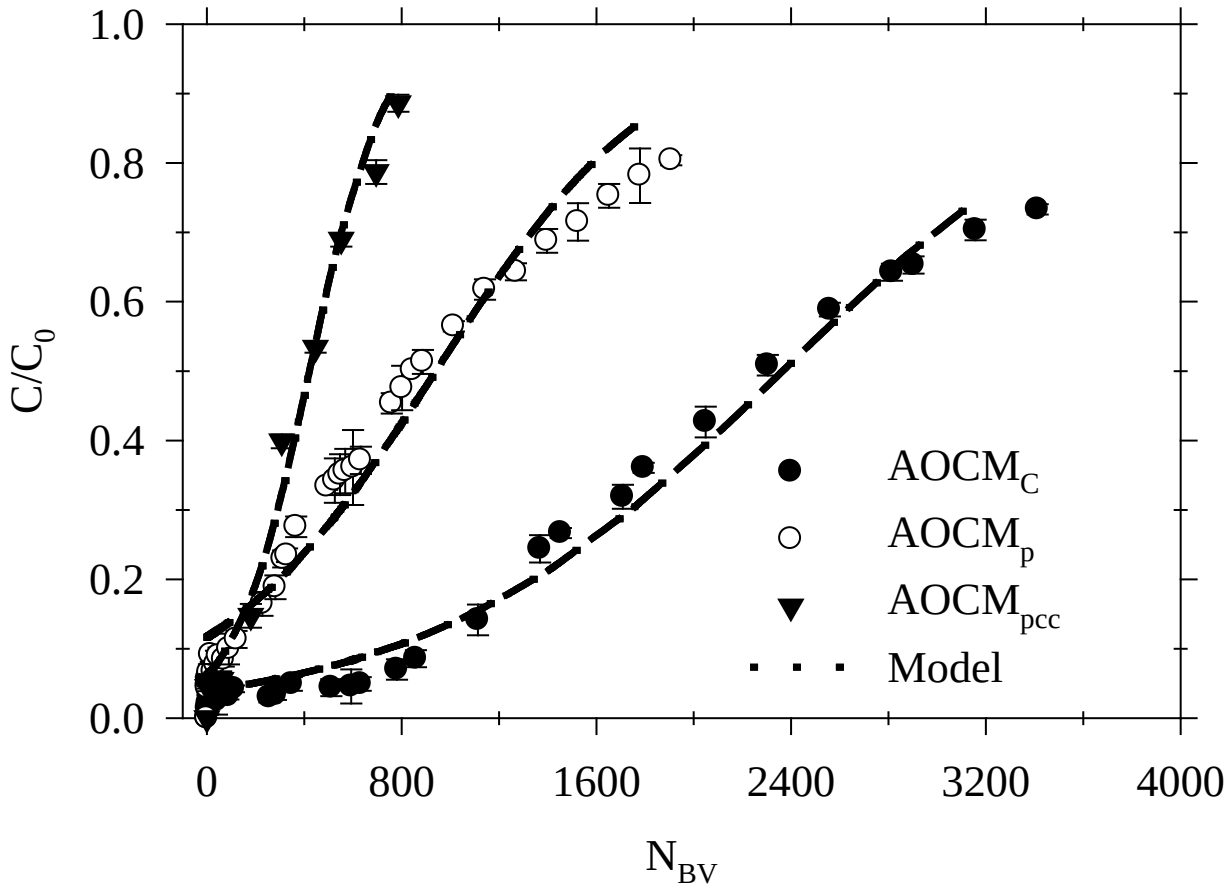

Figure 5-2. Breakthrough curves for AOCM (2 – 4.75 mm) with an influent pH of 7.0 and C_0 of 0.5 mg/L at a surface loading rate of 40 L/min-m^2. Range bar represent standard deviation between duplicate samples.

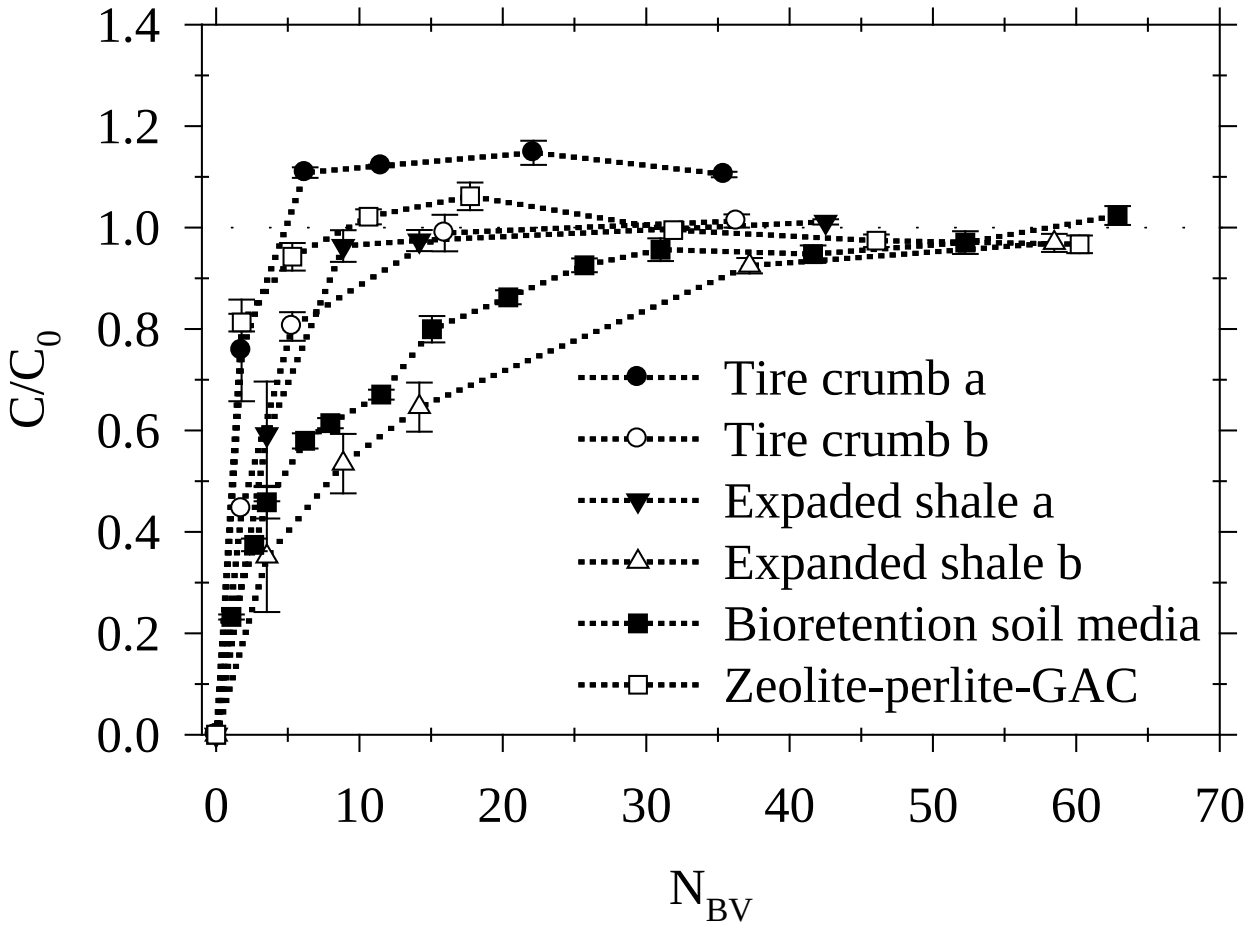

Figure 5-3. Breakthrough curves for commercially available media with an influent pH of 7.0 and C_0 of 0.5 mg/L at a surface loading rate of 40 L/min-m^2. Range bar represent standard deviation between duplicate samples.

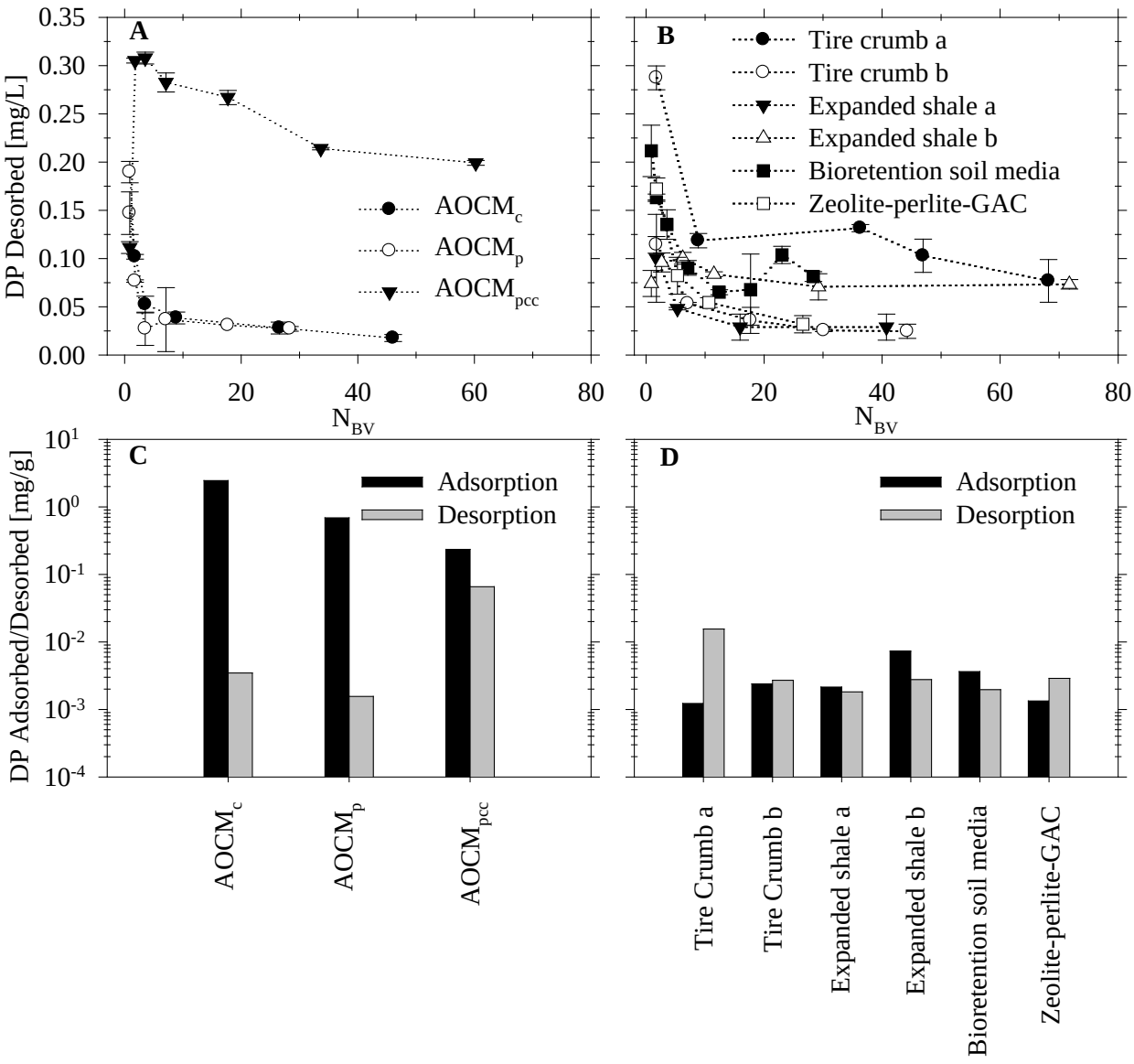

Figure 5-4. Phosphorus desorption from media with D.I. water. Range bar represent standard deviation between duplicate samples.

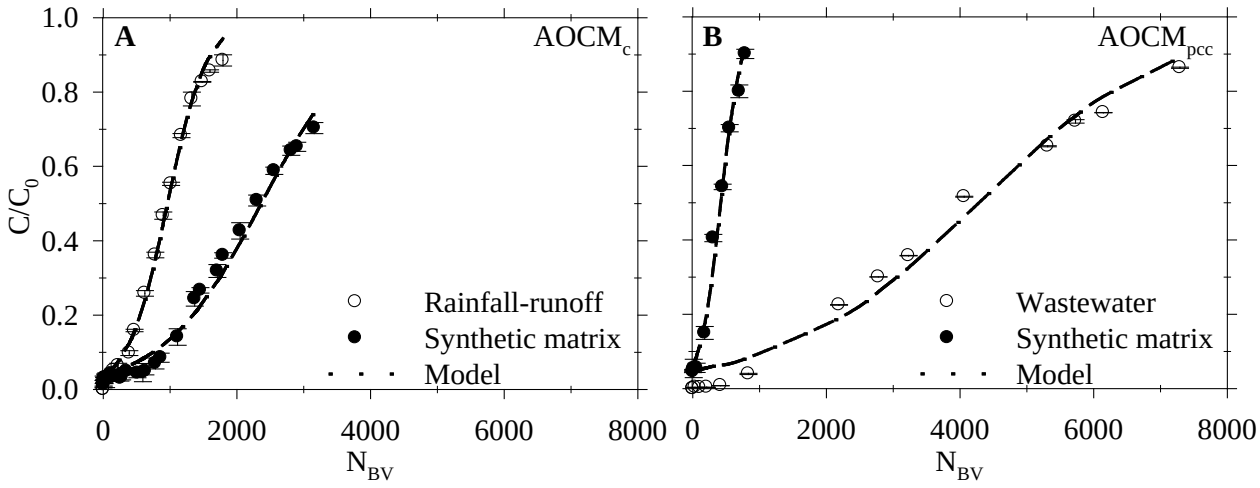

Figure 5-5. A): Breakthrough curves for $AOCM_c$ with rainfall-runoff as influent at a surface loading rate of 40 L/min-m^2 (C_0 = 0.5mg/L); B): Breakthrough curves for AOCMpcc with wastewater as influent at a surface loading rate of 40 L/min-m^2 (C_0 = 0.5 mg/L). Range bar represent standard deviation between duplicate samples.

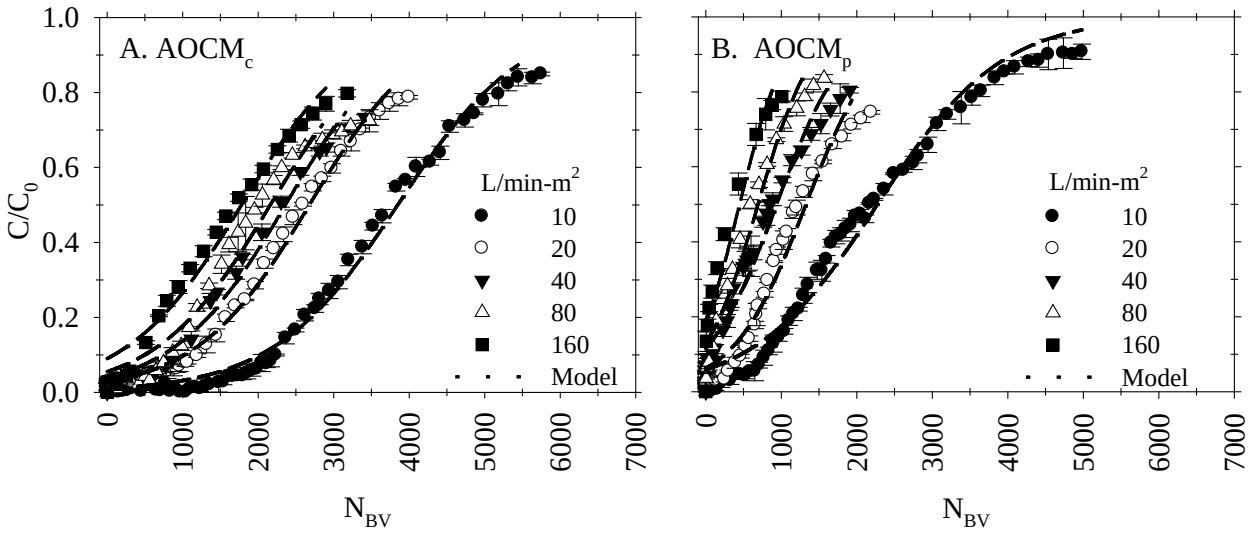

Figure 5-6. Effect of surface loading rate on breakthrough curves of $AOCM_c$ and $AOCM_p$.in synthetic runoff at C_0 = 0.5 mg/L.

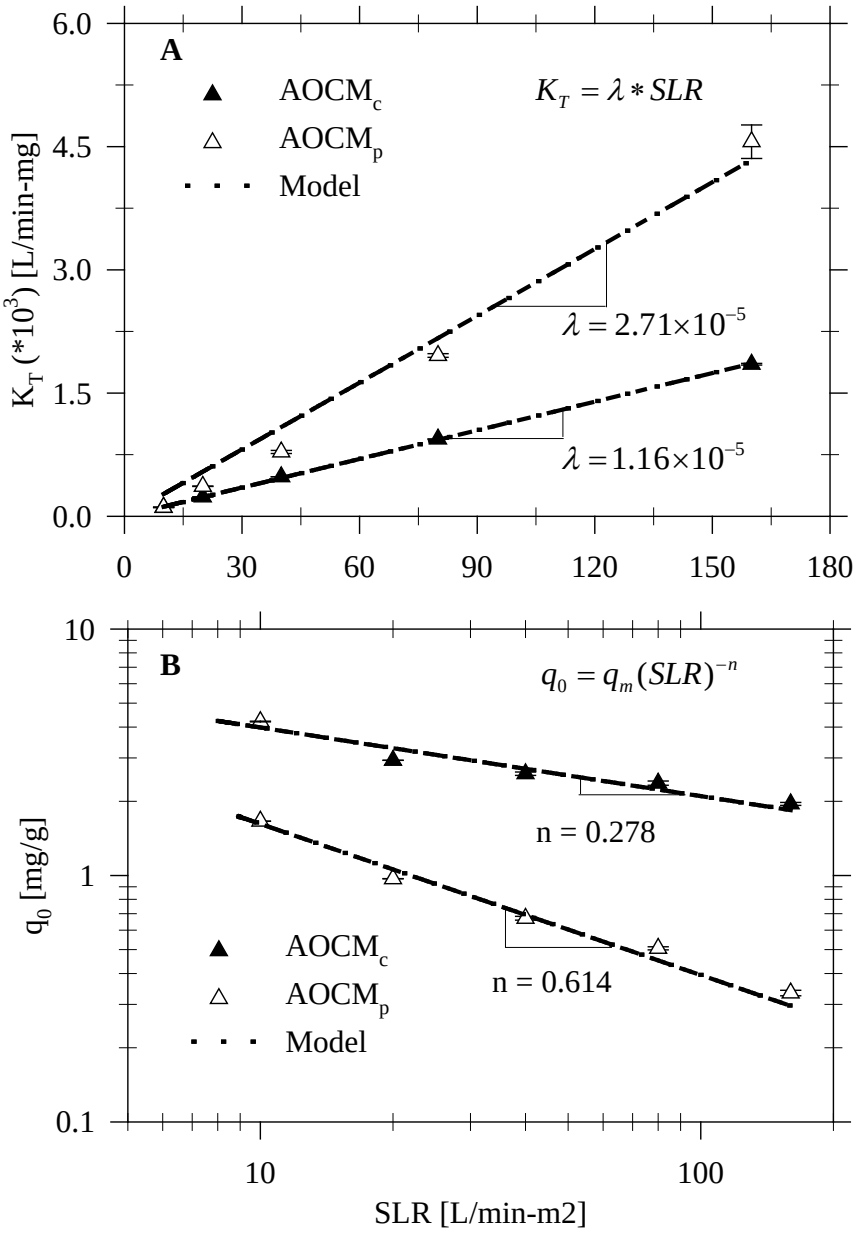

Figure 5-7. Correlations of surface loading rates and Thomas model parameters for $AOCM_c$ and $AOCM_p$.at C_0 = 0.5 mg/L. Range bar represent standard deviation. n and λ for $AOCM_c$ and $AOCM_p$ are significantly different at P = 0.05.

CHAPTER 6
CONCLUSIONS

This research examined a suite of granular filter substrates as potential adsorptive-filtration media for phosphorus control in urban drainage. The media tested were aluminum oxide (AlOx) coated media (AOCM) consisting of three separate substrates: clayey soil ($AOCM_c$), pumice ($AOCM_p$) and Portland cement concrete ($AOCM_{pcc}$) along with their uncoated media substrate (UCM); a set of commercially available media including activated alumina, bioretention soil media, expanded shale (2 gradations), Fe-coated perlite, tire crumb B&G (2 gradations) and Zeolite-perlite-GAC. The media were evaluated through 3 qualitative descriptions of equilibrium isotherm, kinetics and column breakthrough under equivalent conditions of surrogate matrix using DI water. Additionally, metal leaching during adsorption and P desorption after media exhaustion were also monitored. Furthermore, media phenomena of AOCM were investigated as functions of media coating and substrates as well as synthetic runoff, actual rainfall-runoff and wastewater matrices.

Batch equilibrium studies were firstly conducted between the three substrates based AOCM&UCM and aqueous phosphorus species (as dissolved phosphorus, DP). Equilibrium was modeled as Freundlich isotherms for three matrices: rainfall-runoff, wastewater and de-ionized (DI) water as a surrogate runoff matrix. When comparing the suite of media; results demonstrated that each AOCM exhibited significantly higher capacities than the corresponding UCM substrate in surrogate matrix. With the exception of the concrete-based substrate the uncoated clay or pumice had relatively small equilibria capacity across the entire DP range from 0.05 to 50 mg/L in comparison to AOCM of the same substrate. This result supports the study's hypothesis that the

inclusion of AlOx either as an admixture (a chemical addition to the water cement ratio) or coating will statistically significantly increase adsorption capacity. Previous studies have demonstrated ligand exchange as a mechanism for phosphate adsorption onto hydrous metal oxide surfaces. In addition to ligand exchange, results of this study indicate that additional mechanisms, for example surface precipitation for the concrete-based substrate ($AOCM_{pcc}$), occur. $AOCM_c$ and $AOCM_{pcc}$ both provided similar high equilibrium capacity as compared to $AOCM_p$. In contrast, the equilibrium capacity of the UCM_{pcc} dominated the uncoated clay and pumice substrates due to surface precipitation. While a controlled reproducible DI surrogate matrix was utilized to compare isotherms for each AOCM and companion substrate; isotherm results from this surrogate matrix were compared to uncontrolled environmental rainfall-runoff and wastewater matrices. While the DI surrogate matrix generated the highest equilibrium capacity across the range of DP concentrations examined for $AOCM_c$ and $AOCM_p$, this surrogate matrix generated the lowest equilibrium capacity for $AOCM_{pcc}$ as compared to the actual environmental matrices. Examining each AOCM type separately, the rainfall-runoff and wastewater matrices generated isotherms that were similar for each matrix across the range of concentrations examined. With ligand exchange as the primary adsorption mechanisms, the decreased equilibrium capacity of $AOCM_c$ and $AOCM_p$ loaded by rainfall-runoff and wastewater matrices can be attributed to multiple anion competition, such as SO_4^{2-} competing with phosphate for media exchange sites. In contrast, $AOCM_{pcc}$ capacity combines the dominant mechanism of surface precipitation, ternary complexation with Ca^{2+} and ligand exchange to generate nearly identical

equilibrium capacity across the entire DP concentration range which was significantly greater than the surrogate DI matrix.

Results from batch equilibrium experiments of the suite of commercially available media exhibited significantly varied capacities. The unified sorption coefficient K_u demonstrated the distribution of partitioning coefficient of sorbate between the aqueous and solid phase at various equilibrium concentrations and provided a quantitative index of media capacity, which can be evaluated and compared among different media. Results indicated that activated alumina, Fe-coated perlite and $AOCM_c$ were three media with good P removal potential while the others such as tire crumb, expanded shale, ZPG and bioretention soil media exhibited limited capacities. The possible treated water contamination due to media application was examined through metal leaching tests. Al, Ca, Fe and Mg were found to be the major metals released into the water sample. It was also found the high P removal efficiency of activated alumina and Fe-coated perlite were accompanied by a significant amount of Al and Fe leaching, imposing an environmental concern of these media application. On the contrary, $AOCM_c$ seemed to be able to satisfy both P removal and minimal contamination requirement and thus it is considered as a promising cost effective adsorptive media for P treatment.

Overall mass transfer rates of DP from a series of aqueous solutions by the suite of granular filter media in a re-circulating reactor was also monitored and modeled. Kinetic rates are examined in a synthetic runoff matrix, an actual rainfall-runoff matrix, and a secondary effluent wastewater matrix. Kinetics parameters are developed based on simulation of monitored data with a 2^{nd} order potential driving model for overall mass

transfer and an empirical model to identify intra-media diffusion as a rate limiting mechanism. Compared to the UCM controls for each AOCM, the Al-Ox coated media achieved significantly higher kinetic rates and equilibrium capacity as irrespective of the aqueous matrix. The role of the AOCM substrates did not illustrate a significant effect in a DI matrix. While the kinetic rates for the commercially available media were all below that of AOCM forms in a DI matrix, these media exhibited varied capacity and decreased in the order from Fe-coated perlite, activated alumina, expanded shale and bioretention soil media. Tire crumb (B&G) media used for green roof applications and zeolite-perlite-GAC mass transfer rates to and from were equal and therefore net equilibrium capacity was not significantly greater than 0. For the DI matrix the 2nd order potential driving model simulated the overall mass transfer rate and the intra-media diffusion model identified the rate limiting diffusion of the permeable AOCM and other media. The DI matrix is a controlled and reproducible matrix that allows comparison of media on an equivalent basis but a basis that may not represent the complex interactions of actual matrices such as rainfall-runoff and wastewater.

In order to examine the kinetic rates of DP mass transfer for actual aqueous matrices, municipal wet weather flow (rainfall-runoff, C_0 = 2.7 mg/L) and dry weather (secondary wastewater, C_0 = 11.1 mg/L) matrices are tested with AOCM and UCM. Again each AOCM out-performed the UCM substrate. However, while the type of AOCM substrate had an insignificant effect in the synthetic matrix, $AOCM_p$ kinetics rates and equilibrium capacity are significantly lower than $AOCM_c$ and $AOCM_{pcc}$ in both rainfall-runoff and wastewater matrices.

The choice of an aqueous matrix impacts resulting media parameters as developed from the 2nd order model. Therefore to investigate the effect of the aqueous matrix the DP concentration in each matrix (synthetic and actual) are adjusted to that of actual rainfall-runoff (2.7 mg/L) to eliminate the interference of different driving forces. The presence of SO_4^{2-} and Ca^{2+} in the actual matrices can exert contrary effects on phosphate mass transfer, as SO_4^{2-} competes for the active sites with phosphate ions through ligand exchange and Ca^{2+} enhances the surface precipitation of phosphate as $Ca_3(PO_4)_2$. Results demonstrated that the competition effects of SO_4^{2-} dominates in the rainfall-runoff matrix and decreases the AOCM overall mass transfer rate. While this competitive effect is observed for $AOCM_c$ and $AOCM_p$ in wastewater, surface precipitation overweighed the competition effect for $AOCM_{pcc}$, due to the high concentration of Ca^{2+} (56 mg/L) in the aqueous matrix as well as the alkaline condition in aqueous phase created through contact with concrete-based media, resulting in a faster kinetics.

Finally, column adsorption breakthrough experiments were conducted at a surface loading rate of 40 L/min-m^2 and initial P concentration of 0.5 mg/L in a fixed bed reactor with L/D =5 for all of the media studied, followed by desorption tests 24 hrs later. In these breakthrough and desorption examinations the aqueous matrix utilized is a controlled synthetic runoff matrix of D.I. water, recognizing that while this matrix does not provide the complexity of rainfall-runoff or wastewater, the matrix is consistently reproducible for comparative or parameterization studies.

Results indicate that $AOCM_c$ had higher breakthrough (X/M_b) and exhaustion (X/M_{exh}) capacity as compared to $AOCM_{pcc}$ and $AOCM_p$; $AOCM_c$ largely as a function of

the substrate providing higher specific surface area for the AlOx. While $AOCM_{pcc}$ has a higher breakthrough capacity than $AOCM_p$ the exhaustion capacity is lower; both of these results a function of surface precipitates and the instability thereof at the $AOCM_{pcc}$ surface, in addition to ligand exchange generated by the AlOx. In contrast the primary adsorption mechanism of $AOCM_c$ and $AOCM_p$ is ligand exchange. Results also indicate the non-engineered media has very limited DP breakthrough capacity (adsorption rate ≈ desorption rate) compared to the AlOx adsorptive media. Leaching results using D.I. water at a pH of 7.0 and an SLR of 40 L/min-m^2 indicate that a significant, in some cases a predominant fraction of DP adsorbed, is subsequently leached despite a 24 hour inter-event time providing for intra-particle mass transfer. In contrast, all of the three AOCM exhibit low desorption with $AOCM_c$ providing the lowest leaching concentrations and $AOCM_{pcc}$ providing a higher but nominal level of leaching from surface precipitates. Comparing breakthrough results between the synthetic matrix and rainfall-runoff or wastewater matrices for $AOCM_c$ and $AOCM_{pcc}$ respectively; results illustrate differing behavior. Competing solutes reduce the breakthrough capacity of $AOCM_c$ primarily functioning through ligand exchange. In contrast, the additional mechanism of calcium-based precipitation by $AOCM_{pcc}$ generated by the CaO on the hydrated cementitious surface and the higher Ca concentrations in solution results in an increase in breakthrough capacity for $AOCM_{pcc}$ in wastewater. Results indicate that the surface properties of the media whether providing ligand exchange or a separate mechanism such as chemical precipitation must be considered in conjunction with the aqueous matrix.

SLR ranging from 10 to 160 L/min-m^2, typical of SLRs to runoff filter systems, is a primary explanatory variable for DP breakthrough from adsorptive media. Increasing SLR results in consistently lower BVs at breakthrough and exhaustion levels. The Thomas model reproduced physical model data across all SLRs. The Thomas model rate constant (K_T) and media-phase capacity (q_0) are a function of SLR for a given adsorptive media; media where the adsorption rate >> desorption rate or media that did not include a significant surface precipitation mechanism in addition to an exchange reaction. Mathematical relationships (linear and power law) to SLR are demonstrated for K_T and q_0, respectively. The proportionality constants relating K_T and SLR are significantly different ($p = 0.05$) as are the power law exponent relating q_0 and SLR for the adsorptive media tested.

LIST OF REFERENCES

Ádám K., Krogstad T., Vråle L., Søvik A. K. and Jenssen P. D. (2007). "Phosphorus retention in the filter materials shellsand and Filtrate P® -Batch and column experiment with synthetic P solution and secondary wastewater." Ecol. Eng., 29, 200 – 208

Agyei N. M., Strydom C. A. and Potgieter J. H. (2002). "The removal of phosphate ions from aqueous solution by fly ash, slag, ordinary Portland cement and related blends." Cem. Concr. Res, 32, 1889 – 1897

Akbal F. (2005). "Adsorption of basic dyes from aqueous solution onto pumice powder." J. Colloid Interface Sci., 286, 455 – 458

Aksu Z., Çağatay Ş. Ş. And Gönen F. (2007). "Continuous fixed bed biosorption of reactive dyes by dried Rhizopus arrhizus: determination of column capacity." 143, 362 – 371

Aksu Z. and Gönen F. (2004). "biosorption of phenol by immobilized activated sludge in a continuous packed bed: prediction of breakthrough curves." Process Biochem., 39, 599 - 613

Aldridge K. T. and Ganf G. G. (2003). "Modification of sediment redox potential by three contrasting macrophytes: implications for phosphorus adsorption/desorption." Mar. Freshwater Res., 54, 87 – 94

Alvin W. M. Ip, Barford J. P. and McKay G. (2010). "A comparative study on the kinetics and mechanisms of removal of Reactive Black 5 by adsorption onto activated carbons and bone char." Chem. Eng. J., 157, 434 - 442

Appan A. and Wang H. (2000). "Sorption isotherms and kinetics of sediment phosphorus in a tropical reservoir." J. Environ. Eng. 126 (11), 993 – 998

Arias M., Da Silva-Carballal J., García-Río L., Mejuto J. and Núñez A. (2006). "Retention of phosphorus by iron and aluminum-oxide-coated quartz particles." J. Colloid Interface Sci., 295, 65 – 70

Ayari F., Srasra E., and Trabelsi-Ayadi M. (2005). "Characterization of bentonitic clays and their use as adsorbent." Desalination, 185, 391 – 397

Ayoub G. M., Koopman B. and Pandy N. (2001). "Coated filter media for low-concentration of phosphorus removal." Water Environ. Res., 73, 478 - 485

Barrett M. E., Walsh P. M., Malina J. F., and Charbeneau R. J. (1998). "Performance of vegetative controls for treating highway runoff." J. Environ. Eng., 124 (11), 1121-1128

Boari G., Liberti L. and Passino R. (1976). “Selective renovation of eutrophic wastes: phosphate removal.” Water Res., 10, 421 - 428

Boujelben N., Bouzid J., Elouear Z., Feki M., Jamoussi F. and Montiel A.(2008).“ Phosphorus removal from aqueous solution using iron coated natural and engineered sorbents.” J. Hazard. Mater., 151, 103 – 110

Bowes M.J., House W.A., Hadgkinson R.A. and Leach D.V. (2005). “Phosphorus-discharge hysteresis during storm events along a rivers catchment: the river swale,UK.” Water Res., 29, 751-762

Bowman B. T. (1981). “Anomalies in the log Freundlich equation resulting in deviations in adsorption K values of pesticides and other organic compounds when the system of units is changed.” J. Environ. Sci. Health B 16 (2), 113 - 123

Bowman B. T. (1982). “Conversion of Freundlich adsorption K values to the mole fraction format and the use of S_y values to express relative adsorption of pesticides.” Soil Sci. Soc. Am. J., 46, 740 – 743

Braja M. D. (2001). “Principles of Geotechnical Engineering” 5th edition, Thomson Learning

Bubba M. D., Arias C. A. and Brix H. (2003). “Phosphorus adsorption maximum of sandsfor use as media in subsurface flow constructed reed beds as measured by the Langmuir isotherm.” Water Res., 37, 3390 – 3400

Chandrasekharan R., Zhang L., Ostroverkhov V., Prakash S., Wu Y., Shen Y. and Shannon M. A.(2008). “High-temperature hydroxylation of alumina crystalline surfaces.” Surf. Sci., 602, 1466 - 1474

Chang Y., Li C.W. and Benjamin M. M. (1997). “Iron oxide-coated media for NOM sorption and particulate filtration.” J. Am. Water Works Assoc., 89, 100 – 113

Chen J. P., Chua M-L and Zhang B. (2002). “Effects of competitive ions, humic acid and pH on removal of ammonium and phosphorous from the synthetic industrial effluent by ion exchange resins.” Waste Manage., 22, 711–719

Chen Z., Xing B. and McGill W. B. (1999). “A unified sorption variable for environmental applications of the Freundlich Equation.” J. Environ. Qual., 28, 1422 – 1428

Christidis G. E., Scott P. W. and Dunham A. C. (1997). “Acid activation and bleaching capacity of bentonites from the islands of Milos and Chios, Aegean, Greece.” Appl. Clay Sci., 12, 329 – 347

Chitrakar R., Tezuka S., Sonoda A., Sakane K., Ooi K. and Hirotsu T. (2006). “Selective adsorption of phosphate from seawater and wastewater by amorphous zirconium hydroxide.” J. Colloid Interface Sci., 297, 426 – 433

Chitrakar R., Tezuka S., Sonoda A., Sakane K., Ooi K. and Takahiro H. (2006). “Phosphate adsorption on synthetic goethite and akaganeite.” J. Colloid Interface Sci., 298, 602 – 608

Choy K. K. H., Porter J. F. and McKay G. (2004). “Intraparticle diffusion in single and multi component acid dye adsorption from wastewater onto carbon.” Chem. Eng. J., 103, 133 - 145

Coles C. A. and Yong R. N. (2006). “Use of equilibrium and initial metal concentrations in determining Freundlich isotherms for soils and sediments.” Eng. Geol., 85, 19 – 25

Colombo C., Barrón V. and Torrent J. (1994). “Phosphate adsorption and desorption in relation to morphology and crystal properties of synthetic hematites.” Geochim. Cosmochim Acta, 58 (4), 1261 – 1269

Comings K. J., Booth D. B., and Horner R. R. (2000). “Storm water pollutant removal by two wet ponds in Bellevue, Washington.” J. Environ. Eng., 126 (4), 321-330

Costa H. S., Pereira M. M. and Andrade G. I. (2007). “Characterization of calcium phosphate coating and zinc incorporation on the porous alumina scaffolds.” Mat. Res., 10 (1), 27 – 29

Danny C. K., Ko K., Porter J. F. and Mckay G.(2000). “Optimized correlations for the fixed-bed adsorption metal ions on bone char.” 55, 5819 - 5829

Danny C. K., Ko K., Porter J. F. and Mckay G. (2001). “Determination of solid-phase loading for the removal of metal ion form effluents using fixed-bed adsorbers.” Envion. Sci. Technol., 35, 2797 – 2803

Das J., Patra B. S., Baliarsingh N. and Parida K. M. (2006). “Adsorption of phosphate by layered double hydroxides in aqueous solutions.” Appl. Clay Sci., 32, 252 – 260

Davis A. P. (2007). “Field performance of bioretention: water quality.” Environ. Eng. Sci., 24 (8) 1048 - 1064

Davis A. P., Hunt W. F., Traver R. G. and Clar M. (2009). “Bioretention technology: overview of current practice and future needs.” J. Environ. Eng., 135 (3), 109 – 117

Davis P., Shokouhian M., Sharma H., and Minami C. (2006). “Water qualityimprovement through bioretention media: nitrogen and phosphorus removal.” Water Environ. Res., 78(3), 284-293

Dayton E. A., Basta N. T., Jakober C. A. and Hattey J. A. (2003). “ Using treatment residuals to reduce phosphorus in agriculture runoff.” J. Am. Water Works Assoc., 95 (4), 151 – 158

Dean C. M., Sansalone J. J., Cartleedge F. K. and Pardue J. H. (2005). “Influence of hydrology on rainfall-runoff metal element speciation.” J. Environ. Eng., 131 (4), 632 – 642

Dechesne M., Barraud S., and Bardin J. P. (2005). “Experimental assessment of stormwater infiltration basin evolution.” J. Environ. Eng., 131 (7), 1090-1098

Drapper D., Tomlinson R. and Williams P. (2000). “Pollutant concentrations in road runoff: Southeast Queensland case study.” J. Environ. Eng.**,** 124, 313–320

Drizo A., Forget C., Chapuis R. P. and Comeau Y. (2006). “Phosphorus removal by electric arc furnace steel slag and serpentinite.” Water Res., 40 (8), 1547 – 1554

Duda A.M. (1993). “Addressing nonpoint sources of water pollution must become an international priority. Water Sci. Technol., 28, 1-11

Eaton A. D., Clesceri L. S. and Greenberg A. E. (1998). “Standard Methods for the Examination of Water and Wastewater.” 20th Edition. American Public Health Association, American Water Works Association and Water Environment Federation.

Edwards A. C. and Withers P. J. A. (2007). “Linking phosphorus sources to impacts in different types of water body.” Soil Use Manage., 23, 133 – 143

Edzwald J. K., Toensing D. C. and Leung M. C-Y (1976). “Phosphate adsorption reactions with clay minerals.” Environ. Sci. Technol., 10 (5), 485 – 490

Everett D. H. (1993). “Some problems in the study of the heterogeneity of solid surfaces.” Langmuir, 9, 2586 – 2592

Erickson A. J., Gulliver J. S. and Weiss P. T. (2007). “Enhanced sand filtration for storm water phosphorus removal.” J. Environ. Eng., 133 (5), 485 - 497

Floriano M. A. (1994). “The structure of pumice by neutron diffraction.” J. Appl. Cryst., 27, 271 – 277

Fontes M. P. F. and Weed S. B. (1996). “Phosphate adsorption by clays from Brazilian Oxisols: relationships with specific surface area and mineralogy.” Geoderma, 72, 37 – 51

Forbes M. G., Dickson K. R., Golden T. D., Hudak P. and Doyle R. D. (2004). “Dissolved phosphorus retention of light-weight expanded shale and masonry sand used in subsurface flow treatment wetlands.” Environ. Sci. Technol., 38, 892 – 898

Fu J. F., Zhao Y. Q., Razali M. and Bruen M. (2008). “Response surface optimization of phosphorus species adsorption onto powdered alum sludge.” J. Environ. Sci. Health, Part A, 43, 1100 – 1107

Gao Y., Wahi R., Kan A. T., Falkner J. C., Colvin V. L. and Tomson M. B. (2004). “Adsorption of cadmium on anatase nanoparticless effect of crystal size and pH.” Langmuir, 20, 9585 - 9593

Genç-Fuhrman H., Bregnhøj H., and McConchie D. (2005). “Arsenate removal from water using sand-red mud columns.” Water Res., 39, 2944 – 2954

Genz A., Kornmüller A. and Jekel M. (2004). “Advanced phosphorus removal from membrane filtrates by adsorption on activated aluminum oxide and granulated ferric hydroxide.” Water Res., 38, 3523 – 3530

Georgantas D. A. and Grigoropoulou H. P. (2007). “Orthophosphate and metaphosphateion removal from aqueous solution using alum and aluminum hydroxide.” J. Colloid Interface Sci., 315, 70 – 79

Gervin L., and Brix H. (2001). “Removal of nutrients from combined sewer overflows and lake water in a vertical-flow constructed wetland system.” Water Sci. Technol., 44(11-12), 171-176

Goldberg S., Lebron I., Suarez D. L. and Hinedi Z. R. (2001). “Surface characterization of amorphous aluminum oxides.” Soil Sci. Soc. Am. J., 65, 78 – 86

Goldberg S. and Sposito G. (1985). “On the mechanism of specific phosphate adsorption by hydroxylated mineral surfaces: A review.” Commun. Soil Sci. Plant Anal., 16, 801 – 821

Gomez E., Durillon C., Rofes G. and Picot B. (1999). “Phosphate adsorption and release from sediments of brackish lagoons: pH, O_2 and loading influence.” Water Res., 33, 2437 – 2447

Gray S., Kinross J., Read P. and Marland A. (2000). “The nutrient assimilative capacity of maerl as a substrate in constructed wetland systems for waste treatment.” Water Res., 34, 2183 – 2190

Guan X- H., Liu Q., Chen G- H., Shang C. (2005). “Surface complexation of condensed phosphate to aluminum hydroxide: An ATR-FTIR spectroscopic investigation.” J. Colloid Interface Sci., 289, 319 – 327

Gustafsson J. P., Renman A., Renman G. and Poll K. (2008). “Phosphate removal by mineral-based sorbents used in filters for small-scale wastewater treatment.” Water Res., 42, 189 – 197

Hameed B. H. and Daud F. B. M. (2008). “Adsorption studies of basic dye on activated carbon derived from agriculture waste: *Hevea brasiliensis* seed coat.” Chem. Eng. J., 139, 48 – 55

Hardin M. E.I. (2006). “The effectiveness of a specifically designed green roof stormwater treatment system irrigated with recycled stormwater runoff to achieve pollutant removal and stormwater volume reduction.” Master thesis, University of Central Florida

Havens K. E. and Schelske C. L. (2004). “The importance of considering biological processes when setting total maximum daily loads (TMDL) for phosphorus in shallow lakes and reservoirs.” Environ. Pollut., 113 (1), 1 – 9

Heal K. V., Smith K. A., Younger P. L. and McHaffie H. and Batty L. C. (2004). “Removing P from sewage effluent and agriculture runoff using ochre recovered from mine eater treatment”. In: Valsami-Jones, E. (Ed.), Phosphorus in Environmental Technology: Removal, Recovery and Applications. IWA Publishing, London, 320 – 334

Hietala S. L., Smith D. M., Golden J. L. and Brinker C. J. (1989). “Anomalously low surface area and density in the silica-alumina gel system.” J. Am. Ceram. Soc. 72, 2354 -2358

Hietala S. L., Smith D. M., Brinker C. J., Hurd A. J., Carim A. H. and Dando N. (1990). “ Structural studies of anomalous behavior in the silica-alumina gel system.” J. Am Ceram. Soc., 73, 2815 - 2821

Hsieh C.-h and Davis A.P. (2005). “Evaluation and optimization of bioretention media for treatment of urban storm water runoff,” J. Environ. Eng., 131(11), 1521-1531

Hsieh C.-h., Davis A.P. and Needelman B.A. (2007). “Bioretention column studies of phosphorus removal from urban stormwater runoff,” Water Environ. Res., 79(2), 177-184

Ho Y. and McKay G. (1999). “Pseudo-second order model for sorption processes.” Process Biochem., 34, 451 - 465

Huang C. (1975). “Adsorption of phosphate at the hydrous γ-Al_2O_3 electrolyte interface.” J. Colloid Interface Sci., 53, 178 – 186

Huang W., Wang S., Zhu Z., Li L., Yao X., Rudolph V. and Haghseresht F. (2008). “Phosphate removal from wastewater using red mud.” J. Hazard. Mater., 158, 35 – 42

Hunt W. F., Jarrett A. R., Smith J. T., and Sharkey L. J. (2006). “Evaluating bioretention hydrology and nutrient removal at three field sites in North Carolina.” J. Irrig. Drain. Eng., 132 (6), 600 – 608

Hunt W. F., Smith J. T., Jadlock S. J., Hathaway J. M. and Eubanks P. R. (2008). “Pollutant removal and peak flow mitigation by a bioretention cell in urban charlotte, N.C.” J. of Environ. Eng., 134 (5), 403 – 408

Johnson B. B., Ivanov A. V., Antzutkin O. N. and Forsling W. (2002). “^{31}P nuclear magnetic resonance study of the adsorption of phosphate and phenyl phosphate on γ-Al_2O_3.” Langmuir, 18, 1104 – 1111

Johansson L. (1999). “Industrial by-products and natural substrata as phosphorus sorbents.” Environ. Technol., 20, 309 – 316

Kang S-K, Choo K-H and Lim K-H (2003). “Use of iron oxide particles as adsorbents to enhance phosphorus removal form secondary wastewater effluent.” Separ. Sci. Technol., 38 (15)., 3853 – 3874

Karaca S., Gürses A., Ejder M. and Açıkyıdız M. (2004). “Kinetic modeling of liquid-phase adsorption of phosphate on dolomite.” J. Colloid Interface Sci., 277, 257 – 263

Karageorgiou K., Paschalis M. and Anastassakis G. N. (2007). “Removal of phosphate species from solution by adsorption onto calcite used as natural adsorbent.” J. Hazard. Mater., 39, 447 – 452

Karathanasis A. D. and Shumaker P. D. (2009). “Organic and inorganic phosphate interactions with soil hydroxyl-interlayered minerals.” J. Soils Sediments, 9, 501 - 510

Khaled A., Nemr A. E., Amany E-S and Abdelwahab O. (2009). “Treatment of artificial textile dye effluent containing Direct Yellow 12 by orange peel carbon.” Desalination, 238, 210 - 232

Kim J., Mann J. D. and Kwon S. (2006). “Enhanced adsorption and regeneration with lignocelluloses-based phosphorus removal media using molecular coating nanotechnology.” J. Environ. Sci. Health, Part A, 41, 87 – 100

Kim J-Y., Ma J., Howerter K., Garofalo G., and Sansalone J.J. (2008). “Interactions Of Phosphorus With Anthropogenic And Engineered Particulate Matter As A Function Of Mass, Number And Surface Area”, *Urban Water Systems, Monograph 11*, Edited by James W. CHI Publications, Guelph, Ontario, 20 pp. February.

Kim Y. and Kirkpatrick R. J. (2004). “An investigation of phosphate adsorbed on aluminum oxyhydroxide and oxide phases by nuclear magnetic resonance.” Eur. J. Soil Sci., 55, 243 – 251

Kitis M., Kaplan S. S., Karakaya E., Yigit N. O. and Civelekoglu G. (2007). “Adsorption of natural organic matter from waters by iorn coated pumice.” Chemosphere, 66, 130 - 138

Klute A. (1986). “Methods of soil analysis Part 1: Physical and mineralogical methods.” American Society of Agronomy, Inc., Soil Science Society of America, Inc., Madison, Wisconsin, USA

Ko H., Davis A. P., Kim J-Y, and Kim K-W (2007). “Arsenic removal by a colloidal iron oxide coated sand.” J. Environ.Eng., 133(9), 891-898

Koh J-H, Wankat P. C. and Wang N.-H. L. (1998). “Pore and surface diffusion and bulk phase mass transfer in packed and fluidized beds.” Ind. Eng. Chem. Res., 37, 228 – 239

Köse T. E. and Öztürk N. (2008). “Boron removal from aqueous solutions by ion-exchange resin: column sorption-elution studies.” J. Hazard. Mater., 152, 744 – 749

Kostura B., Kulveitová H. and Leško J. (2005). “Blast furnace slags as sorbents of phosphate form water solutions.” Water Res., 39, 1795 – 1802

Kuzawa K., Jung Y-J., Kiso Y., Yamada T., Nagai M. and Lee T-G (2006). “Phosphate removal and recovery with a synthetic hydrotalcite as an adsorbent.” Chemosphere., 62, 45 – 52

Lee V. K. C., Porter J. F. and McKay G. (2000). “Development of fixed-bed adsorber correlation models.” Ind. Eng. Chem. Res., 39 (7), 2427 -2433

Lee V. K. C, Porter J. F., and Mckay G. (2003). “Fixed bed modeling for acid dye adsorption onto activated carbon.” J. Chem. Techol. Biotechnol., 78, 1281 – 1289

Li H. and Davis A. P. (2008). “Urban particle capture in bioretention media I: Laboratory and field studies.” J. Environ. Eng., 134 (6), 409 – 418

Lin C. Y. and Yang D. H. (2002). “Removal of pollutants from wastewater by coal bottom ash.” J. Environ. Sci. Health, Part A: Toxic/Hazard. Subst. Environ., 37, 1509 – 1522

Lisi R. D., Park J. K. and Stier J. C. (2004). “Mitigating nutrient leaching with a sub surface drainage layer of granulated tires.” Waste Mange., 24, 831 – 839

Liu H. S., Mead J. L. and Stacer R. G. (2000). “Environmental effects of recycled rubber in light-fill applications.” Rubber Chem. Technol., 73, 551 – 564

Liu D., Sansalone J. J., and Cartledge F. K. (2005a). “Adsorption kinetics for urban rainfall-runoff metals by composite oxide-coated polymeric media.” J. Environ. Eng.,131 (8), 1168 - 1177

Liu D., Sansalone J. J., and Cartledge F. K. (2005b). “Comparison of sorptive filter media for treatment of metals in runoff.” J. Environ. Eng., 131 (8), 1178 – 1186

Liu D., Teng Z., Sansalone J. J. and Cartledge F. K. (2001). “Surface characteristics of sorptive-filtration storm water media. I: Low-density ($\rho_s < 1.0$) oxide-coatd buoyant media.” J. Environ. Eng., 127 (10), 868 – 878

Liu X. (1999). “FTIR spectroscopic studies of silication of γ – alumina with FCC catalysts Via steaming.” J. Phys. Chem. B, 103, 2647 - 2652

Lu S-G, Bai S-Q and Shan H-D (2008). “Mechanisms of phosphate removal from aqueous solution by blast furnace slag and steel furnace slag.” J. Zhejiang Univ. Sci. A, 9 (1), 125 – 132

Ma J. (2005). “Speciation, equilibrium distribution and kinetics of rainfall-runoff phosphorus in adsorptive-filtration unit operation and process.” PhD dissertation, Louisiana State University

Makris K. C., Hassan E-H, Harris W. G., O’Connor G. A. and Obreza T. A. (2004). “Intraparticle phosphorus diffusion in a drinking water treatment residual at room temperature.” J. Colloid Interface Sci., 277, 417 – 423

Malkoc E. and Nuboglu Y. (2006). “Fixed bed studies for the sorption of chromium (VI) onto tea factory waste.” Chem. Eng. Sci., 61, 4363 – 4372

Mantovaneli I. C. C., Ferretti E. C., Simões M. R. and Ferreira da Silva C. (2004). “The effect of temperature and flow rate on the clarification of the aqueous stevia extract in a fixed-bed column with zeolites.” Braz. J. Chem. Eng., 21 (3), 449 - 458

Marchi G., Guilherme L. R. G. and Lima J. M. (2006). “Adsorption/Desorption of organic anions in Brazilian oxisols.” Commun. Soil Sci. Plant Anal., 37, 1367 – 1379

Mehta P.K., (1987). “Concrete Structure, Properties, and Materials.” Prentice-Hall, Inc. New Jersey, pp. 453.

Metcal and Eddy (2003). “Wastewater engineering: treatment and reuse.” McGraw Hill.

Millero F., Huang F., Zhu X., Liu X. and Zhang, J (2001). “Adsorption and desorption of phosphate oncalcite and aragonite in seawater.” Aqua. Geochem., 7, 33–56

Morillo E., Undabeytia T., Cabrera A., Villaverde J. and Maqueda C. (2004). “Effect of soil type on adsorption-desorption, mobility, and activity of the herbicide norflurazon.” J. Agric. Food Chem., 52, 884 – 890

Mortula M., Gibbons M. and Gagnon G. A. (2007). “Phosphorus adsorption by naturally-occurring materials and industrial by-products.” J. Environ. Eng. Sci., 6, 157 – 164

Namasivayam C. and Sangeetha D. (2004). “Equilibrium and kinetic studies of adsorption of phosphate onto $ZnCl_2$ activated coir pith carbon.” J. Colloid Interface Sci., 280, 359 – 65

Nooney M. G., Campbell A., Murrell T. S., Lin X. F., Hossner L. R., Chusuei C. C. and Goodman D. W. (1998). “Nucleation and growth of phosphate on metal oxide thin films.” Langmuir, 14, 2750 – 2755

Oğuz E. (2005). “Sorption of phosphate from solid/liquid interface by fly ash.” Colloids and Surfaces A: physiochem. Eng. Aspects, 262, 113 – 117

Oğuz E., Gürses A. and Canpolat N. (2003). “Removal of phosphate form wastewater.” Cem. Concr. Res., 33, 1109 – 1112

Oleszkiewicz J. A. and Barnard J. L. (2006). “Nutrient removal technology in North America and the European Union: a review.” Water Qual. Res. J. Can., 41 (4), 449 – 462

Önal M. and Sarıkaya Y. (2007). “Preparation and characterization of acid-activated bentonite powders.” Powder Technol., 172, 14 – 18

Onar A. N., Balkaya N. and Akyüz T. (1996). “Phosphate removal by adsorption.” Environ. Tech., 17 (2), 207 – 213

Özacar M. (2003a). “Equilibrium and kinetic modeling of adsorption of phosphorus on calcined alunite.” Adsorption, 9, 125 - 132

Özacar M. (2003b). “Phosphate adsorption characteristics of alunite to be used as a cement additive.” Cem. Concr. Res., 33, 1583 – 1587

Rao J. R. and Viraraghavan T. (2007). “Biosorption of phenol from an aqueous solution by Aspergillus niger biomass.” 85, 165 – 171

Raposo F., De La Rubia M. A. and Borja R. (2009) “Methylene blue number as useful indicator to evaluate the adsorptive capacity of granular activated carbon in batch

Read P. and Fernandes T. (2003). “Management of environmental impacts of marine aquaculture in Europe.” Aquaculture, 226 (1-4), 139 – 163

Pafitt R. L. (1978). “Anion adsorption by soils and soil materials.” Adv. Agron., 30, 1 – 50

Panuccio M. R., Sorgonà A., Rizzo M. and Cacco G. (2009). “Cadmium adsorption on vermiculite, zeolite and pumice: Batch experimental studies.” J. Environ Manage. 90, 364 - 374

Penn C. J., Mullins G. L. and Zelazny L. W. (2005). “Mineralogy in relation to phosphorus sorption and dissolved phosphorus losses in runoff.” Soil Sci. Soc. Am. J., 69, 1532 - 1540

Pokhrel D. and Viraraghavan T. (2008). “Arsenic removal in an iron oxide-coated fungal biomass column: analysis of breakthrough curves.” Bioresour. Technol., 99, 2067 – 2071

Pollio F. X. and Kumin R. (1968). “Tertiary treatment of municipal sewage effluents.” Environ.Sci. Technol., 2 (1), 54 - 61

Rajan S. S.S. (1975). “Adsorption of divalent phosphate on hydrous aluminum oxide.” Nature, 253, 434 – 436

Rocha M. S. D., Iha K., Faleiros A. C., Corat E. J., Suárez-Iha M. E. V. (1997). “Freundlich’s isotherm extended by statistical mechanics.” J. Colloid Interface Sci., 185, 493 – 496

Sakadevan K. and Bavor H. J. (1998). “Phosphate adsorption characteristics of soils, slags and zeolite to be used as substrates in constructed wetland systems.” Water Res., 32, 393 – 399

Sansalone J. J. (2005). “Perspective on the synthesis of unit operations and process (UOP) concepts with hydrologic controls for rainfall-runoff”, J. Environ. Eng, 131 (7), 995 - 997.

Sansalone J. J. and Buchberger S. G. (1997). “Partitioning and first fluch of metals in urban roadway storm water.” J. Environ. Eng., 123 (2), 134 - 143

Sansalone J. J., Koran J. M., Smithson J. A., and Buchberger S. G. (1998). “Physical characteristics of urban roadway solids transported during rain.” J. Environ. Eng., 124 (5), 427 – 440

Sansalone J. J., Liu B. and Ying G. (2010). “Volumetic Filtration of rainfall-runoff. II: event-based and interevent nutrient fate.” J. Environ. Eng., 136 (12)

Sansalone J. J. and Ma J. (2009). “Parametric evaluation of batch equilibria for stormwater phosphorus adsorption on aluminum oxide media”, J. Envion. Eng, 135 (9), 737 – 746

Sansalone J.J., and Teng Z. (2005a). “Transient rainfall-runoff loadings to a partial exfiltration system: implications for urban water quantity and quality.” J. Environ. Eng., 130 (9), 990-1007

Sansalone J.J. and Teng Z. (2005b). “Transient rainfall-runoff loadings to a partial exfiltration system: implications for urban water quantity and quality”, J. Environ. Eng., 131 (8), 1155-1167

Schwarzenbach R. P., Gschwend P. M., Imboden D. M. “Environmental Organic Chemistry” 2nd ed. (2002). Wiley: Hoboken, NJ

Seo D. C., Cho J. S., Lee H. J., and Heo J. S. (2005). “Phosphorus retention capacity of filter media for stimating the longevity of constructed wetland.” Water Res., 39(11), 2445-2457

Shilton A., Pratt S., Drizo A., Mahmood, B., Banker S., Billings L., Glenny S. and Luo D. (2005). “ ‘Active’ filters for upgrading phosphorus removal from pond systems.” Water Sci.Technol., 51 (12), 111–116

Shin E. W. and Han J. S. (2004). “Phosphate adsorption on aluminum-impregnated mesoporous silicates: Surface structure and behavior of adsorbents.” Environ.Sci Technol., 38, 912 – 917

Sibrell P. L., Montgomery G. A., Ritenour K. L. and Tucker T. W. (2009). “Removal of phosphorus from agricultural wastewaters using adsorption media prepared from acid mine drainage sludge.” Water Res., 43, 2240 – 2250

Sivakumar P. and Palanisamy P. N. (2009). “Adsorptive removal of reactive and direct dyes using non-conventional adsorbent – column studies.” J. Sci. Ind. Res., 894 - 899

Smidt E., Eckhardt K., Lechner P., Schulten H. and Leinweber P. (2005). “Characterization of different decomposition stages of biowaste using FT-IR spectroscopy and pyrolysis-field ionization mass spectrometry.” Biodegradation, 16, 67 – 79

Sperlich A., Werner A., Benz A., Amy G., Worch E. and Jekel M. (2005). “Breakthrough Behavior of Granular Ferric Hydroxide (GFH) Fixed-Bed Adsorption Filters: Modeling and Experimental Approaches.”., Water Res., 39, 1190-1198.

Suzuki M. (1990). “Adsorption engineering”, Elsevier Science, Chemical engineering monographs; vol. 25

Teng Z.and Sansalone J.J. (2004). “In situ partial exfiltration of rainfall runoff. II: particle separation.” J. Environ. Eng., 130 (9), 1008-1020

Thirunavukkarasu O.S., Viraraghavan T. and Subramanian K.S. (2003). “Arsenic removal from drinking water using iron oxide-coated Sand.” Water Air, Soil Pollut., 142, 95-111

Tien C. (1994). “Adsorption calculation and modeling”, Butterworth-Heinemann series in chemical engineering, Newton, MA

Urano K. and Tachikawa H. (1991). “Process development for removal and recovery of phosphorus from wastewater by a new adsorbent. 1. Preparation method and adsorption capability of a new adsorbent.” Ind. Eng. Chem. Res., 30, 1893 – 1896

U. S. Environmental Protection Agency (USEPA). (1986). “Quality criteria for water.” Office of Water Regulation and Standards, US Government Printing Office (PB81-226759), Washington, DC 20460

U. S. Environmental Protection Agency (USEPA) (1993). “Handbook: Urban Runoff Pollution Prevention and Control Planning.” *EPA l625/R-93/004*, Office of Research and Development, Washington, DC

U. S. Environmental Protection Agency (USEPA) (1996). “National Water Quality Inventory”, Reports Congress, U. S. Environmental Protection Agency, Office of Water: Washington, D. C., Sec. 1.

U. S. Environmental Protection Agency (USEPA). (2002a). “Environmental assessment for the final effluent limitations guidelines, pre-treatment standards for new and existing sources and new source performance standards for the centralized waste treatment.”

U. S. Environmental Protection Agency (USEPA). (2002b). National water quality inventory: 2000 Report. *EPA-841-R-02-001*, USEPA, Washington, DC.

U. S. Environmental Protection Agency (USEPA) (2003). “Decentralized approaches to wastewater treatment” [online]. available from http://www.epa.gov/owm/septic/pubs/septic_presentation.pdf

U. S. Geological Survey (1999). “The quality of our nation’s waters: nutrients andpesticides.” U.S. Geological Survey Circular 1225. USGS Information Services, Denver, CO, 88 pp.

Van der Zee S. E. A. T. M. and van Riemsdijk (1988). “Model for long-term phosphate reaction kinetics in soil.” J. Environ. Qual., 17, 35 - 41

Van Raij B., and Peech M. (1972). “Electrochemical properties of some oxides and alfisols of the tropics.” Soil Sci. Soc. Am. Proc., 36, 587 – 593

Walker Jr. and William W. (2003). “Consideration of variability and uncertainty on phosphorus total maximum daily loads for lakes.” J. Water Resour. Plann. Mange., 129 (4), 337 – 344

Wang G. T., Chen, S., Barber, M. E., and Yonge, D. R. (2004). “Modeling flow and pollutant removal of wet detention pond treating stormwater runoff.” J. Environ. Eng., 130 (11), 1315-1321

Wang M. K. and Tzou Y. M. (1995). “Phosphate sorption by calcite, and iron-rich calcareous soils.” Geoderma, 65, 249 – 261

Water Environment Federation and ASCE (WEF/ASCE) (1998). “Urban runoff quality management.” WEF Manual of Practice No. 23, ASCE Manual and Rep on Engineering Practice No. 87, WEF, Alexandria, Va., ASCE, Reston, Va

Wei X., Viadero Jr. R. C. and Bhojappa S. (2008). “Phosphorus removal by acid mine drainage sludge from secondary effluents of municipal wastewater treatment plants.” Water Res., 42, 3275 – 3284

Wu J. S., Holman, R. E., and Dorney, J. R. (1996). “Systematic evaluation of pollution removal by urban wet detention ponds.” J. Environ. Eng., 122 (11), 983-988

Wu T., Gnecco, I., Berretta, C., Ma, J. and Sansalone, J.J.(2008). “Stormwater phosphorus adsorption on oxide-coated media”, Proceedings of the Water Environment Federation, Session 91 through Session 100 , pp. 6945-6957(13), Chicago, IL

Yang Y., Tomlinson D., Kennedy S. and Zhao Y. Q. (2006). “Dewatered alum sludge: a potential adsorbent for phosphorus removal.” Water Sci. Tech., 54 (5), 207 – 213

Yang Y., Zhao Y. Q., Babatunde A. O., Wang L., Ren Y. X., and Han Y. (2006). “Characteristics and mechanisms of phosphate adsorption on dewatered alum sludge.” Sep. Purif. Technol., 51, 193 – 200

Yoon S., Prezzi M., Siddiki N. Z. and Kim B. (2006). “Construction of a test embankment using a sand-tire shred mixture as fill material.” Waste Mange., 26, 1033 – 1044

Yoshida H., Jitsukawa H. and Galinada W. A. (2004). “Breakthrough and elution curves for adsorption of phosphates on an OH-type strongly basic ion exchanger.” Ind. Eng. Chem. Res., 43, 3394 – 3402

Yoshida I. (1983). “Studies on the selective adsorption of anion by metal-ion loaded ion-exchanges resin.” Sep. Sci. Technol., 18 (1), 73 - 82

Yu M-J, Li X. and Ahn W-S (2008). “Adsorptive removal of arsenate and orthophosphate anions by mesoporous alumina.” Microporous Mesoporous Mater., 113, 197 – 203

Zeng L., Li X. and Liu J. (2004). “Adsorptive removal of phosphate from aqueous solutions using iron oxide tailings.” Water Res., 38, 1318 – 1326

Zhao D. and Sengupta A. K. (1997). “Ultimate removal of phosphorus from wastewater using a new class of polymetric ion exchangers.” Water Res., 32 (5), 1613 - 1625

BIOGRAPHICAL SKETCH

Tingting Wu received her bachelor's degree in environmental engineering from Tongji University, People's Republic of China, in 2001. She got her master's degree in chemical and biomolecular engineering from National University of Singapore, Singapore, in 2005. She started her doctoral degree in the Department of Environmental Engineering and Science at University of Florida in August 2006. Her graduate research was focused on equilibria and kinetics of granular filter materials for mass transfer of phosphorus in urban water. She worked under the guidance of Dr. John J. Sansalone. Tingting Wu received the degree of Doctor of Philosophy from University of Florida in December 2010.